INVESTIGATION OF PARP1 AS A THERAPEUTIC TARGET FOR GLIOBLASTOMA

By

KRISHNA PANCHAL

A thesis submitted in partial fulfilment for the requirements for the degree of Masters of Science (by Research) at the University of Central Lancashire

February 2019

STUDENT DECLARATION FORM

Concurrent registration for two or more academic awards

I declare that while registered as a candidate for the research degree, I have not been a registered candidate or enrolled student for another award of the University or other academic or professional institution

Material submitted for another award

I declare that no material contained in the thesis has been used in any other submission for an academic award and is solely my own work

Collaboration

Where a candidate's research programme is part of a collaborative project, the thesis must indicate in addition clearly the candidate's individual contribution and the extent of the collaboration. Please state below:

_____

Signature of Candidate _____

Type of Award _____

School _____

Investigation of PARP1 as a Therapeutic Target for Glioblastoma

Krishna Panchal and Dr. Philip Welsby

Masters of Science (by Research)

School of Pharmacy and Biomedical Sciences, University of Central Lancashire

Abstract

Glioblastoma (GBM) is the most common and aggressive primary central nervous system malignancy. It is a grade IV tumour, the incidence of which peaks during the 75-84 age group, however, it can occur at any age, including childhood. Incidence is also slightly higher in men compared to in women, possibly due to the significantly less active retinoblastoma protein in males compared to in women. Despite current treatment options including surgical resection, radiation and chemotherapy, GBM has the poorest overall survival rate of gliomas, with only 0.05-4% of patients surviving 5 years after diagnosis. A combination of increasing drug resistance and the inability of many drugs to cross the blood-brain barrier, requires novel therapies for GBM to be established. Combination treatments have been proven to have a beneficial effect on increasing the sensitivity of GBM cells to therapy. This study investigated whether PARP1 could be a therapeutic target for GBM, measuring the effects of PARP1 inhibition by olaparib, alone and in combination with temozolomide and cisplatin on cell viability, proliferation, cell cycle arrest, apoptosis and autophagy in U87-MG grade IV glioblastoma and SVG p12 foetal glia cell lines cultured under normoxic (21% O_2) and hypoxic (1% O_2) conditions. The results show that olaparib monotherapy had little effect on cell viability in U87-MG cells. It decreased proliferation following 48- and 72-hours of treatment under normoxia. The combination treatment of olaparib and cisplatin was observed to induce apoptosis in a greater proportion of U87-MG cells in comparison to olaparib monotherapy under both normoxia and hypoxia following 48- and 72-hours. Whereas, both combinations with temozolomide and cisplatin induced greater autophagy when compared to olaparib following 24-hours of treatment. In the comet assay, olaparib was also observed to induce DNA damage in the U87-MG cells 24-hours after treatment. In conclusion the results of this study show that olaparib induces cytotoxic effects on glioma cells and has the potential to become an alternative treatment for GBM, whether alone or in combination with the current chemotherapeutics.

Table of Contents

Table of Figures:

List of Tables:

Acknowledgments

There are many people who I would like to thank for their support and guidance, and for helping me through the course of this Masters by Research degree. Firstly, I would like to thank my supervisor Dr. Philip Welsby for his excellent guidance, patience and mentorship throughout this year. With his help, I have learnt several new laboratory techniques and with his support this MSc has been possible. In addition, a huge thank you to the rest of my supervisory team, Dr. Gail Welsby and Dr. Izabela Stasik for their insightful knowledge in the development and support of my research.

I would like to thank Dr. Julie Burrow for providing me with the training and assistance in the cell culture laboratory, and to Joud Sabouni whom also offered guidance during this year whenever it was required.

A special thanks to my laboratory partner and best friend, Jess Gardner for being there to talk to during the stressful times. We encouraged and supported each other throughout this year, and lab work would not have been the same without you.

Finally, and most importantly, I would like to express my deepest gratitude to my family, who I cannot thank enough. I could not have achieved what I have without their love and continuous support throughout this year. Thank you for your encouragement to help me get to where I am today.

Abbreviations

5-ALA	5-aminolevulinic acid
ADP	Adenosine diphosphate
ANOVA	Analysis of Variance
ATCC	American Type Culture Collection
ATP	Adenosine triphosphate
BBB	Blood Brain Barrier
BRCA	Breast Cancer susceptibility gene
CFDA-SE	Carboxyfluorescein Diacetate Succinimidyl Ester
CNS	Central Nervous System
CT	Computerised Tomography
DNA	Deoxyribonucleic acid
DSB	Double Stranded Breaks
DTI	Diffusion Tensor Imaging
ECACC	The European Collection of Authenticated Cell Cultures
EDTA	Ethylenediaminetetraacetic acid
EGFR	Epidermal Growth Factor Receptor
EMA	European Medicines Agency
EMEM	Eagles Minimum Essential Media
ER	Endoplasmic Reticulum
FBS	Foetal Bovine Serum
GY	Gray Units
NEAA	Non-Essential Amino Acids
FDA	Food and Drug Administration
GBM	Glioblastoma
GLUT-1	Glucose Transporter-1
H_2O_2	Hydrogen peroxide
HCl	Hydrogen Chloride
HIF	Hypoxia-Inducible Factor
HR	Homologous Recombination
$IC_{50/25}$	Inhibitory Concentration of 50/25%
IDH	Isocitrate Dehydrogenase
MGMT	O^6-methylguanine methyltransferase
MOA	Mechanism of Action
MRI	Magnetic Resonance Imaging
mRNA	Messenger Ribonucleic acid
NAD^+	Nicotinamide Adenine Dinucleotide

NaOH	Sodium Hydroxide
NADPH	Nicotinamide Adenine Dinucleotide Phosphate
NOS	Not Otherwise Specified
O^6MeG	O^6-methylguanine
PAR	Poly-(ADP-ribose)
PARP	Poly-(ADP-ribose) Polymerase
PARPi	Poly-(ADP-ribose) Polymerase Inhibitor
PBS	Phosphate-Buffered Saline
PI	Propidium Iodide
RT	Radiation Therapy
SEM	Standard Error of Mean
siRNA	Small interfering RNA
SSB	Single Stranded Breaks
TMZ	Temozolomide
VEGFR	Vascular Endothelial Growth Factor Receptor
WHO	World Health Organisation

Chapter 1:

Introduction

1.1 Cancer

Cancer is the second leading cause of death worldwide and was responsible for an estimated 9.6 million deaths in 2018 (Bray, *et al*., 2018), and it is predicted that in the UK, 1 in 2 people born after 1960 will be diagnosed with some form of cancer during their lifetime. There are over 100 types of cancers worldwide, but the most common are breast, lung, prostate and bowel cancer (NHS, 2016), however the probability of developing cancer depends on many factors, such as age, genetics, and exposure to risk factors (Cancer Research UK, 2018). The highest proportion of cases diagnosed at an early stage, for all cancers combined, is by the route of screening (Cancer Research UK, 2018). The initial treatment option for most cancer types is surgery, as solid tumours can usually be surgically removed, but also other commonly used treatments are chemotherapy and radiotherapy (NHS, 2016). Cancer can also metastasise by spreading to another area of the body from its site of origin and this is when a primary cancer becomes secondary.

One cancer with a high mortality rate is a grade IV glioblastoma (GBM), a type of glioma, which affects the central nervous system (CNS), especially the brain. The incidence of GBM usually peaks during the 75-84 age group, but it can also affect younger people (Davis, 2016). This study employed U87-MG and SVG p12 glial cell lines to study the anti-cancer effects of three drugs, namely olaparib, temozolomide and cisplatin.

1.2 Glioma

Less than 2% of all primary cancers are comprised of brain tumours, which when they originate in the neuroglial cells, are referred to as gliomas (Longworth, 2005). Gliomas are the most common intracranial tumours and approximately 30% of all brain and central nervous system (CNS) tumours are made up of gliomas, and also, they represent approximately 80% of all malignant brain tumours in adults (Goodenberger & Jenkins, 2012). Despite their prevalence, the aetiology of gliomas remains largely unknown, but when diagnosed they cause significant mortality and morbidity (Ostrom, *et al*., 2014). People of all ages can be affected but are most often diagnosed in adults aged 45-60 years and young children <6 years, and they are more commonly seen in men compared to women.

Gliomas have been classified following genomic studies which identified individual molecular subtypes within “glioma” that were seen to correlate with biological aetiology, prognosis and response to therapy. By determining these subtypes, it suggests that molecular genetic tests are and will be useful, further than classical histology, for the clinical classification of gliomas (Goodenberger & Jenkins, 2012).

1.2.1 Classification & Grading

Depending on their cell of origin, gliomas have been divided into four main types: astrocytic, oligodendroglial, a mix of these two cell types (oligoastrocytic), and ependymal tumours (Ostrom, *et al*., 2014). Further classifications have been summarised in Table 1.1.

Gliomas are categorised according to the World Health Organisation (WHO) grading system, where grades I-IV are based on the malignant behaviour of the tumour. The most frequently occurring histological types of gliomas in adults are astrocytoma (grade I-IV), oligodendroglioma (grade II-III), and oligoastrocytoma (grade II-III) (Table 1.1), with ependymomas (grade I-III) being extremely rare (Ostrom, *et al*., 2014). The grades of the tumours are also classified according to their likely rate of growth; from grade I being the slowest growing, to grade IV being fast growing (Longworth, 2005). Grades I-III are classed as low-grade gliomas, while grade IV gliomas are referred to as high-grade due to their rapid progression (Louis, *et al*., 2018).

Table 1.1: The classification of glioma tumours according to the 2016 WHO classification system: identifying the grade, incidence, and the approximate age of onset (Louis, *et al*., 2016).

Glioma type	Name	Grade	Incidence (% of all brain tumours)	Age
Astrocytic tumours	Pilocytic astrocytoma	Grade I	5-6%	First 2 decades
	Subependymal giant cell astrocytoma	Grade II	<1%	2-20
	Pilomyxoid astrocytoma		1.9%	10-18 months
	Pleomorphic xanthoastrocytoma		<1%	10-30
	Diffuse astrocytoma		10-15%	30-40
	Anaplastic astrocytoma	Grade III	10-15%	45-50
	Glioblastoma	Grade IV	12-15%	45-84
Oligodendroglial tumours	Oligodendroglioma	Grade II	2.5%	40-45
	Anaplastic oligodendroglioma	Grade III	1.2%	45-50
Oligoastrocytic tumours	Oligoastrocytoma	Grade II	1.8%	35-45
	Anaplastic oligoastrocytoma	Grade III	1%	40-45
Ependymal tumours	Subependymoma	Grade I	0.7%	50-60
	Myxopapillary ependymoma		0.3%	20-35
	Ependymoma	Grade II	4.7%	<16, 30-40
	Anaplastic ependymoma	Grade III	1%	<16

1.3 Glioblastoma

Glioblastoma (GBM) is the most common and aggressive primary CNS malignancy, comprising approximately 16% of all primary brain and CNS neoplasms (Thakkar, *et al*., 2014) and 60-75% of astrocytic tumours (Young, *et al*., 2015). A term previously synonymous with glioblastoma was glioblastoma multiforme, however “multiforme” is no longer associated with the WHO classification (Young, *et al*., 2015). GBM is now divided into three types, namely wild-type, mutant-type, and not otherwise specified. This will be discussed further in the next paragraph. GBM is a grade IV tumour, whose cell type of origin is yet to be elucidated (Jawhari, *et al*., 2016). The age of incidence of GBM peaks during the 75-84 age group, however it can occur at any age, including childhood. Incidence is also slightly higher in men compared to in women (Davis, 2016), with males being diagnosed twice as often compared to females. A possible reason for this was

found when researchers established that the retinoblastoma protein, which is known to reduce the risk of cancer, is significantly less active in male brain cells than in female brain cells (Purdy, 2014; Sun, *et al*., 2014). Glioblastoma has the poorest overall survival rate of gliomas, with only 0.05-4% of patients surviving 5 years after diagnosis. Age is significantly associated with survival in all gliomas, but the effect is most obvious in GBM patients (Ostrom, *et al*., 2014). It constitutes the second leading cause of death by cancer in children after leukaemia and the third leading in adults (Jawhari, *et al*., 2016). GBM can be classified as either primary or secondary, depending on its site of origin and clinical presentation. The majority of glioblastomas (~80-85%) are primary tumours, that can arise without a known precursor. These primary tumours develop rapidly, as most patients show either signs or symptoms less than six months before diagnosis. Secondary GBM is where a low-grade tumour from elsewhere in the body that has metastasised and transformed into GBM overtime. These patients will usually show signs and/or symptoms for longer than six months (Goodenberger & Jenkins, 2012). Those diagnosed with a primary GBM tend to be older aged and have a poorer prognosis, compared to those with secondary GBM (Davis, 2016).

According to the 2016 CNS WHO classification system, glioblastomas are divided into glioblastoma isocitrate dehydrogenase (IDH) wild-type, glioblastoma IDH mutant-type and glioblastoma not otherwise specified (NOS). IDH wild-type accounts for about 90-95% of cases and is most frequently associated with the clinically defined primary or *de-novo* glioblastoma and is predominantly observed in patients aged 55+. IDH mutant-type accounts for only 10% of cases mainly arising in younger patients. IDH wild and mutant-type are classified as grade IV tumours by the 2016 WHO classification. The glioblastoma NOS designation is a diagnosis for those tumours for which a full IDH evaluation cannot be completed. However, a full IDH evaluation differs for glioblastomas present in older patients compared to those in younger adults (Louis, *et al*., 2016).

Isocitrate dehydrogenase is a catalytic isozyme encoded by five genes that express the three key IDH human types, that are involved in the citric acid cycle and it also plays a role in the protection of cells against oxidative damage. Mutations within IDH1 and IDH2 occur in 70-80% of low-grade gliomas and secondary glioblastomas, but only in a small proportion of primary glioblastomas (~5-10%) (Ostrom, *et al*., 2014). These mutations alter the function of the enzymes, resulting in the production of 2-hydroxyglutarate, a potential oncometabolite, and lack of nicotinamide adenine dinucleotide phosphate (NADPH) production (Cohen, *et al*., 2013)**.** These mutations are associated with glioblastoma IDH mutant-type and is believed to arise spontaneously (Brown, *et al*., 2010). IDH1 and IDH2 mutated GBM has a better prognosis compared to

GBM IDH-wild type. Patients with GBM IDH-mutant type have a mean overall survival time of 27.1 months, which is more than twice as long as than those with GBM IDH-wild type (11.3 months) (Ohgaki & Kleihues, 2013).

The GBM tumour environment contains areas of low tumour oxygenation, also known as hypoxia (Jawhari, *et al*., 2016), a condition frequent in solid tumours. Due to GBM being an extremely hypoxic tumour, deep and remote areas of the growth suffer from a low oxygen partial-pressure, which could drop to 1% or less. Although, expectations are that these conditions should slow tumour growth, instead the cancer cells develop processes overtime enabling them to not only survive hypoxia, but to also become more aggressive. In the midst of these adaptive responses, autophagy, a catabolic mechanism, aids in the survival of tumour cells. This survival pathway allows cell components to be degraded resulting in the production of energy (adenosine triphosphate (ATP)) and metabolic precursors to be further recycled by the cellular anabolism (Jawhari, *et al*., 2016). Hypoxia constitutes a major issue for GBM patients, since it induces tumour cell invasion into healthy brain tissue in order to evade the adverse environment. As well as being a major obstacle for therapy, tumour invasion is also the leading cause of death in GBM patients (Monteiro, *et al*., 2017). Due to this reason, a large amount of research has been focused on characterising the molecular and cellular pathways which regulate GBM cell invasiveness. Since the hypoxic condition is a major inducer of the invasive phenotype, understanding how hypoxia triggers GBM cells to invade, or how this can be prevented, is essential for the development of novel and more effective therapies against glioblastoma (Monteiro, *et al*., 2017).

1.4 Diagnosis of GBM

Symptoms of glioblastoma can vary widely, as they are dependent on the size and the location of the tumour. The most commonly observed symptoms include headaches, nausea, dizziness, seizures, physical weakness, visual loss, memory problems, personality changes or stroke-like symptoms (Young, *et al*., 2015). Symptoms can worsen as the tumour progresses. During the first stage of diagnosis when a patient presents any neurological symptoms, a physical exam will be performed. This will include neurologic functions tests, such as muscle strength, alertness, eye and mouth movement and coordination. If, following this, a tumour is suspected, imaging tests including either magnetic resonance imaging (MRI) or computerised tomography (CT) will be done to identify any abnormalities in the patient's brain (Ramakrishna, 2017). Determination of a patient's tumour subtype requires an invasive biopsy or surgical resection in order to perform genomic analysis (Davis, 2016).

1.5 Treatment of GBM

Treatment options for GBM patients are limited and have remained largely unchanged over the past 40 years. This includes surgical resection, radiation and chemotherapy (Young, *et al*., 2015). Complete and extensive surgical resection of the tumour is most likely impossible, because GBM tumours are frequently invasive and are often located in essential areas of the brain; areas which control speech, motor function, and the senses. Therefore, the amount of tumour which is safe to be removed will be surgically resected. However, due to the high degree of invasiveness, radical resection of the primary mass of tumour is non-curative, and invading GBM cells will remain within the brain region, resulting in later GBM progression or recurrence (Davis, 2016). The importance of aggressive surgical resection when possible has been demonstrated by multiple studies, by showing trends of a better outcome in those patients who have a greater extent of resection (Kuhnt, *et al*., 2011). A surgical resection of 98% or more of the tumour volume has a median survival of 13 months, compared to 8.8 months for resections of less than 98% (Lacroix, *et al*., 2001). Thus, a significant correlation is seen between the extent of resection and longer progression-free survival and overall survival.

More recently enhancements in surgical and pre-operative brain mapping techniques have also made it possible to achieve more extensive surgical resection, while preserving function and quality of life (Davis, 2016). The use of imaging techniques, such as functional MRI and diffusion tensor imaging (DTI) in pre-operative planning, as well as ultrasound, CT scans, and MRI with direct stimulation during surgery has made multimodal neuro-navigation and the integration of patient-specific anatomic and function data possible. Regardless of these technologies, differentiating between normal brain cells and tumour cells continues to be a great challenge, and the use of 5-aminolevulinic acid (5-ALA) dye for fluorescent guidance is more effective than neuro-navigation-guided surgery alone (Zhao, *et al*., 2013). However, there are limitations to these novel techniques, such as cost, the need for specialised equipment, operators and surgery suites. Therefore, further studies are required to elucidate the clinical benefits, prior to being established as the standard care for patients with GBM (Davis, 2016).

Opportunities for new therapies for recurrent and newly diagnosed GBM have come to light by significant advances in the knowledge and understanding of the molecular pathology of GBM and the accompanying cell signalling pathways. Due to survival being short-term, new advances in treatment are greatly required to prolong a GBM patient's survival (Davis, 2016).

1.5.1 Radiation & Chemotherapy

Following surgical resection, the patient will commonly wait as long as four weeks for the craniotomy wound to heal, before commencing therapy. Post-operative radiation therapy (RT) alone was the standard treatment until 2005, until a pivotal phase III trial improved the standard of care for GBM. It was confirmed that external beam RT combined with temozolomide (TMZ) chemotherapy was more effective than RT alone (Stupp, *et al*., 2005; Davis, 2016).

RT occupies an integral role in GBM treatment. Analysis of the relationship between survival and the dose of radiation administered, revealed a dose-effect relationship. The usual dose of 60 gray units (Gy), given in 30 fractions of 2 Gy, provided superior survival in comparison to lower doses (Mann, *et al*., 2017); and a dose escalation beyond this identified increased toxicity, without additional survival benefits (Davis, 2016). However, from recent findings patients who received TMZ chemotherapy along with RT had a median survival of 14.6 months, compared to 12.1 months with RT alone. The cohort of patients who received TMZ plus RT also had a higher proportion of long-term survivors compared to those who received RT alone (27% vs. 11% at two years; 10% vs. 2% at five years, respectively) (Stupp, *et al*., 2009). RT and alkylating chemotherapy exert their therapeutic effects by initiating DNA damage, cytotoxicity and triggering apoptosis (Davis, 2016).

1.5.2 Temozolomide

Temozolomide is an imidazotetrazine derivative of the alkylating agent dacarbazine and a prodrug of the anti-cancer drug, Temodar (Moody & Wheelhouse, 2014). TMZ was approved in 2005 by the US Food and Drug Administration (FDA) for the treatment of newly diagnosed adult GBM. TMZ is administered orally, due to its lipophilic nature allowing it to penetrate through the blood-brain-barrier (BBB). As a DNA alkylating agent, it induces cell cycle arrest during the G2/M phase, eventually resulting in apoptosis. The cytotoxicity caused by TMZ is mediated in genomic DNA by its addition of methyl groups at N^7 and O^6 sites on guanines, and the N^3 site on adenines. Alkylation of the O^6 site on guanine results in the insertion of a thymine base instead of a cytosine opposite to the methyl-guanine, during subsequent DNA replication, which can ultimately cause cell death (Fig.1.1) (Lee, 2016).

However, 50% of patients given TMZ do not respond to it, and this is primarily due to the over-expression of the O^6-methylguanine methyltransferase (MGMT) enzyme (Lee, 2016). The *MGMT* gene codes for the MGMT enzyme, which is involved in DNA repair, thus patients with methylated (non-activated) *MGMT* present with compromised DNA repair. Activation of the MGMT enzyme can cause interference with the effects of treatment, therefore, patients who express methylated *MGMT* benefit further when undergoing chemotherapy with TMZ and RT (Stupp, *et al*., 2009; Davis, 2016).

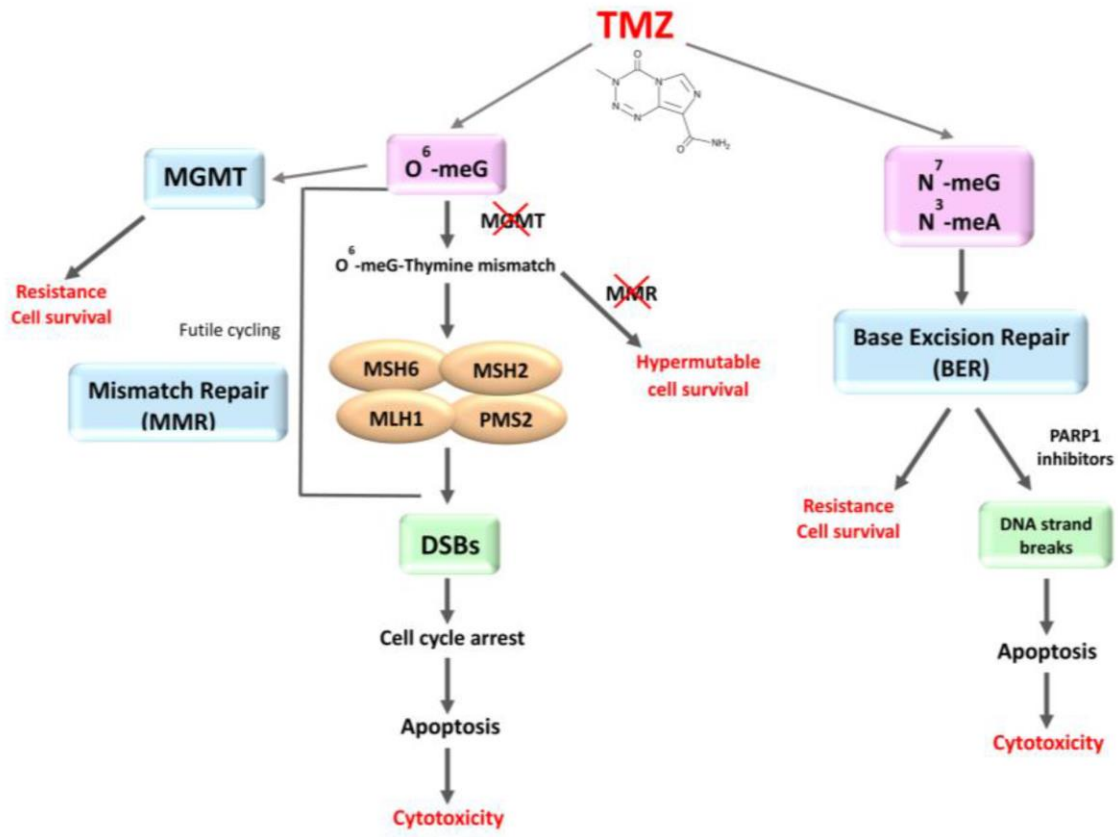

Figure 1.1: Flow diagram showing the mechanism of action of temozolomide for the treatment of cancer, leading to the induction of cytotoxicity (Annovazzi, *et al*., 2017).

1.5.3 Cisplatin

Otherwise known as cisplatinum, or *cis*-diamminedichloroplatinum (II), cisplatin is a well-known chemotherapeutic drug. It has been used as a treatment for numerous human cancers, such as bladder, testicular, ovarian, head and neck, and lung cancers. Its mechanism of action (MOA) has been associated with its ability to cross-link with the N^7 reactive centre of purine bases in DNA. This causes interference with DNA repair mechanisms, initiating DNA damage in cells and blocking cell division, to consequently induce apoptotic cell death (Dasari & Tchounwou, 2014). Even though cisplatin is one of the most commonly used and effective anti-cancer drugs, high doses are frequently

required for it to penetrate the BBB; which usually causes intolerable adverse effects in patients. Furthermore, ~90-95% of cisplatin becomes irreversibly bound to plasma proteins, resulting in only 5-10% of the drug which is fraction free to exert anti-tumour effects (Coluccia, *et al*., 2018). Regarding brain tumours, cisplatin has been used as a treatment for recurrent childhood brain tumours (Dasari & Tchounwou, 2014). As TMZ is a prodrug that can display inconsistent activities *in vitro*, in this project cisplatin was used as a consistent control.

1.6 PARP1

PARP (poly ADP-ribose polymerase) enzymes comprise of a large family of 18 proteins (Dziadkowiec, *et al*., 2016). PARP1 is an abundant nuclear protein that is involved in many cellular processes from DNA repair to cell death. Recognition of DNA breaks by PARP1 is one of the initial steps that occur following DNA damage. When DNA strand breaks occur, particularly due to ionising radiation or DNA alkylating agents, including temozolomide, PARP1 binds to the break sites through its N-terminal zinc finger motifs which are located in the DNA-binding domain. This causes activation of its catalytic C-terminal domain which initiates hydrolysis of NAD^+, by transferring an ADP-ribose moiety, to synthesise poly-(ADP-ribose) (PAR) polymers, which are covalently bound to different acceptor proteins or to PARP1 itself. The auto-poly(ADP-ribosyl)ation results in chromatin decondensation at the break site, allowing access for repair enzymes. A key mechanism of PARP1-dependent decondensation is that the removal of the H1 linker histone from transcription initiation sites is facilitated by an activated PARP1. Removal of H1 causes chromatin decondensation, allowing repair enzymes to cleave to the damaged DNA sites, forming a repair complex (Malyuchenko, *et al*., 2015). Eventually, PARP1 undergoes a molecular modification that ultimately results in its reduced affinity for DNA. The dissociation of PARP1 from DNA is required for DNA repair completion (Dziadkowiec, *et al*., 2016). The active involvement of PARP1 in DNA repair occurs only upon minimal genotoxic damage. Stronger damage would trigger apoptosis, though more extensive DNA damage would cause overactivation of PARP1, resulting in cell necrosis (Fig.1.2) (Malyuchenko, *et al*., 2015).

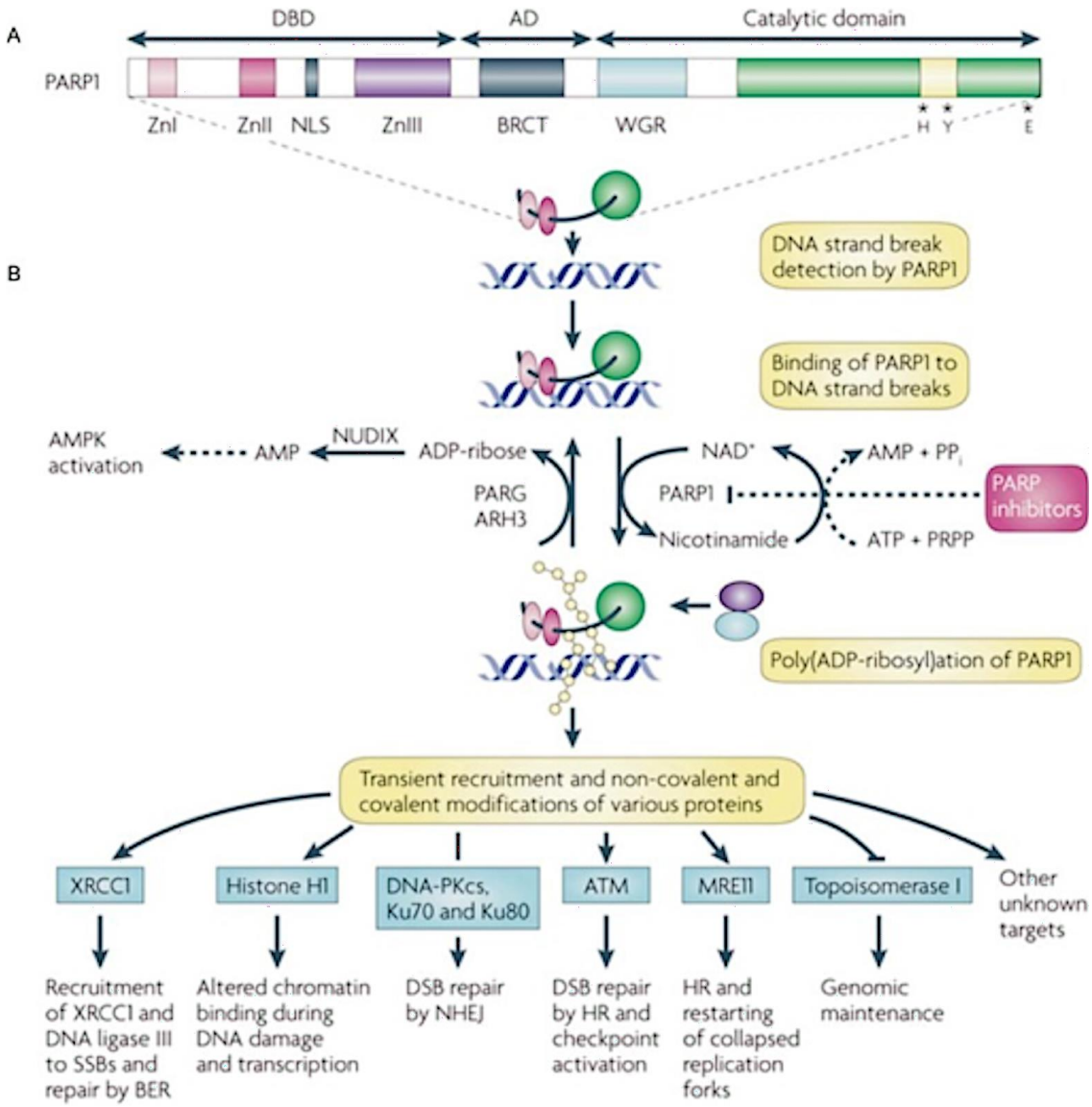

Figure 1.2: Diagrams A and B depicting the role of PARP1 in the DNA repair pathway (Chen, 2011).

Abundant data have found PARP1 to be involved in carcinogenesis. Inhibition of PARP1 by olaparib leads to disruption of many cellular pathways. Disturbances in the DNA repair process and inhibition of the transcription of various genes involved in DNA replication and cell cycle regulation are caused by the loss of PARP1. Under-expression of the enzyme leads to genome shuffling and chromosomal abnormalities, and it may contribute to overall genome instability. In contrast, increased expression of PARP1 has been observed in many tumours, including GBM, which is considered as a prognostic factor associated with poor survival (Malyuchenko, *et al*., 2015).

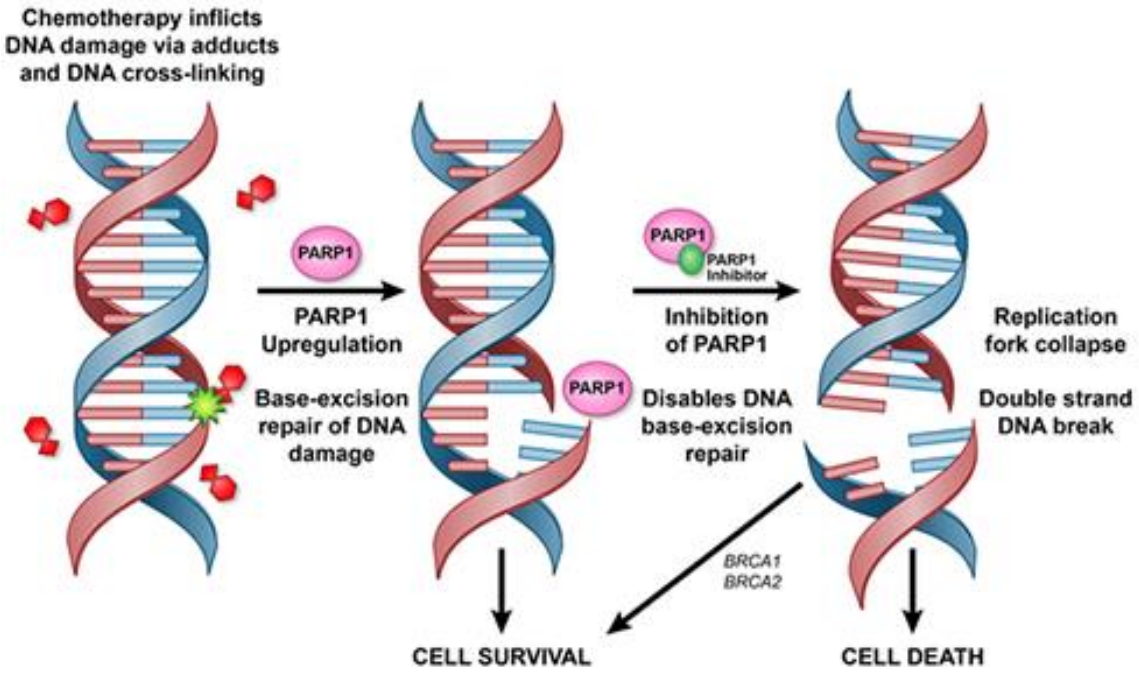

Figure 1.3: Diagram showing the mechanism of action of PARP1 and PARP inhibitors on DNA following chemotherapy (Powell, 2014).

Even though PARP1 is over-expressed in the nuclei of GBM cells, it is barely detectable in normal brain tissue (Fulton, *et al*., 2018). Therefore, PARP may represent a tumour-specific treatment target. As well as assisting rapidly dividing cancer cells with DNA repair, PARP1 counteracts apoptotic cell death. Interference of PARP function by inhibition renders cancer cells to be more prone to the cytotoxic effects of DNA-damaging treatments (Karpel-Massler, *et al*., 2014).

1.7 Olaparib

Also known by the trade name Lynparza, olaparib is used as a targeted therapy, and in 2014, was approved by the FDA as treatment for advanced ovarian cancer in patients with inherited *BRCA* mutations who have had three or more types of chemotherapy. The FDA granted regular approval for olaparib, in 2017, as maintenance therapy for patients with recurring epithelial ovarian, fallopian tube, or primary peritoneal cancer, who were either partially or completely responsive to platinum-based chemotherapy (Sharples, 2017). This was further approved by the European Medicines Agency (EMA) in 2018 (AstraZeneca, 2018). Olaparib was granted regular approval by the FDA in January 2018 also for the treatment of deleterious or suspected deleterious germline-*BRCA*-mutated, HER2-negative metastatic breast cancer in patients who had received chemotherapy in

the neoadjuvant, adjuvant or metastatic setting. This is the first FDA-approved treatment for these patients (FDA, 2018).

In recent studies, olaparib has been investigated for the treatment of glioblastoma. The OPARATIC trial managed by Professor Anthony Chalmers (University of Glasgow) obtained results of olaparib successfully penetrating both the core and outer-area of recurrent GBM, despite failing to penetrate an intact BBB (Jenkins, 2017). It was able to leak through because the barrier is disrupted in GBM. By elucidating that olaparib was able to reach the tumours, it can be utilised to enhance current treatments and make them more effective. Olaparib combined with low dose TMZ was also discovered as being safe and endurable, which allowed promising 6-month progression-free survival rates. These results suggest olaparib could be a potential treatment strategy for GBM tumours. This study has already caused two further clinical trials to commence, PARADIGM and PARADIGM-2, which investigate olaparib in combination with TMZ and radiotherapy in patients with newly diagnosed GBM (Jenkins, 2017).

Olaparib is a member of a class of drugs, known as PARP enzyme inhibitors. The focus in this project will be on PARP1 inhibition by olaparib. PARP inhibitors (PARPi), such as olaparib, sensitise cancer cells to DNA damaging agents and functions through synthetic lethality in cells containing defects in homologous recombination (HR) DNA repair (Lim & Tan, 2017). Single-strand breaks (SSBs) activate PARP1 in order to repair the damage. Olaparib inhibits PARP by trapping it at the unrepaired SSB sites on DNA, which induces the production of DNA double-strand breaks (DSBs), that require HR for successful repair (Brown, *et al*., 2016). The accumulation of these breaks induces cell apoptosis, which subsequently allows the effects of the therapeutics to be more effective and cause enhanced apoptosis (Fig.1.3) (Chalmers, 2017). Preclinical studies have indicated that only 10-100 nM of olaparib is required to achieve >90% PARP inhibition (Chalmers, *et al*., 2016).

1.8 Drug Resistance

Effectiveness of cancer therapy becomes limited due to drug resistance – a serious issue that results when diseases become tolerant to pharmaceutical treatments. There are two broad categories into which resistance to chemotherapeutics can be divided: intrinsic or acquired. Intrinsic drug resistance refers to the pre-existence of resistance-mediating factors in the bulk of the tumour cells even before receiving chemotherapy, causing the therapy to be ineffective. However, acquired resistance can develop during treatment. These tumours can be initially susceptible, but resistance can be due to

mutations arising during treatment. Various other adaptive responses, including increased expression of the therapeutic target and activation of alternative compensatory signalling pathways can also result in acquired drug resistance (Holohan, *et al*., 2013).

Treatment of drug resistant GBM is a complex goal due to the heterogeneous nature of GBM tumours and the inherent issues of treating any cancer of the CNS because of the limited repair mechanisms and anatomic complications. The molecular pathways by which GBM presents resistance to apoptosis, are only partially understood. However, by understanding the molecular relationship between GBM cells and their environment is vital since these abnormalities could determine tumour formation and progression. This process can be reversible via therapeutic targeting, resulting in restoration of susceptibility to apoptosis. Thus, by recognising the cellular and molecular mechanisms that are involved in drug resistance is an essential target for the treatment of GBM (Haar, *et al*., 2012).

GBM can become resistant to current post-operative therapies, contributing to the poor survival prognosis of GBM patients. Evidence is available that increased PARP1 expression and treatment resistance of tumours are correlated (Malyuchenko, *et al*., 2015). Upregulation of PARP1 enhances the anti-apoptotic feature of GBM, leading to resistance to DNA-damaging therapeutic agents. Therefore, restoring apoptotic sensitivity is of vital importance to render GBM cells sensitive to treatment (Karpel-Massler, *et al*., 2014). PARP1 can also become resistant to PARPi, though it is largely unknown how this resistance develops. (Murnyák, *et al*., 2017). PARPi have been seen to cause synthetic lethality in cells with defects in HR DNA repair as a result of molecular abnormalities including BRCA mutations. Resistance of PARPi can therefore also be caused when *BRCA1/2* function is restored through mutations which result in repair of the open reading frames of the gene (Lim & Tan, 2017).

1.9 Combination Therapies

Administration of combination drug regimens is one way to make treatment resistant GBM responsive to drug therapy, as such treatments have the potential to overcome intrinsic and acquired resistance to therapy. The majority of all GBMs develop treatment resistance after administration of TMZ, radiation, or the combination of TMZ and radiation (Karpel-Massler, *et al*., 2014). The discovery of small molecule PARPi was driven by their potential to enhance the cytotoxic effects of commonly used cancer therapies for GBM.

Temozolomide mediates its cytotoxic effects by binding alkyl groups to nitrogen atoms in guanine bases in DNA. The synergistic interaction of TMZ and PARPi has appeared, at least partly, to be dependent upon the ability of PARPi to trap PARP on DNA. Olaparib has found to have a great ability to trap PARP1 on DNA, which enhances the cytotoxic effects of TMZ to a great extent. The TMZ-PARPi synergistic effect is suggested to be associated to the role of PARP1 in the repair of abasic sites in DNA (short “gaps” in the double helix which lack a base). PARP1 especially attaches to DNA lesions with 5’-deoxyribose phosphate ends, as opposed to 5’-phosphate ends; possibly elucidating why TMZ induces a greater level of PARP DNA binding, and also in the presence of TMZ why more DNA-PARP complexes occur, which in turn enhances cytotoxic effects of PARPi caused by efficient PARP trapping. In preclinical models, the TMZ-PARPi combination has been seen to be effective in targeting models of GBM, also including models which are usually TMZ-resistant. High doses of PARPi treatment combined with a low dose of TMZ has improved TMZ efficacy; dose-limiting toxicity is often a factor of TMZ treatment. Therefore, a combined treatment approach that utilises a low dose of TMZ with an increased dose of a PARPi may reduce toxicity while still maintaining efficacy (Dréan, *et al*., 2016).

Early studies demonstrated that PARP inhibition causes radio-sensitisation in mammalian cells (Malyuchenko, *et al*., 2015; Ben-Hur, *et al*., 1985). Later it was discovered that various PARPi, such as olaparib, enhanced the radio-sensitisation efficacy in some cell lines. Other studies observed that PARPi selectively induces radio-sensitisation of actively replicating cells during the S-phase of the cell cycle. Therefore, this observation suggests a mechanism that PARP inhibition increases the sensitivity to ionising radiation as inhibition prevents SSBs repair, converting them into DSBs during the movement of the replication fork in the S-phase, hence resulting in cell death (Malyuchenko, *et al*., 2015). These radio-sensitising effects of PARP inhibition have been observed in multiple glioma cell lines but are only present in actively dividing cells. Since normal brain tissue is comprised almost entirely of non-dividing cells, combining radiotherapy with PARPi is expected to improve its therapeutic effects (Fulton, *et al*., 2018).

1.10 Model Cell Lines

U87-MG cells are epithelial cells, derived from brain tissue and are a grade IV glioblastoma cell line that were developed almost 50 years ago (Pontén & Macintyre, 1968). U87-MG cells are possibly the most commonly used cell line for research on human glioma as there were 408 publications on PubMed, which used these cells, in

2018. This cell line is currently available from the American Type Culture Collection (ATCC), but the original cell line was generated by Uppsala. These two versions of the cell line are not identical, possibly due to the occurrence of cross-contamination, but they both are glioblastoma cell lines (Allen, *et al*., 2016).

SVG p12 cells are fibroblast cells, derived from brain tissue and are a human foetal glial cell line that was generated in 1985 (Major, *et al*., 1985). SVG p12 cells have been provided by the ATCC since 1987 and have been used in various research studies where cells of neural origin are required (Henriksen, *et al*., 2014).

1.11 Gaps in Knowledge

Over the past decade, a vast amount of research has been performed on glioblastoma, with numerous published papers focusing on prognosis, treatment response and treatment targets; though, not many studies have caused changes in patient outcome. A novel approach for therapy is greatly required to address the overwhelmingly poor survival and treatment results for patients diagnosed with GBM (Ozdemir-Kaynak, *et al*., 2018).

Olaparib's effects in GBM are currently being studied, and due to the illness causing the BBB in patients to become leaky, this allows olaparib to enter the CNS (Chalmers, 2017). However, limited knowledge is available about whether the drug has a potential to be a treatment for GBM. Therefore, more testing is required to ensure it can be used as a treatment alone or in combination with the current standard chemotherapeutics. Also, due to the intra-tumoural environment of GBM being hypoxic (Jawhari, *et al*., 2016), the MOA of olaparib in low oxygen conditions also requires research in order to establish whether olaparib would be effective on hypoxic cancer cells.

Inhibiting PARP1 may be a potential and promising therapeutic target, though no previous study has determined the expression characteristics and prognostic role associated with the molecular heterogeneity in astrocytomas, including GBM, of PARP1 (Murnyák, *et al*., 2017). Therefore, thorough research is required, so its role as a DNA repair protein in GBM can be elucidated.

These experiments are necessary because currently there is no curative treatment for GBM and the survival rate is considerably low (Lee, 2016). Therefore, investigation into whether olaparib can improve a patient's chances of survival is required. However,

if survival is an unrealistic goal, it could be observed whether olaparib can be used to improve a patient's life conditions. This may be possible if olaparib has fewer side effects or even less harmful effects, compared to those caused by current chemotherapeutic agents.

1.12 Hypothesis

The overall survival rate of glioblastoma is very poor, and as the treatment options are limited, a novel therapy is highly required. Therefore, in this study it was decided to investigate the effects of olaparib, a PARP1 inhibitor, on U87-MG cells. Olaparib was investigated alone and in combination with either TMZ and cisplatin in various assays.

It is hypothesised that olaparib will cause enhanced cytotoxicity in glioblastoma cells when used as a treatment alone and in combination with standard chemotherapeutic agents.

Main Aim: To investigate olaparib as a novel treatment for glioblastoma when administered either alone or in combination with other standard chemotherapeutic agents, such as temozolomide and cisplatin.

Objectives:

- To establish whether olaparib effects the growth, viability, proliferation, cell cycle arrest, apoptosis, autophagy and colony formation of glioma cells.
- To confirm DNA damage by olaparib by performing the comet assay.
- To establish the effects of olaparib in both normoxic and hypoxic conditions.
- To determine the cytotoxic effects of olaparib alone and in combination with either temozolomide and cisplatin on glioma cells.

Chapter 2:

Materials and Methods

2.1 Materials

Consumables were of the highest grade commercially available and purchased from the following suppliers: SVG p12 and U87-MG cell lines (The European Collection of Authenticated Cell Cultures (ECACC)), olaparib, temozolomide, cisplatin (Cambridge Bioscience), Eagles Minimum Essential Media (EMEM), Trypan blue (Lonza), PrestoBlue® viability reagent (ThermoFisher Scientific), propidium iodide (PI) dye (Sigma), carboxyfluorescein diacetate succinimidyl ester (CFDA-SE) (ThermoFisher Scientific), apoptosis assay kit (ThermoFisher Scientific), autophagy kit (Enzo), Hoescht 33342 (Life Technologies), crystal violet (Sigma). All other consumables were of the highest available and purchased from Sigma.

2.2 Tissue Culture

SVG p12 and U87-MG cell lines were maintained in EMEM supplemented with 10% foetal bovine serum (FBS), 1mM sodium pyruvate, 2mM L-glutamine and 1% non-essential amino acids in a 37°C humidified atmosphere with 5% CO_2. When approximately 80% confluency was reached, the cell monolayers were washed with 1x phosphate-buffered saline (PBS) solution, which was replaced with trypsin and returned to the incubator to allow the cells to detach from the surface of the flask for approximately 5 minutes. After detachment, EMEM was added to neutralise the trypsin. The cells were gently re-suspended to ensure a single cell suspension was obtained before passaging or seeding into plates for experimental analysis.

2.3 PrestoBlue® Cell Viability Assay

Both concentration and time-dependent effects on cell viability were measured over 3-days of drug treatment. SVG p12 and U87-MG cells were seeded at 1000 cells/well in 96-well plates prior to drug treatment with olaparib, temozolomide and cisplatin at various concentrations (0.001 mM, 0.003 mM, 0.01 mM, 0.03 mM, 0.1 mM, 0.3 mM) to measure cell viability at 24, 48 and 72-hour time-points. Following treatment, PrestoBlue® reagent was added to the wells and after an incubation period of 1-hour, the fluorescence was measured at Ex 535 nm/Em 612 nm using the Tecan GENios Pro plate reader. This assay was performed in normoxic (21% O_2) and in hypoxic (1% O_2) conditions to compare the viability of the drug treated cells in normal and reduced oxygen levels. From the concentration-time curves, the IC_{50} and IC_{25} values were determined for each of the drug treatments using GraphPad Prism software.

2.4 CFDA-SE Cell Proliferation Assay & PI staining for Cell Cycle Assay

SVG p12 and U87-MG cells were seeded at 50,000 cells/well in 6-well plates for the day 0 controls and 10,000 cells/well in 12-well plates for measuring the effects of drug treatment on cell proliferation and cell cycle over a period of 7-days. This assay was performed in both normoxic and hypoxic conditions. Following seeding, the cells were incubated for 24-hours prior to the addition of carboxyfluorescein diacetate succinimidyl ester (CFDA-SE) dye (5 μM in PBS). After 10 minutes, the CFDA-SE solution was replaced with fresh medium and incubated for 2-hours prior to drug treatment and the drug treatments were added to the appropriately labelled wells using the previously calculated IC_{25} values of olaparib (100 μM), temozolomide (100 μM) and cisplatin (10 μM). Day 0 controls and then 24, 48, 72, 144 and 168-hours post-treatment, cells were harvested by trypsinisation, followed by fixation in 70% ice cold methanol until the samples were analysed. Before analysis, cells were counterstained with propidium iodide (PI; 5μg/ml in 1X PBS with 250 μg/mlRNase) and incubated for 1-hour at 37°C in the dark. Changes in cell proliferation and cell cycle were measured at Ex 492 nm/Em 517 nm by flow cytometry where 5000 events were analysed using the Guava® easyCyte 12HT benchtop flow cytometer (Merck Millipore, UK).

2.5 Annexin V & PI Staining for Cell Apoptosis Assay

Effects of olaparib, TMZ and cisplatin on apoptosis, in normoxia and in hypoxia, were investigated on SVG p12 and U87-MG cells, over 3-days. The cell lines were seeded at 25,000 cells/well in a 24-well plate and incubated for 24-hours, prior to drug treatment. Previously calculated IC_{50} values of each of the drugs were used: a concentration of 300 μM for all three drug treatments. At 24, 48 and 72-hours post-treatment, the cells were harvested by trypsinisation. Prior to analysis, the PI (1 μg/ml) and Annexin V stains were prepared and added to each labelled sample according to the manufacturer's instructions (ThermoFisher Scientific), before transferring into a 96-well plate. After incubation for 30 minutes at room temperature, the samples were analysed by flow cytometry where 5000 events were analysed using the Guava® easyCyte 12HT benchtop flow cytometer, at Ex 488 nm/Em 530 nm and 575 nm (Merck Millipore, UK).

2.6 Autophagy Assay

SVG p12 and U87-MG cell lines were seeded at 50,000 cells/well in 24-well plates to investigate the effects on autophagy at 24-hours. This assay was performed in both normoxia and hypoxia in order to compare the differences in normal oxygen conditions and in reduced oxygen conditions. Each appropriate well was drug treated with the previous calculated IC_{50} values: a concentration of 300 μM for all three drug treatments, including the combination treatment wells 24-hours before analysis. The positive controls, rapamycin (10 μM) and chloroquine (200 μM), were added to the appropriate wells 16-18 hours prior to harvesting. The following day, the 1X assay buffer and the diluted CYTO-ID green stain solution (0.5 μl/ml) were prepared, as per the manufacturer's instructions (Enzo) and protected from light. The cells were harvested by trypsinisation and centrifuged for 5 minutes, at 4°C, at 100 xg. After removing the supernatant, the cells were resuspended in EMEM and diluted CYTO-ID stain solution; 1 X assay buffer was added to the unstained samples instead of the stain. The samples were incubated for 30 minutes at 37°C, in the dark, before centrifugation again. Finally, the cells were resuspended in PBS, transferred into a 96-well plate and analysed by flow cytometry where 5000 events were analysed using the Guava® easyCyte 12HT benchtop flow cytometer, at Ex 483 nm/Em 506 nm (Merck Millipore, UK). The normoxia and hypoxia graphs were created by calculating the percentage of each of the non-treated controls for each cell line. Whereas, for the normoxia and hypoxia comparison graphs, percentages were calculated from the normoxia non-treated control for each cell line.

2.7 Comet Assay

SVG p12 and U87-MG cells were seeded at 50,000 cells/well in 6-well plates to measure DNA damage at the individual eukaryotic cell level. This assay was performed in normoxic conditions only. A final concentration of 300 μM, obtained from the previously calculated IC_{50} values, was used of olaparib, TMZ and cisplatin to treat the cells. 24-hours after drug treating, the full comet assay was performed: the cells were harvested by trypsinisation and counted to calculate the volume of cell mix needed to get a total of 20,000 cells. The samples were centrifuged before removing the supernatant, and the resulting cells were embedded onto microscope slides by combining with 1% low melting-point agarose. Dilute H_2O_2 was added to a set of untreated cells to be measured as a positive control. Slides were emerged into a pre-made lysis solution (2.5 M Sodium Chloride, 0.1 M EDTA (ethylenediaminetetraacetic acid) disodium salt, 10 mM Tris-Hydrogen Chloride (HCl)), Triton-X-100, and the pH was adjusted to 10 with sodium

hydroxide (NaOH)) and incubated for 1-hour at 4°C. After incubation, slides were placed in pre-chilled electrophoresis solution (0.3 M NaOH, 1 mM EDTA) for 40 minutes at 4°C, prior to running the samples for electrophoresis at 25V for 30 minutes. The next step was neutralisation where the slides were washed with three changes, at 5 minutes each at 4°C, of neutralisation buffer (0.4 M Tris Base, pH 7.5 adjusted with concentrated HCl). Finally, the slides were stained with Hoechst (1 µg/ml), covered with a cover slip and left to dry at 4°C overnight. Analysis was performed using the ZEN Pro software, using a magnification of 10x, the DAPI filter, an excitation wavelength of 335-383 nm and an emission wavelength of 420-470 nm, on which two different analysis methods were used to obtain results.

2.8 Clonogenic Assay

The ability of a single cell to form a colony was measured using SVG p12 and U87-MG cell lines, in both normoxic and hypoxic conditions. The cells were seeded at 1,500 cells/well in 6-well plates, which were incubated for 24-hours prior to drug treating. Either olaparib, TMZ or cisplatin was added to the appropriate wells at a final concentration of 10 µM. Following 4-hours incubation, the EMEM in the wells was discarded and replaced with fresh EMEM. After 10-days, media was discarded, and cells were washed with ice cold PBS; fixed with 100% ice cold methanol for 10 minutes; and then at room temperature stained with crystal violet for 10 minutes. After crystal violet (1%) was removed, the wells were washed 3 x with distilled H_2O, then left to air dry overnight, before the colonies were counted using a digital colony counter.

2.9 Statistical Analysis

Statistical analysis was performed in GraphPad Prism software version 5 (GraphPad Software, GraphPad Software Inc., USA). An ANOVA (analysis of variance) with a Bonferroni's post hoc test was performed to determine significance with a value of $p<0.05$ used to identify significant differences. Appropriate vehicle controls were tested and, unless otherwise stated, had no significant effect when compared to the non-treated control. To show significance, * indicates comparison to the respective control, † indicates comparison between drug treatments (* $p<0.05$, ** $p<0.01$, *** $p<0.001$). Note that all data were suppressed as mean ± standard error of the mean (SEM) and, unless otherwise specified, of 5 independent repeats.

Chapter 3:

Results

3.1 Growth Curves

The growth of SVG p12 and U87-MG cells, prior to the addition of treatment, was determined over 9-days and the data was represented as growth curves (Fig. 3.1A and 3.1B). The results show that each cell line seems to grow significantly (p<0.05) in normoxic conditions compared to in hypoxia, especially from day 5 to day 9.

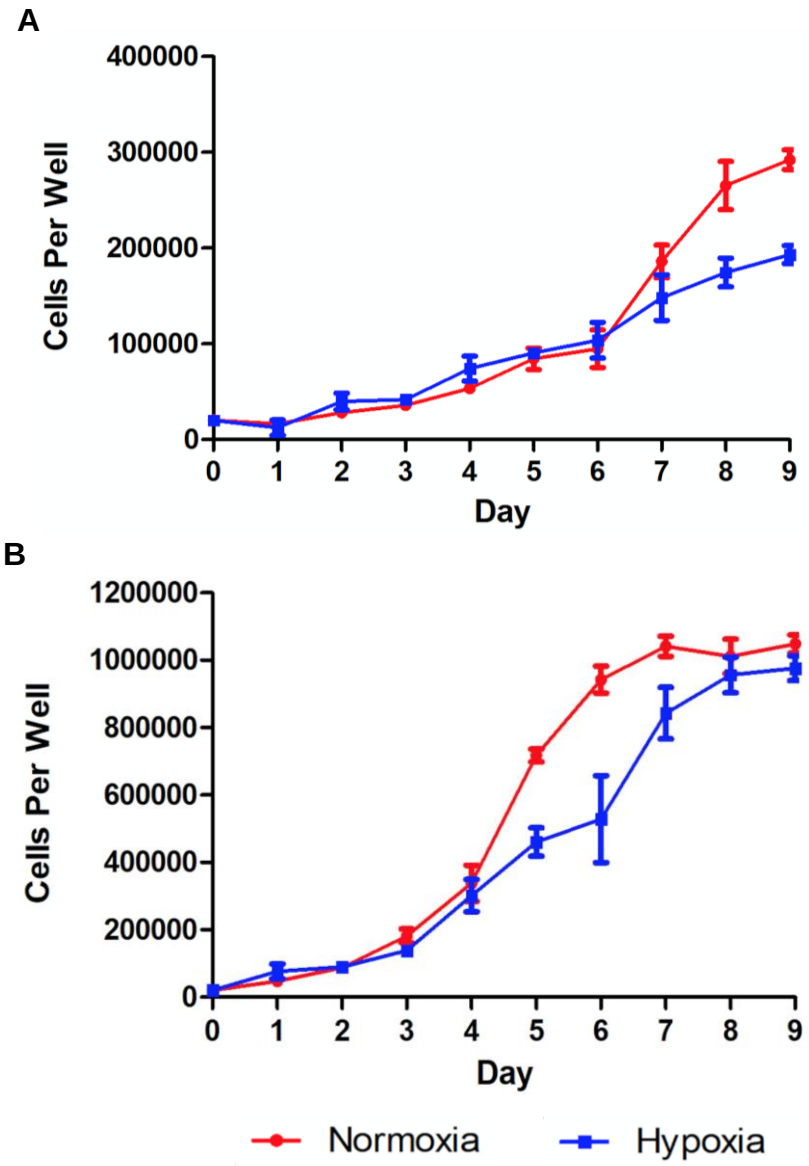

Figure 3.1: Graphs showing the growth of SVG p12 (A) and U87-MG cells (B) under normoxia (21% O_2) and hypoxia (1% O_2) without drug treatment. Log phase for SVG p12 cells commences at day 6 in both normoxia and hypoxia, whereas for U87-MG cells, at day 3. For the U87-MG cell line, the log phase finishes at day 8 in both conditions. Data are representative of three independent repeats.

3.2 *Concentration and Time Responses for Cell Viability*

The effect of olaparib, temozolomide and cisplatin on SVG p12 and U87-MG cell viability, in both normoxic and hypoxic conditions, was investigated *in vitro*. All three of these treatments produced concentration- and time-dependent changes under both conditions (Fig.3.4 and Fig.3.5). TMZ and cisplatin produced a concentration- and time-dependent decrease in cell viability in both cell lines, and also in both conditions during the three time-points, an effect not as clearly observed with olaparib (Fig.3.4A, B; Fig.3.5A, B).

3.2.1 **Effects on Cell Viability in Normoxia**

In the concentration range used, olaparib had little effect on cell viability at 24-, 48-, and 72-hours in either SVG p12 or U87-MG cells under normoxia apart from at 72-hours in SVG p12 cells where a significant decrease was observed, when compared to 24-hours, at a concentration of 0.1mM (p<0.001) (Fig.3.4A). However, at this 72-hour time-point, no significant differences were observed between the SVG p12 and U87-MG cells (p>0.05).

TMZ had greater effects on cell viability at all time-points in both cell lines. In SVG p12 cells after 24-hours, in comparison to 48-hours, no significant differences were observed (p>0.05) (Fig.3.4C). However, a significant decrease was observed 72-hours after TMZ treatment compared to 24-hours at concentrations of 0.003 mM, 0.1 mM (p<0.01) and 0.3 mM (p<0.001). 48-hours after TMZ treatment in U87-MG cells, in comparison to 72-hours in SVG p12 cells, presented a significant decrease in the U87-MG cells at a concentration of 0.003 mM (p<0.01). No significant differences were observed in U87-MG cells at neither 24-, 48- or 72-hours after TMZ treatment (Fig.3.4D), when compared to the SVG p12 cells at the equivalent time-points (Fig.3.4C).

Following 48-hours of treatment with cisplatin in SVG p12 cells, a significant difference was observed, when compared to 24-hours (Fig.3.4E) at concentrations of 0.01 mM (p<0.05), 0.03 mM, 0.1 mM and 0.3 mM (p<0.001). The same significant decrease was also observed at 72-hours, in comparison to 24-hours (37.6 μM vs. 270.3 μM), at the same concentrations. In U87-MG cells, the greatest difference observed was at 72-hours, when compared to 24-hours post-treatment (28.8 μM vs. 592.4 μM). These significantly different decreases occurred at concentrations of 0.01 mM (p<0.05), 0.03 mM, 0.1 mM and 0.3 mM (p<0.001).

Comparisons between TMZ and cisplatin treatments observed various effects on cell viability in both cell lines. In SVG p12 cells, the greatest significant decrease was observed at 72-hours after treatment with cisplatin, when compared with TMZ (37.6 μM vs. 244.5 μM), at concentrations of 0.03 mM, 0.1 mM and 0.3 mM (p<0.001). In U87-MG cells, 72-hours after treatment with TMZ, in comparison to 24-, 48-, and 72-hours after treatment with cisplatin, all identified major differences. The greatest significant decrease was observed 72-hours after cisplatin treatment compared to TMZ (28.8 μM vs. 303.6 μM), at 0.01 mM, 0.03 mM, 0.1 mM and 0.3 mM (p<0.001).

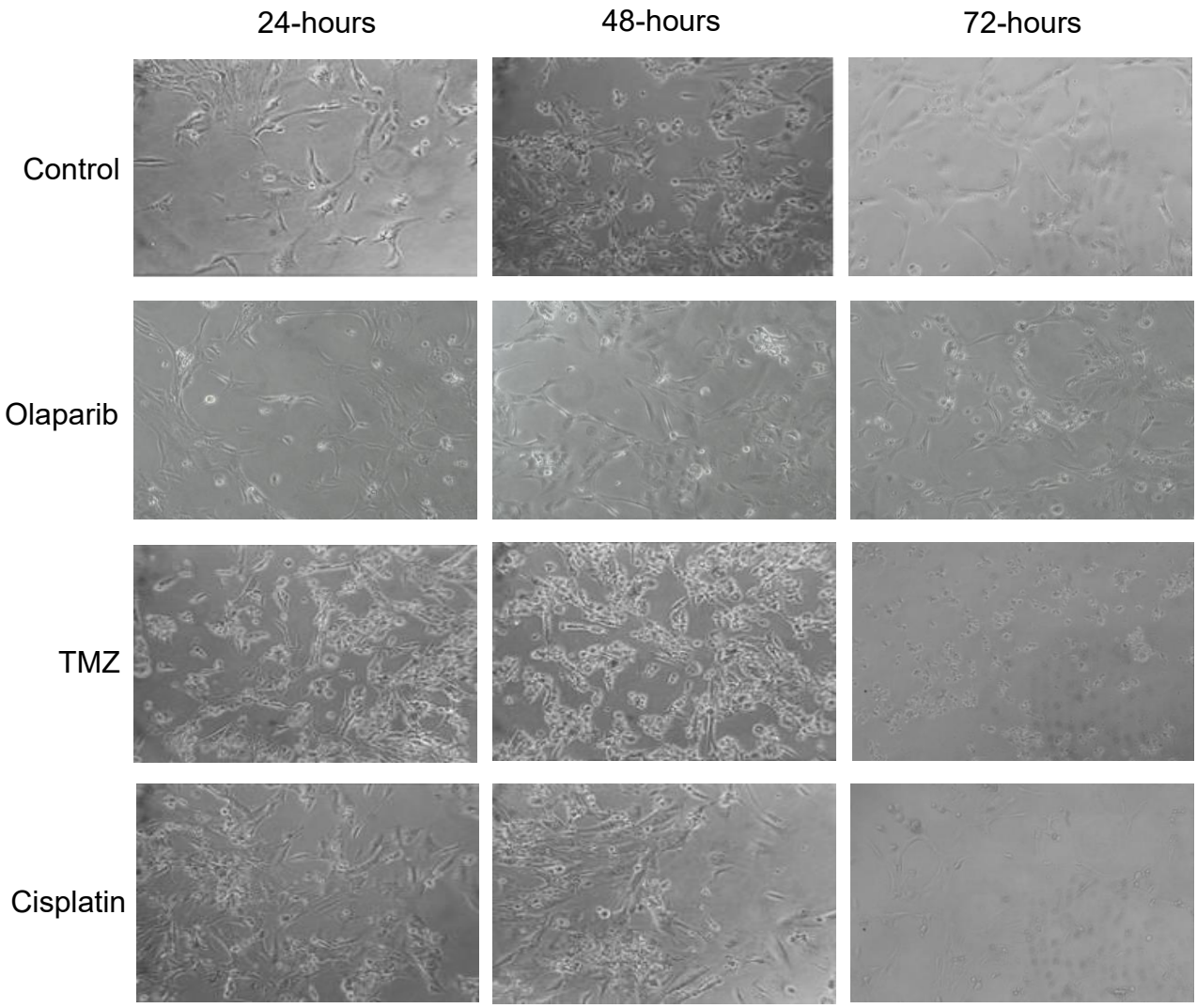

Figure 3.2: Original photographs show representative untreated and treated SVG p12 cells under normoxia (21% O_2) after 24-, 48-, and 72-hours following treatment with either olaparib, temozolomide or cisplatin using the IC_{50} values from the cell viability assay.

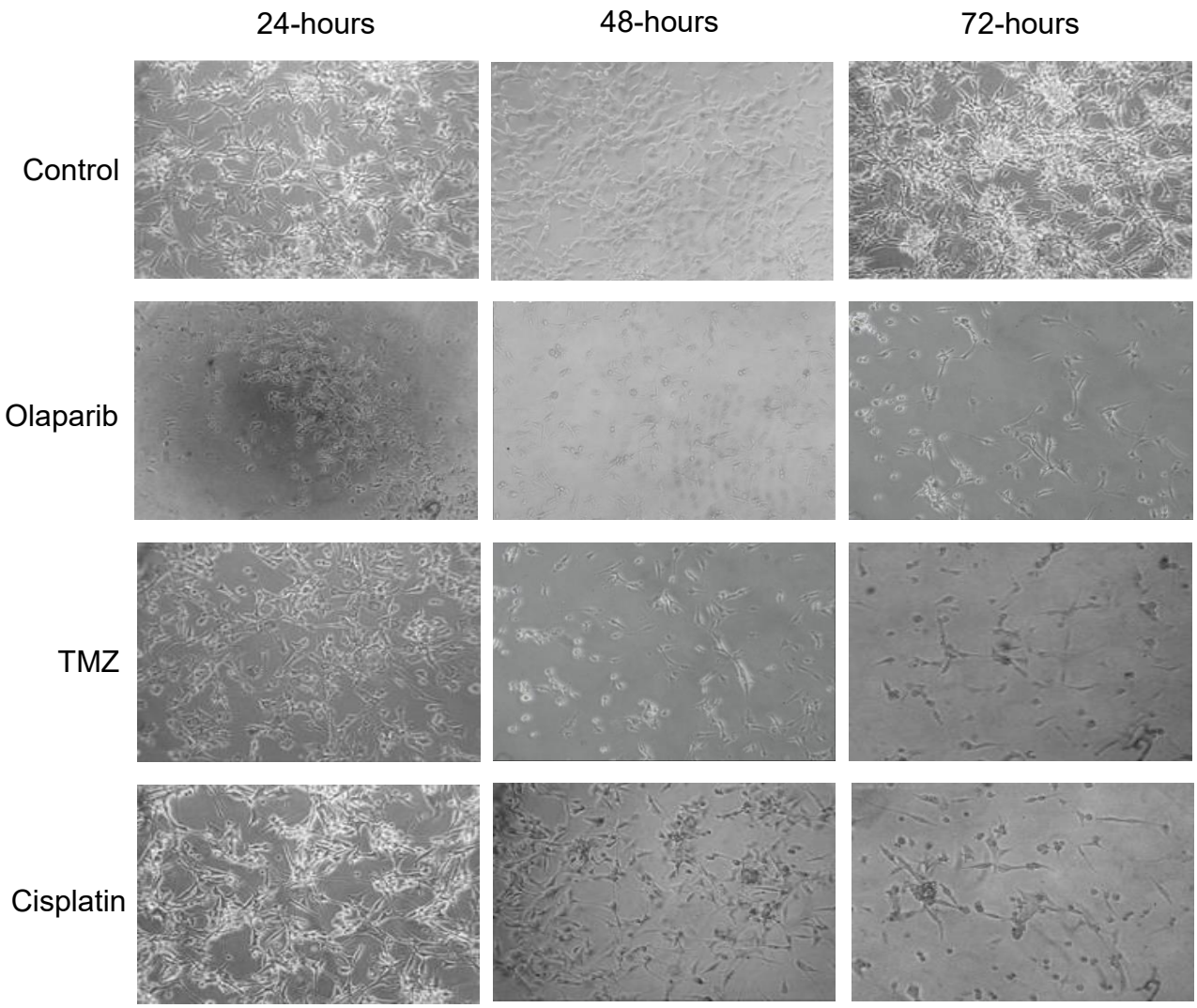

Figure 3.3: Original photographs show representative untreated and treated U87-MG cells under normoxia (21% O_2) after 24-, 48-, and 72-hours following treatment with either olaparib, temozolomide or cisplatin using the IC_{50} values from the cell viability assay.

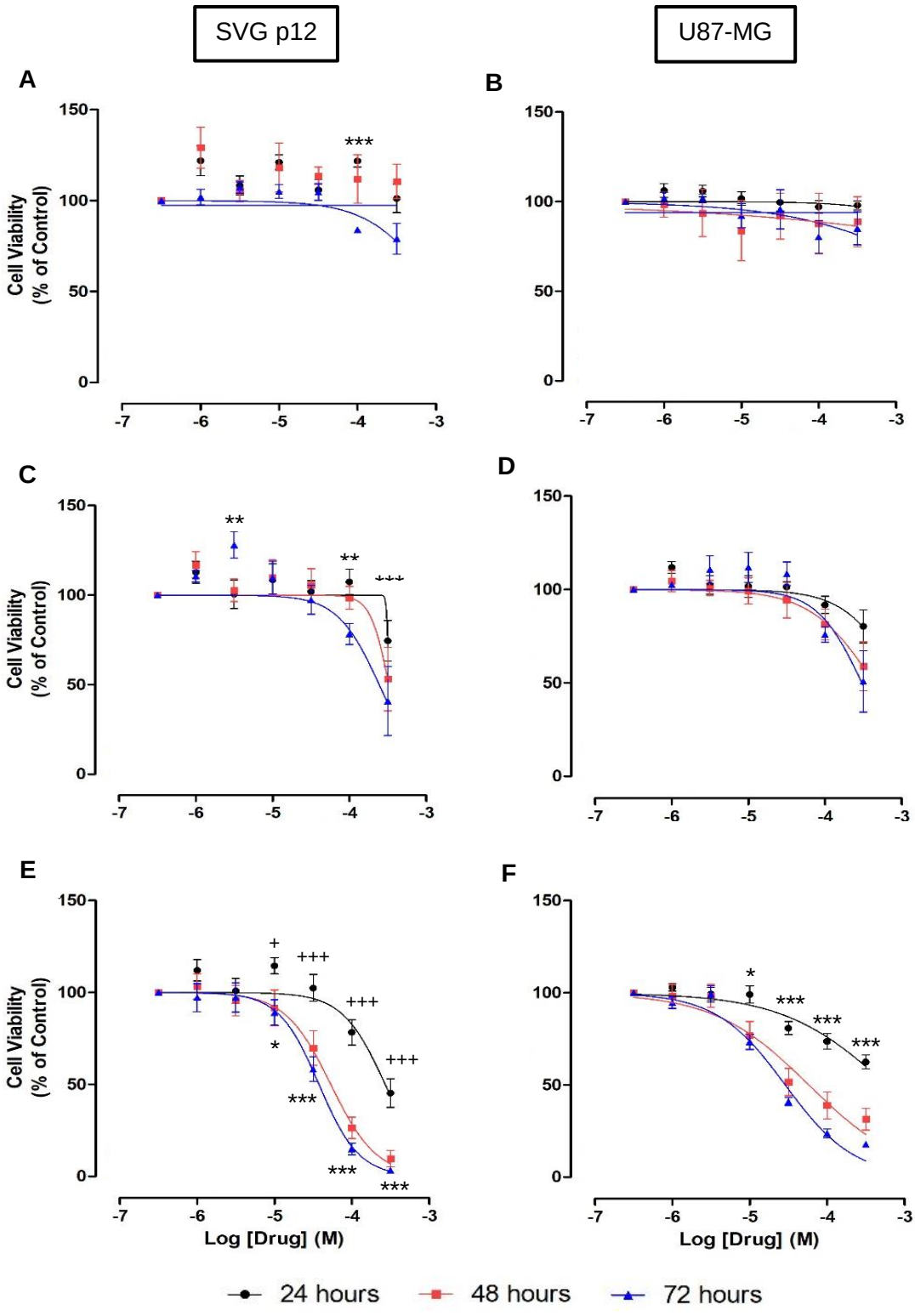

Figure 3.4: Comparison of the effects of olaparib (A, B), temozolomide (C, D) and cisplatin (E, F) on cell viability measured by PrestoBlue® assay under normoxia. Concentration- and time-dependent changes after drug treatment in both SVG p12 (A, C, E) and U87-MG (B, D, F) cell lines in normoxia (21% O_2). Data obtained from the mean±SEM of five consecutive independent repeats. Significant differences are shown within each drug treatment: 24-hours compared to 48-hours (+), 24-hours compared to 72-hours (*).

	Olaparib			Temozolomide			Cisplatin		
	24	48	72	24	48	72	24	48	72
SVG p12	n/a	n/a	*0.0μM*	n/a	327.4μM	244.5μM	270.3μM	53.4μM	37.6μM
U87-MG	*15.0mM*	*5.5M*	*8.0mM*	977.6μM	438.6μM	303.6μM	592.4μM	58.1μM	28.8μM

Table 3.1: IC_{50} values for olaparib, temozolomide and cisplatin following 24-, 48-, and 72-hours of treatment in normoxia. Data represent an average of five experiments. ANOVA with a Bonferroni's post hoc test (p<0.05) was performed to show significance. Some of the values, indicated in italics, have been predicted by extrapolation from the GraphPad Prism software.

	Olaparib			Temozolomide			Cisplatin		
	24	48	72	24	48	72	24	48	72
SVG p12	n/a	n/a	*355.1μM*	316.0μM	241.6μM	123.1μM	134.5μM	25.3μM	19.5μM
U87-MG	*4.6mM*	*16.5mM*	*0.0μM*	397.1μM	153.9μM	144.5μM	108.3μM	12.3μM	9.3μM

Table 3.2: IC_{25} values for olaparib, temozolomide and cisplatin following 24-, 48-, and 72-hours of treatment in normoxia. Data represent an average of five experiments. ANOVA with a Bonferroni's post hoc test (p<0.05) was performed to show significance. Some of the values, indicated in italics, have been predicted by extrapolation from the GraphPad Prism software.

3.2.2 Effects on Cell Viability in Hypoxia

The results show that olaparib had little effect overall on cell viability at 24-, 48-, and 72-hours in SVG p12 and U87-MG cells under hypoxia, apart from at 72-hours in SVG p12 cells, compared to 24-hours, showed a significant decrease in cell viability (Fig.3.5A), at 0.01 mM, 0.03 mM (p<0.05), 0.1 mM (p<0.001) and 0.3 mM (p<0.01). In U87-MG cells (Fig.3.5B) the greatest significant difference was observed again at 72-hours after olaparib treatment, in comparison to 24-hours, at concentrations of 0.1 mM and 0.3 mM (p<0.01).

In SVG p12 cells, the greatest significant difference was observed at 72-hours in comparison to 24-hours following treatment with TMZ (Fig.3.5C), at concentrations of 0.01 mM, 0.03 mM (p<0.01), 0.1 mM and 0.3 mM (p<0.001). 48-hours post-treatment compared to 72-hours showed no significant differences (p>0.05). Similarly, TMZ in U87-MG cells caused the largest significant decrease at 72-hours compared to 24-hours (Fig.3.5D) at concentrations of 0.3 mM (p<0.01). No significant difference (p>0.05) was observed 24-hours post-TMZ treatment when compared to 48-hours, and also when 48-hours post-treatment was compared to 72-hours (p>0.05). No significant differences (p>0.05) were observed between the SVG p12 and U87-MG cells at any time-point.

Following cisplatin treatment, a significant decrease in viability of SVG p12 cells was observed at 72-hours in comparison to 24-hours (22.7 μM vs. 256.2 μM) (Fig.3.5E), at concentrations of 0.01 mM, 0.03 mM, 0.1 mM and 0.3 mM (p<0.001). No significant difference was seen when comparing 72-hours with 48-hours post-cisplatin treatment (p>0.05). In the U87-MG cell line, the largest significant decrease in cell viability was observed at 72-hours after drug treatment compared to 24-hours (21.6 μM vs. 318.2 μM) (Fig.3.5F), at concentrations of 0.03 mM, 0.1 mM and 0.3 mM (p<0.001). When SVG p12 cells were compared to U87-MG cells, a significant decrease was observed in the U87-MG cells at 24-hours following cisplatin treatment (256.2 μM vs. 318.2 μM) at a concentration of 0.03 mM (p<0.05). No significant difference was observed at the other time-points (p>0.05).

When TMZ was compared to cisplatin treatment in SVG p12 cells (Fig.3.5C, E), the greatest decrease in cell viability was seen 72-hours post-TMZ and cisplatin treatment (142.0 μM vs. 22.7 μM), at concentrations of 0.01 mM, 0.3 mM (p<0.05), 0.03 mM and 0.1 mM (p<0.001). A significant decrease in cell viability was observed at 48-hours post-cisplatin treatment in U87-MG cells compared to 72-hours after TMZ treatment (42.9 μM vs. 209.4 μM) (Fig.3.5D, F). This decrease occurred at concentrations of 0.03 mM, 0.1

mM (p<0.001). A greater significant decrease was also observed at 72-hours post-cisplatin treatment when compared to 72-hours post-TMZ treatment (21.6 μM vs. 209.4 μM) at concentrations of 0.01 mM (p<0.01), 0.03 mM and 0.1 mM (p<0.001).

3.2.3 Comparisons of the Effects on Cell Viability in Normoxia and Hypoxia

Olaparib observed to have a similar efficacy on cell viability in both cell lines when normoxia was compared to hypoxia. In the SVG p12 cell line, the largest significant difference was observed at 24-hours after treatment, when normoxia was compared to hypoxia; this was at concentrations of 0.03 mM (p<0.01) and 0.3 mM (p<0.05). No significant difference was seen when comparing 48- and 72-hours after treatment, in the SVG p12 cells (p>0.05) (Fig.3.4A and Fig.3.5A). In the U87-MG cells, no significant difference was observed at 24-, 48- nor 72-hours.

No significant differences were observed in cell viability following TMZ and cisplatin treatment at 24-, 48-, or 72-hours in SVG p12 or U87-MG cells when the two conditions were compared (p>0.05).

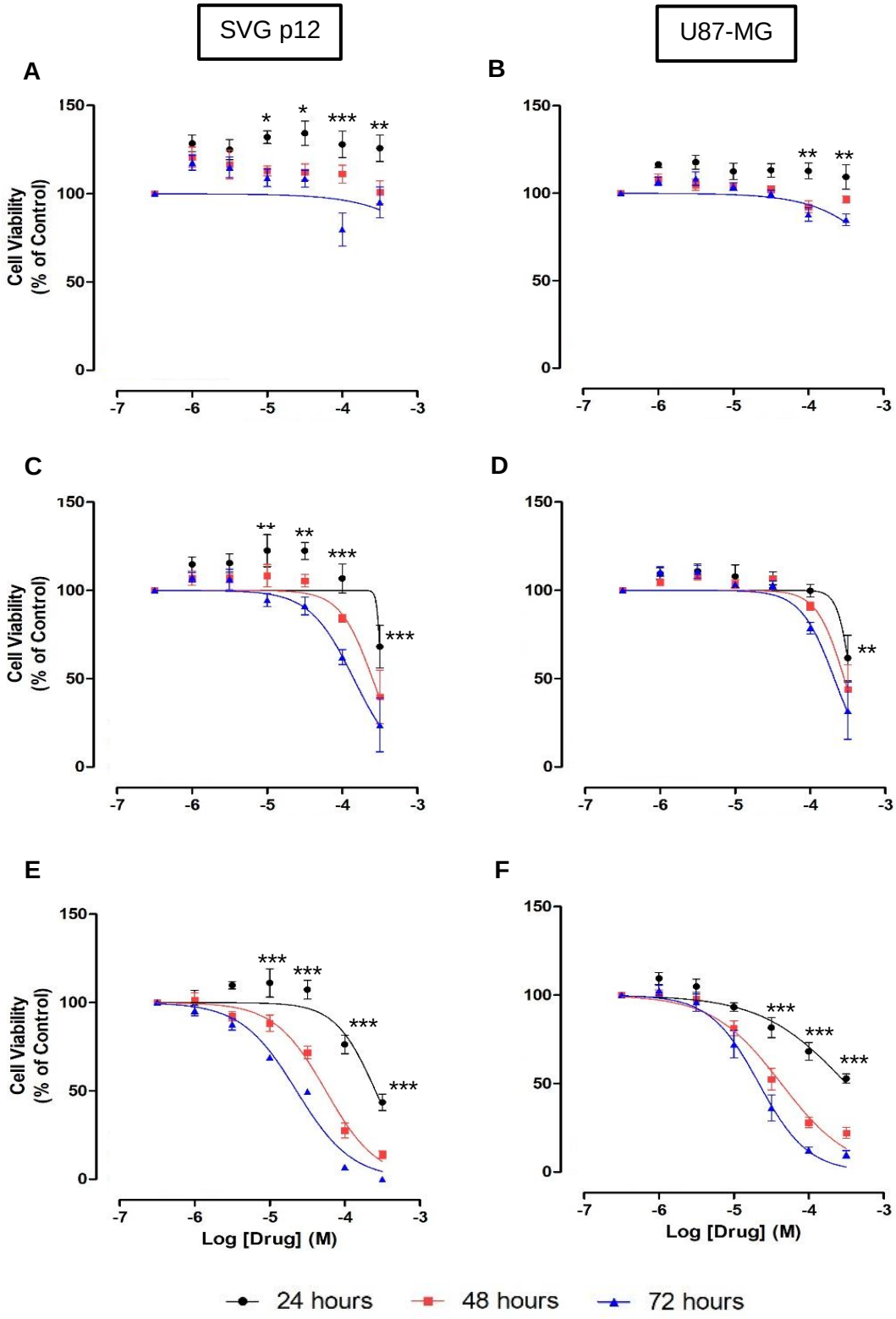

Figure 3.5: Comparison of the effects of olaparib (A, B), temozolomide (C, D) and cisplatin (E, F) on cell viability measured by PrestoBlue® assay under hypoxia. Concentration- and time-dependent changes after drug treatment in both SVG p12 (A, C, E) and U87-MG (B, D, F) cell lines in hypoxia (1% O_2). Data obtained from the mean±SEM of five consecutive independent repeats. Significant differences are shown within each drug treatment: 24-hours compared to 72-hours (*).

	Olaparib			Temozolomide			Cisplatin		
	24	48	72	24	48	72	24	48	72
SVG p12	n/a	n/a	n/a	n/a	252.9μM	142.0μM	256.2μM	55.9μM	22.7μM
U87-MG	n/a	n/a	*1.8mM*	348.7μM	284.7μM	209.4μM	318.2μM	42.9μM	21.6μM

Table 3.3: IC_{50} values for olaparib, temozolomide and cisplatin following 24-, 48-, and 72-hours of treatment in hypoxia. Data represent an average of five experiments. ANOVA with a Bonferroni's post hoc test (p<0.05) was performed to identify significance. Some of the values, indicated in italics, have been predicted by extrapolation from the GraphPad Prism software.

	Olaparib			Temozolomide			Cisplatin		
	24	48	72	24	48	72	24	48	72
SVG p12	n/a	n/a	*1.3mM*	309.8μM	145.6μM	67.4μM	130.2μM	23.5μM	8.9μM
U87-MG	n/a	n/a	*543.3μM*	278.2μM	179.0μM	118.6μM	75.6μM	13.4μM	9.4μM

Table 3.4: IC_{25} values for olaparib, temozolomide and cisplatin following 24-, 48-, and 72-hours of treatment in hypoxia. Data represent an average of five experiments. ANOVA with a Bonferroni's post hoc test (p<0.05) was performed to identify significance. Some of the values, indicated in italics, have been predicted by extrapolation from the GraphPad Prism software.

3.3 *Cell Proliferation*

Based on the IC_{25} values obtained from the cell viability assay, the effect of drug treatment on cell proliferation was investigated *in vitro* under normoxic and hypoxic conditions using CFDA-SE incorporation and flow cytometric analysis. Figure 3.6 shows representative graphs of the right-to-left shift in cell proliferation.

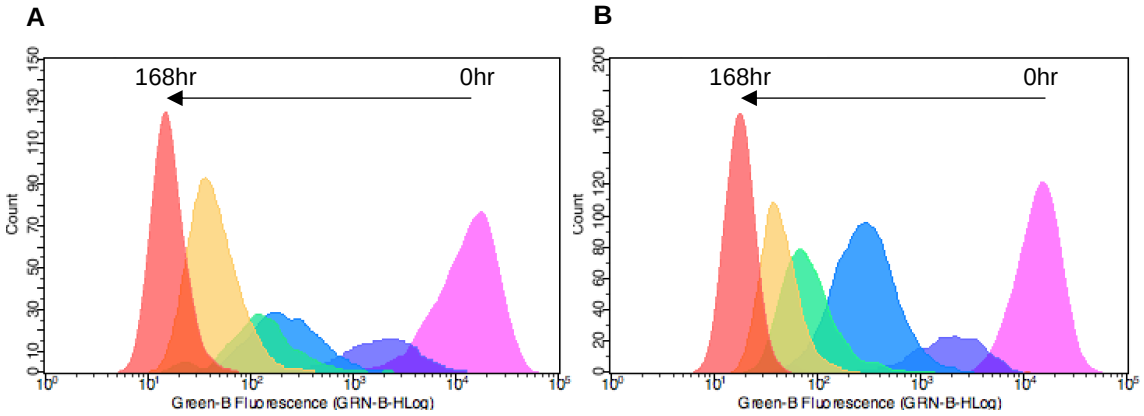

Figure 3.6: Original representative graphs showing the right-to-left in cell proliferation of U87-MG cells measured by CFDA-SE staining and analysed by flow cytometry. (A) normoxia (21% O_2), (B) hypoxia (1% O_2). These original graphs are typical of 5 different experiments using U87-MG cells.

3.3.1 Effects on Cell Proliferation in Normoxia

In each drug treatment, a time-dependent decrease in CFDA-SE fluorescence was observed under normoxia, indicating proliferation is occurring. In SVG p12 cells, little difference was observed in proliferation at 24-, 144-, and 168-hours between the control and all drug treatments (24h: 47±8% vs. olaparib 46±15%; TMZ 40±6%; cisplatin 46±8%) (144h: 3±1% vs. 3±1%; 4±2%; 4±1%) (168h: 2±1% vs. 0±0%; 2±1%; 1±1%) (Fig.3.7A). However, while TMZ and cisplatin treated cells were similar to the control at 48- and 72-hours, it was observed that olaparib treatment may have slowed proliferation as an increase in CFDA-SE fluorescence was observed (48h: 17±4% vs. 32±12%) (72h: 6±2% vs. 17±5%). However, these effects were not significant (p>0.05).

In U87-MG cells, olaparib caused a significant increase in CFDA-SE fluorescence at 24-hours, when compared to the control treatment (56±15% vs. 24±17%) (p<0.01) (Fig.3.7B). Cisplatin was also observed to cause an increase in fluorescence at 24-hours, compared to the control, though this effect was not significant (p>0.05). A slower rate of proliferation was observed between the control and all drug treatments at 48-hours

(19±7% vs. olaparib 31±10%; TMZ 36±8%; cisplatin 36±17%). While TMZ treated cells were similar to the control at 72-hours, olaparib and cisplatin induced an increase in CFDA-SE fluorescence (8±5% vs. 21±14%; 26±15%). Though these results were not significant (p>0.05).

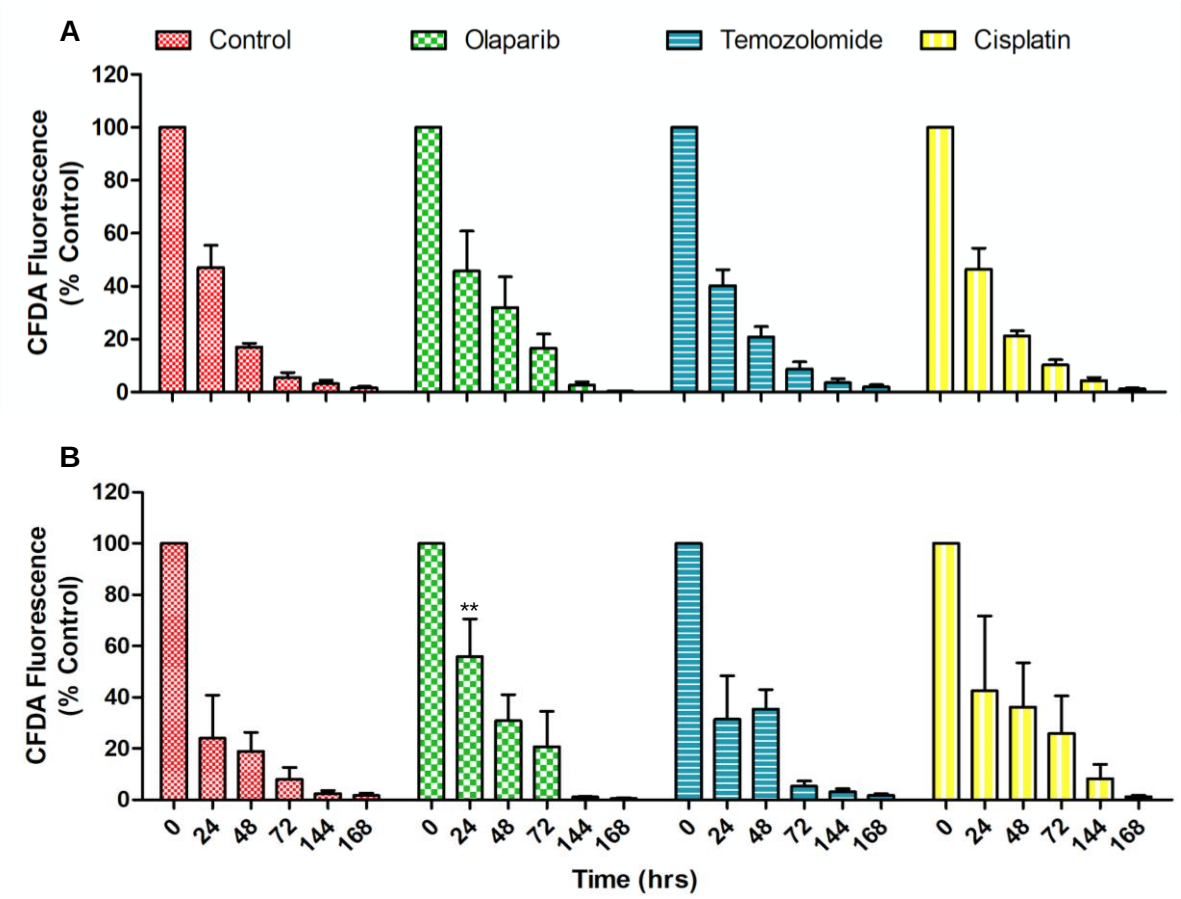

Figure 3.7: Bar charts showing a comparison of the effects of olaparib, temozolomide and cisplatin on cell proliferation measured by CFDA-SE fluorescence under normoxia. CFDA-SE fluorescence presented as a percentage of the respective control after drug treatment in normoxic conditions (21% O_2). (A) SVG p12, (B) U87-MG. Data represent mean±SEM of five independent repeats with significance determined by ANOVA. Significant difference (p<0.05) shown by asterisk (*) is in comparison to the respective control.

3.3.2 Effects on Cell Proliferation in Hypoxia

In hypoxic conditions, for each drug treatment a time-dependent decrease in CFDA-SE fluorescence was observed, signifying that cell proliferation is occurring. In SVG p12 cells, little difference in proliferation was observed at 48-, 72-, 144-, and 168-hours between the non-treated control and all the drug treatments (Fig.3.8A). However, while TMZ-treated SVG p12 cells were similar to the control at 24-hours, olaparib caused an increase in CFDA-SE fluorescence (26±2% vs. 33±7%), though this effect was not significant (p>0.05). Cisplatin produced a significant increase at 24-hours (39±8%) (p<0.05), when compared to the control. At 24-hours, a significant increase in fluorescence was also observed between cisplatin and TMZ treatment (39%±8% vs. 26±3%) (p<0.05).

In U87-MG cells, little difference was observed in proliferation at 144- and 168-hours between the non-treated control and all drug treatments (144h: 1±0% vs. olaparib 1±0%; TMZ 1±1%; cisplatin 2±1%) (168h: 1±0% vs. 1±0%; 1±0%; 1±0%) (Fig.3.8B). Olaparib was observed to cause a decrease in CFDA-SE fluorescence at 24-hours, when compared to the control (20±10% vs. 28±15%), though this effect was not significant (p>0.05). While olaparib treated cells were similar to the control at 48- and 72-hours, TMZ caused an increase in fluorescence at 48-hours (11±4% vs. 17±5%) and cisplatin caused an increase at 48- and 72-hours (48h: 17±5%) (72h: 4±3% vs. 11±8%).

3.3.3 Comparisons on Cell Proliferation in Normoxia and Hypoxia

Olaparib was observed to have similar efficacy overall on cell proliferation in both cell lines under hypoxia compared to normoxia. A significant effect was seen in the olaparib treated U87-MG cells in hypoxia, compared to normoxia. Though, the highest difference was present at 24-hours post-treatment (20±10% vs. 56%±15%) (p<0.01).

No significant differences were observed on cell proliferation following TMZ and cisplatin treatment at 24-, 48-, 72-, 144- or 168-hours in SVG p12 or U87-MG cells when the two conditions were compared (p>0.05).

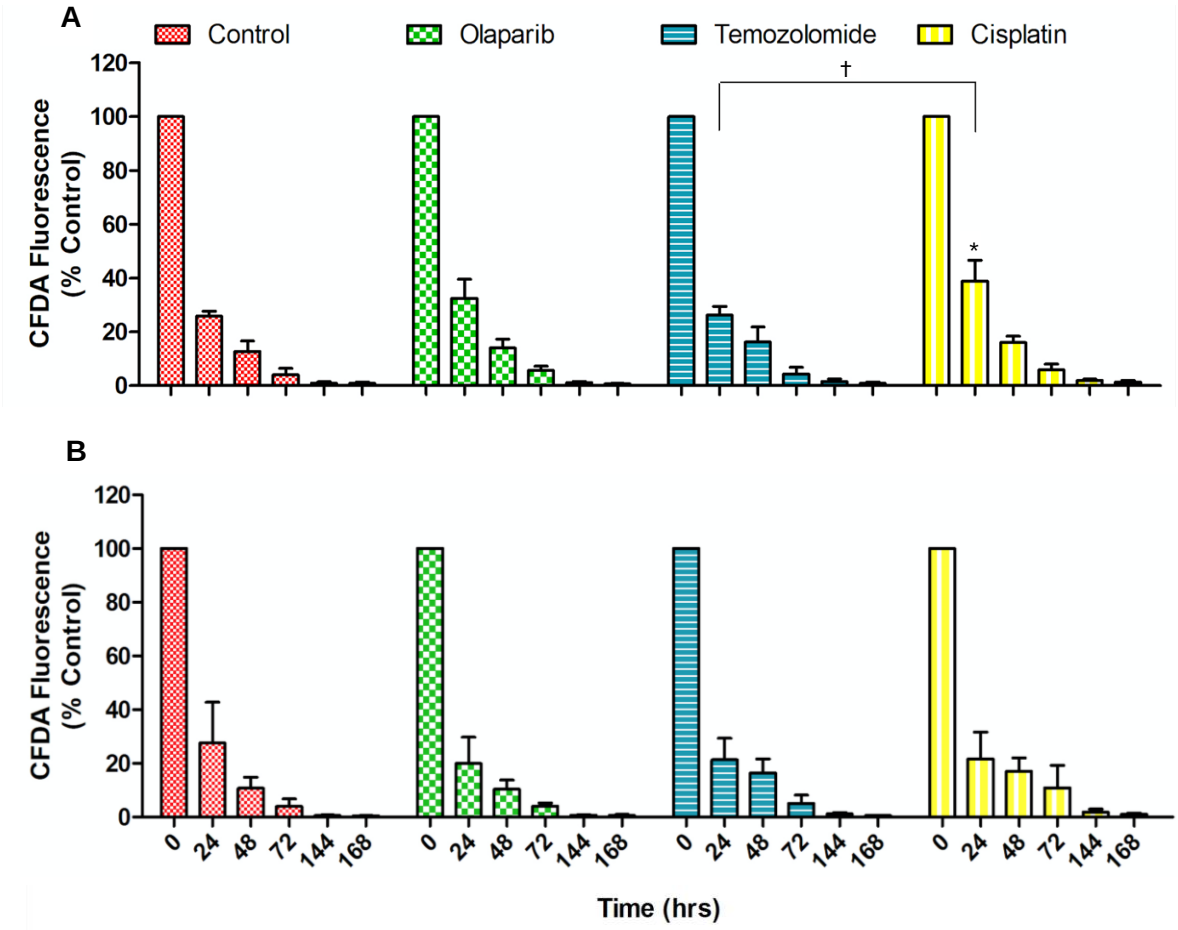

Figure 3.8: Bar charts showing a comparison of the effects of olaparib, temozolomide and cisplatin on cell proliferation measured by CFDA-SE fluorescence under hypoxia. CFDA-SE fluorescence presented as a percentage of the respective control after drug treatment in hypoxic conditions (1% O_2). (A) SVG p12, (B) U87-MG. Data represent mean±SEM of five independent repeats with significance determined by ANOVA. Significant difference (p<0.05) shown by the asterisk (*) is in comparison to the respective control, and † denotes significance between drug treatments.

3.4 *Cell Cycle Analysis*

Based on the IC_{25} values obtained from the cell viability assay, the effect of drug treatment on cell cycle arrest was investigated *in vitro* under normoxic and hypoxic conditions using PI incorporation and flow cytometric analysis. Figure 3.9 represents illustrative graphs of cell cycle arrest for the three drug treatments.

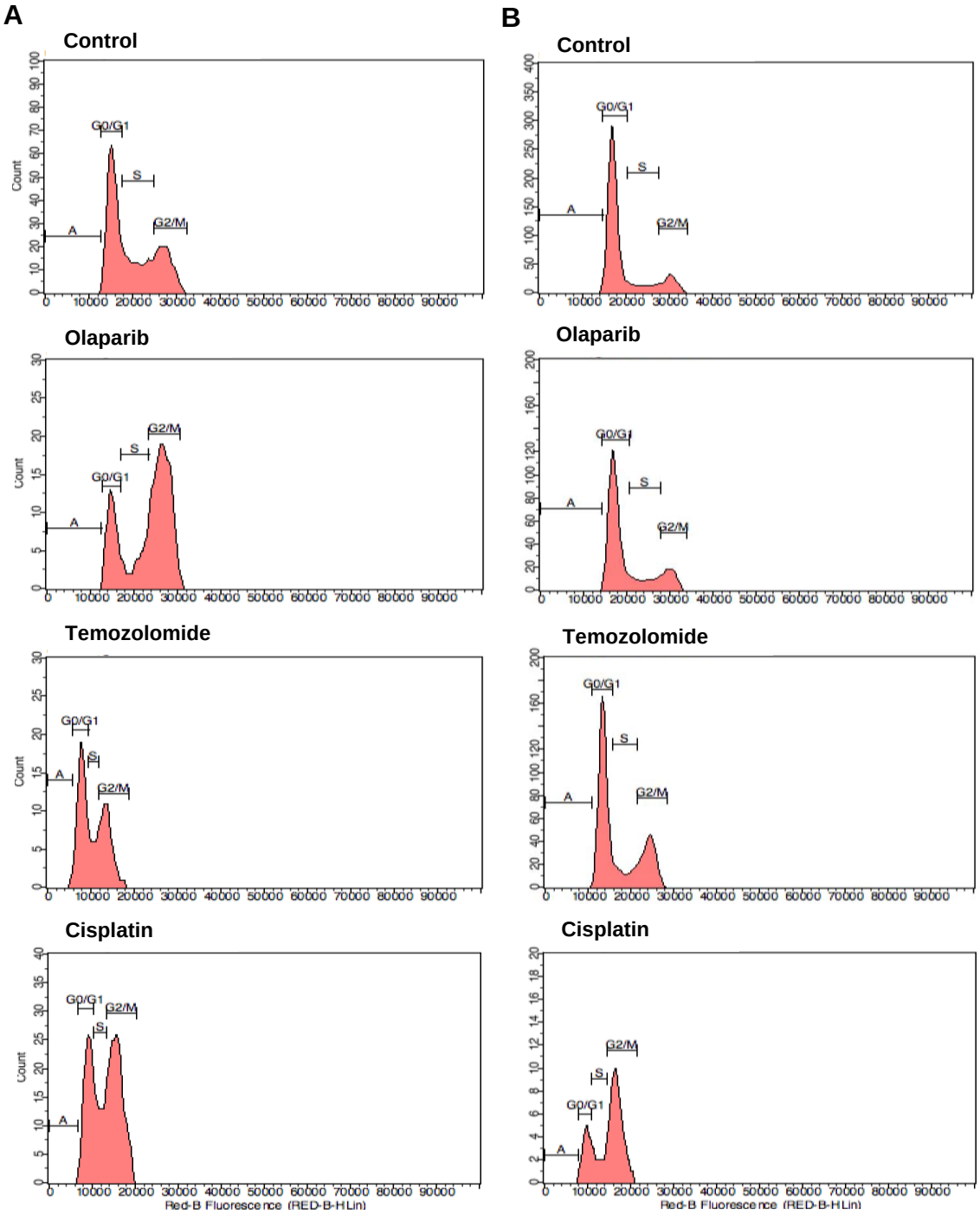

Figure 3.9: Original representative graphs of cell cycle distribution for each treatment in U87-MG cells measured by PI staining and analysed by flow cytometry. (A) normoxia (21% O_2), (B) hypoxia (1% O_2). Graphs are typical of 5 such different experiments.

3.4.1 Cell Cycle Analysis in Normoxia

The control and all three of the drug treatments caused the SVG p12 and U87-MG cells to arrest during one of the four phases of the cell cycle. Even though many statistically significant differences were not observed, variances between the four treatments were present in normoxia (Fig.3.10).

In SVG p12 cells, a decrease in the proportion of cells in the G0/G1 phase of the cell cycle was observed following drug treatment with olaparib (28±6%) and TMZ (29±3%) when compared to control (42±4%), although these differences were not significant (p>0.05) (Fig.3.10A). In contrast, cisplatin treatment had no effect on the proportion of cells in G0/G1 (42±10%), compared to control. Interestingly, following 48-hours of drug treatment, no change in the proportion of cells found in S phase of the cell cycle was observed when compared to control. Changes were observed in G2/M phase, where in comparison to control (42±5%), both TMZ (50±9%) and olaparib (53±9%) increased the population size, however, the data were not significant. Interestingly, cisplatin (34±12%) decreased the proportion of cells in G2/M phase compared to the control, but it did increase the population undergoing apoptosis (7±4%) when compared to control (3±3%).

In U87-MG cells, a decrease in the population of cells in the G0/G1 phase of the cell cycle was observed following drug treatment with olaparib (33±4%) (p<0.05), TMZ (40±7%) and cisplatin (38±4%), when compared to the control (51±5%) (Fig.3.10B). No real change was observed in the proportion of cells found in the S phase for all drug treatments when compared to the control. An increase was observed in the proportion of cells in the G2/M phase following 48-hours of treatment with olaparib (50±6%) (p<0.001), TMZ (37±10%) and cisplatin (39±5%) when compared to the control (28±6%).

When compared to the non-treated control, all drug treatments appeared to cause cell cycle arrest during the G2/M phase in both cell lines, apart from cisplatin in the SVG p12 cells. Overall, olaparib induced the greatest effect in both cell lines compared to TMZ and cisplatin.

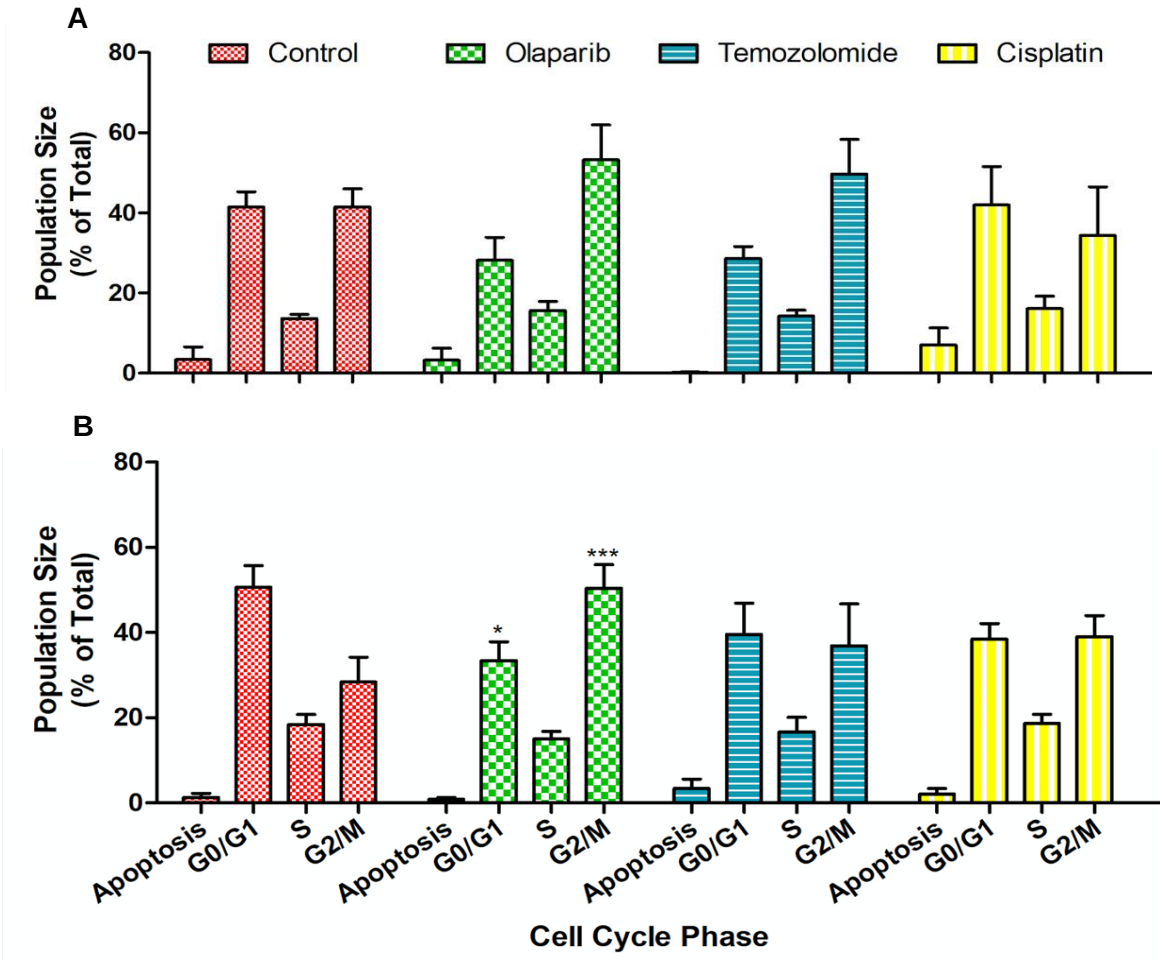

Figure 3.10: Bar charts show comparisons of olaparib, temozolomide and cisplatin on cell cycle arrest measured by PI fluorescence under normoxia. Cell cycle arrest analysis are presented as a percentage of the respective control following 48-hours after drug treatment in normoxic conditions (21% O_2). (A) SVG p12, (B) U87-MG. Data represent mean±SEM of five consecutive independent repeats with significance determined by ANOVA. Significant differences (p<0.05) shown by the asterisks (*) is in comparison to the respective control.

3.4.2 Cell Cycle Analysis in Hypoxia

Various differences of the control treatment and the drug treatments in the SVG p12 and U87-MG cells on cell cycle arrest were observed following 48-hours of drug treatment in hypoxic conditions.

In SVG p12 cells, a decrease in cell cycle analysis was observed in the population of cells in the G0/G1 phase of the cell cycle following drug treatment with olaparib (32±7%), TMZ (37±3%) and cisplatin (31±12%) when compared to the control (42±4%), although these differences were not significant (p>0.05) (Fig.3.11A). A decrease in the G2/M population was observed following TMZ treatment (35±11%) when compared to the control (46±7%). In contrast, no effect was observed on the proportion of cells in G2/M after treatment with olaparib (49±16%) and cisplatin (48±18%), when compared to the control. Changes were observed in apoptosis, where in comparison to the control (0±0%), both olaparib (6±6%) and TMZ (5±5%) increased the population size, although non-significantly.

In the U87-MG cells, a decrease in the proportion of cells in the G0/G1 phase of the cell cycle was observed following olaparib (58±11%), TMZ (54±8%) and cisplatin (30±6%) (p<0.001) treatments, when compared to the control (65±3%) (Fig.3.11B). A small decrease was also observed in the population of cells in the S phase following treatment with olaparib (14±1%) and TMZ (15±2%), compared to the control (17±1%). Changes were observed in the G2/M phase, where in comparison to control (18±2%), olaparib (28±11%), TMZ (28±11%) and cisplatin (50±8%) (p<0.01) increased the population size. Interestingly, only cisplatin (4±3%) increased the apoptotic population of cells, compared to control (0±0%), although the data were not significant. A significant decrease was observed in the proportion of U87-MG cells in the G0/G1 phase following treatment with cisplatin (30±6%), in comparison to olaparib (58±11%) (p<0.01) and TMZ (54±8%) (p<0.05).

All drug treatments induced cell cycle arrest in the G2/M phase in SVG p12 and U87-MG cells, with the exception of TMZ in SVG p12 cells.

3.4.3 Comparisons of Cell Cycle Distribution in Normoxia and Hypoxia

When comparing the two conditions, it was observed that the results were quite similar, with cell cycle arrest in the G2/M phase seeming to be the main effect of drug treatment. In contrast to cell viability, olaparib was similar in efficacy to TMZ and cisplatin treatments. In addition to cell cycle arrest, some results indicate the induction of apoptosis, following 48-hours of drug treatment with IC_{25} concentrations.

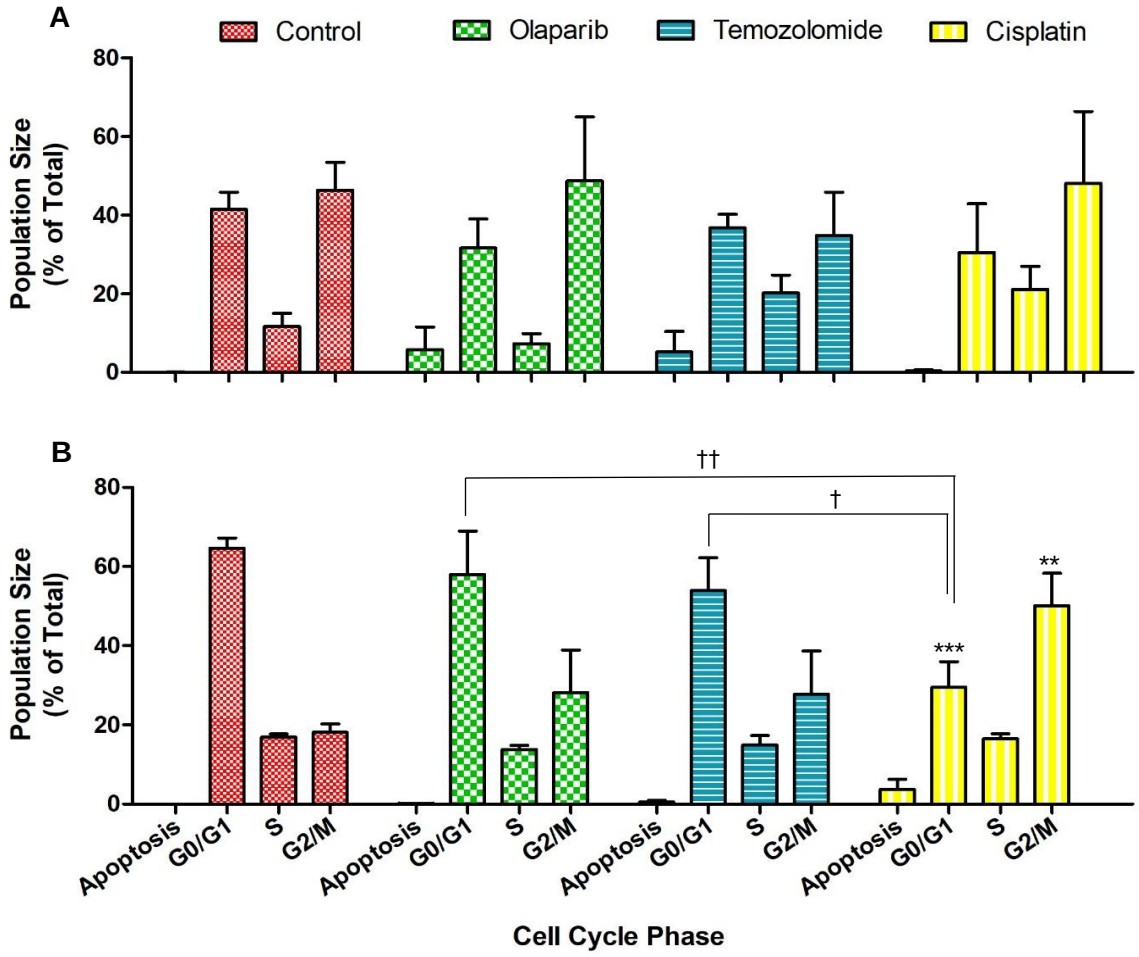

Figure 3.11: Bar charts showing comparisons of olaparib, temozolomide and cisplatin on cell cycle arrest measured by PI fluorescence under hypoxia. Cell cycle arrest analysis presented as a percentage of the respective control following 48-hours after drug treatment in hypoxic conditions (1% O_2). (A) SVG p12, (B) U87-MG. Data represent mean±SEM of five consecutive independent repeats with significance determined by ANOVA. Significant differences (p<0.05) shown by the asterisks (*) is in comparison to the respective control, and † denotes significance between drug treatments.

3.5 *Apoptosis Assay*

Using the IC_{50} values of the three drug treatments (Table 3.1 and 3.3) obtained from the cell viability assay, detection of apoptosis based on the changes that occur in the permeability of cell membranes was investigated *in vitro*, under normoxic and hypoxic conditions using PI and Annexin V incorporation and flow cytometric analysis. Figure 3.12 illustrates representative graphs of apoptotic analysis.

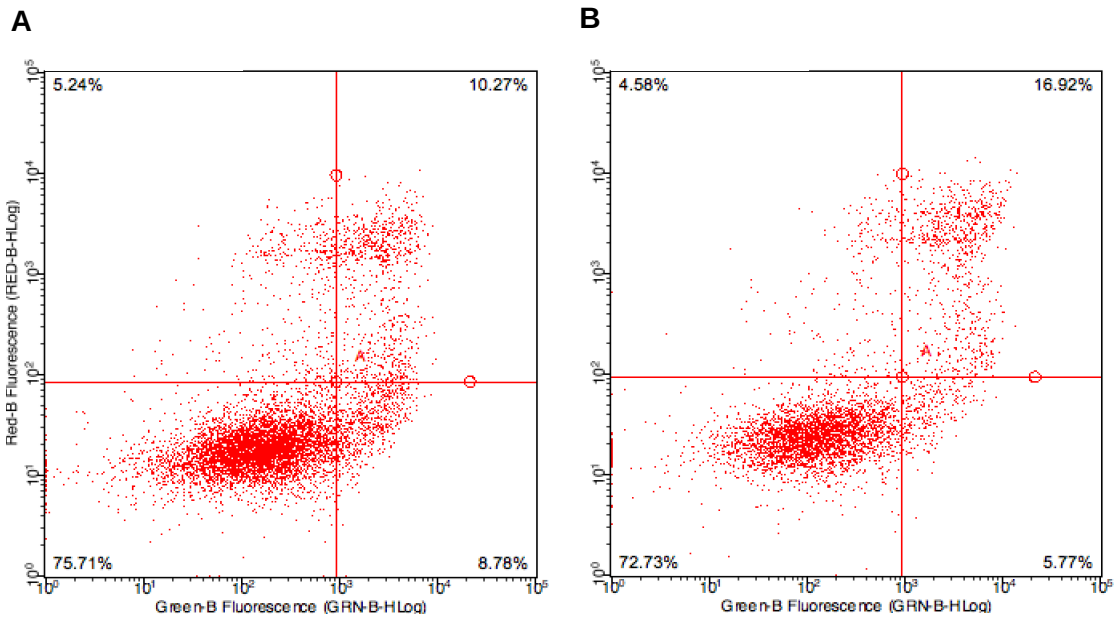

Figure 3.12: Original representative graphs of apoptosis analysis for cisplatin treatment in U87-MG cells measured by PI and Annexin V staining and analysed by flow cytometry. (A) normoxia (21% O_2), (B) hypoxia (1% O_2). Graphs are typical of 5 such different experiments.

3.5.1 <u>Detection of Apoptosis in Normoxia</u>

Across each timepoint, neither olaparib nor TMZ had any effect on apoptosis in SVG p12 cells when compared to control (Fig.3.13A, B, C). For example, at 72-hours, the proportion of live (37±5%) versus apoptotic (44±6%) cells in control was similar to that following treatment with olaparib (33±3% and 48±7%, respectively) and TMZ (33±5% and 44±11%, respectively). In contrast, cisplatin increased the proportion of apoptotic cells (55±10% at 24-hours, 70±3% at 48-hours and 63±1% at 72-hours) over time in comparison to control (51±10%; 62±4%; 44±6%), with a significant increase at 72-hours (p<0.05). While a small increase in the proportion of apoptotic cells was observed

following treatment with the combination of olaparib and TMZ (57±10% at 24-hours, 68±3% at 48-hours and 55±7% at 72-hours) compared to control (51±10% at 24-hours, 62±4% at 48-hours and 44±6% at 72-hours), the most significant effect was with the combination of olaparib and cisplatin, with apoptotic populations significantly increased compared to control at 48- (74±3%) (p<0.05) and 72-hours (66±2%) (p<0.01).

A similar pattern of effect was observed in U87-MG cells (Fig.3.14A, B, C), however there was little effect of the drug treatments at 24-hours. Cisplatin (23±3%), olaparib and TMZ (23±3%) and olaparib and cisplatin (22±3%) increased the population of apoptotic cells at 48-hours, when compared to the control (16±2%). Significant changes were observed at 72-hours for cisplatin alone and when combined with olaparib. A significant decrease was observed in the population of live cells following drug treatment with cisplatin (70±3%) (p<0.001) and olaparib and cisplatin combined (72±2%) (p<0.01), in comparison to the control (83±2%). In contrast, a significant increase in the proportion of apoptotic cells was observed following cisplatin (24±4%) (p<0.01) and olaparib and cisplatin combined (22±3%) (p<0.05) compared to the control (13±1%).

The population of live U87-MG cells significantly decreased following drug treatment with cisplatin (70±3%), in comparison to olaparib (81±1%) and TMZ (82±2%) (p<0.01). A significant increase was also observed following cisplatin (24±4%) treatment in the apoptotic populations, when compared to olaparib (15±1%) (p<0.05) and TMZ (13±1%) (p<0.01). Similarly, the combination treatment of olaparib and cisplatin (72±2%) induced a significant decrease in the proportion of live cells, compared to olaparib (81±1%) (p<0.05). Essentially, cisplatin was more effective than either olaparib or TMZ as a monotherapy.

When SVG p12 cells were compared to U87-MG cells, a similar pattern was observed where the same drug treatments were effective in both cell lines. A higher proportion of apoptosis was observed in the non-treated control in SVG p12 cells compared to U87-MG cells.

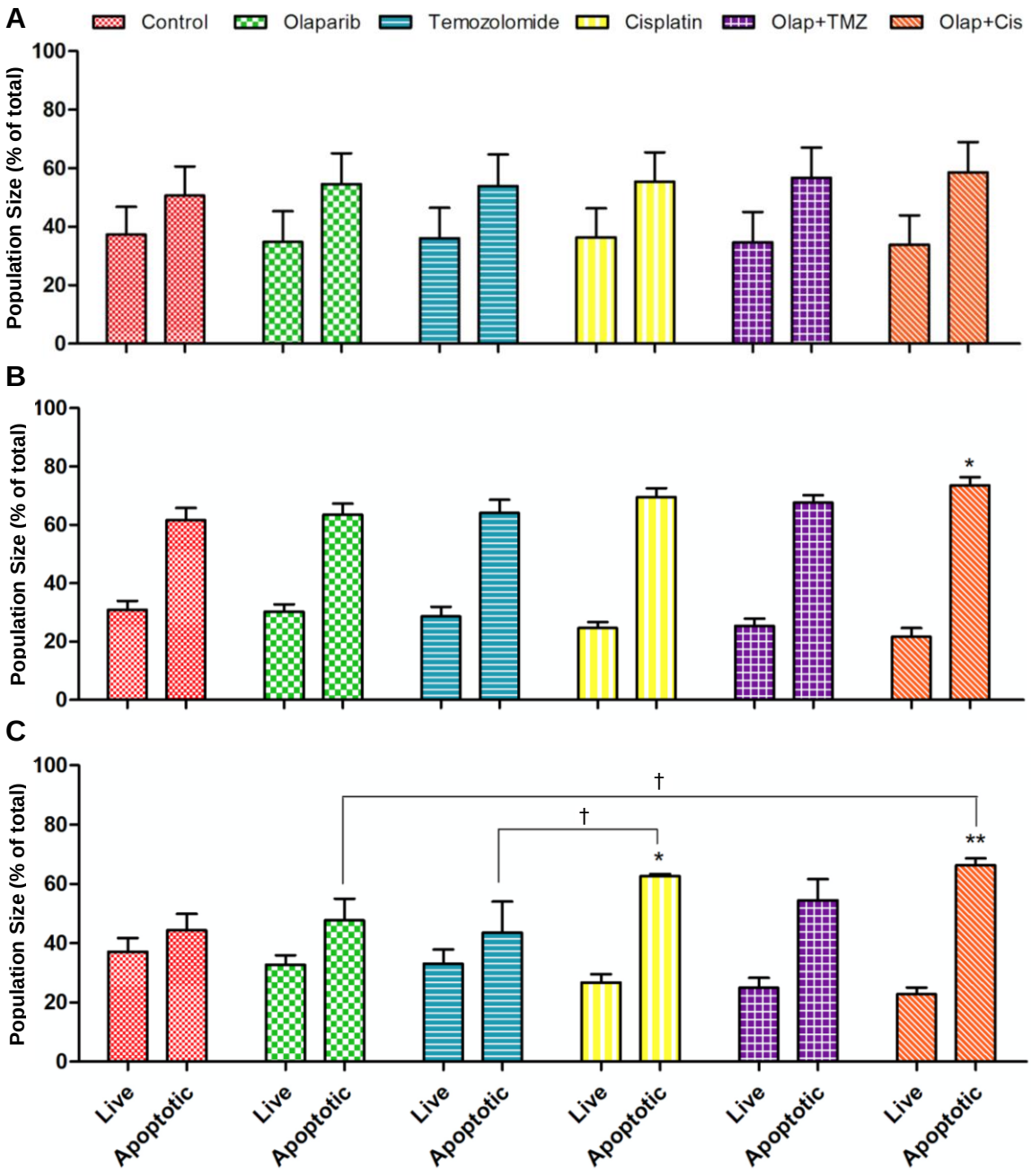

Figure 3.13: Bar charts showing comparisons of various drug treatments on the effects of apoptosis measured by PI and Annexin V fluorescence under normoxia in SVG p12 cells. Apoptotic analysis presented as a percentage of the total following (A) 24-, (B) 48-, and (C) 72-hours after single/combined drug treatment in normoxia (21% O_2). Data represent mean±SEM of five independent repeats with significance determined by ANOVA. Significant differences (p<0.05) shown by the asterisks (*) is in comparison to the respective control, and † denotes significance between drug treatments.

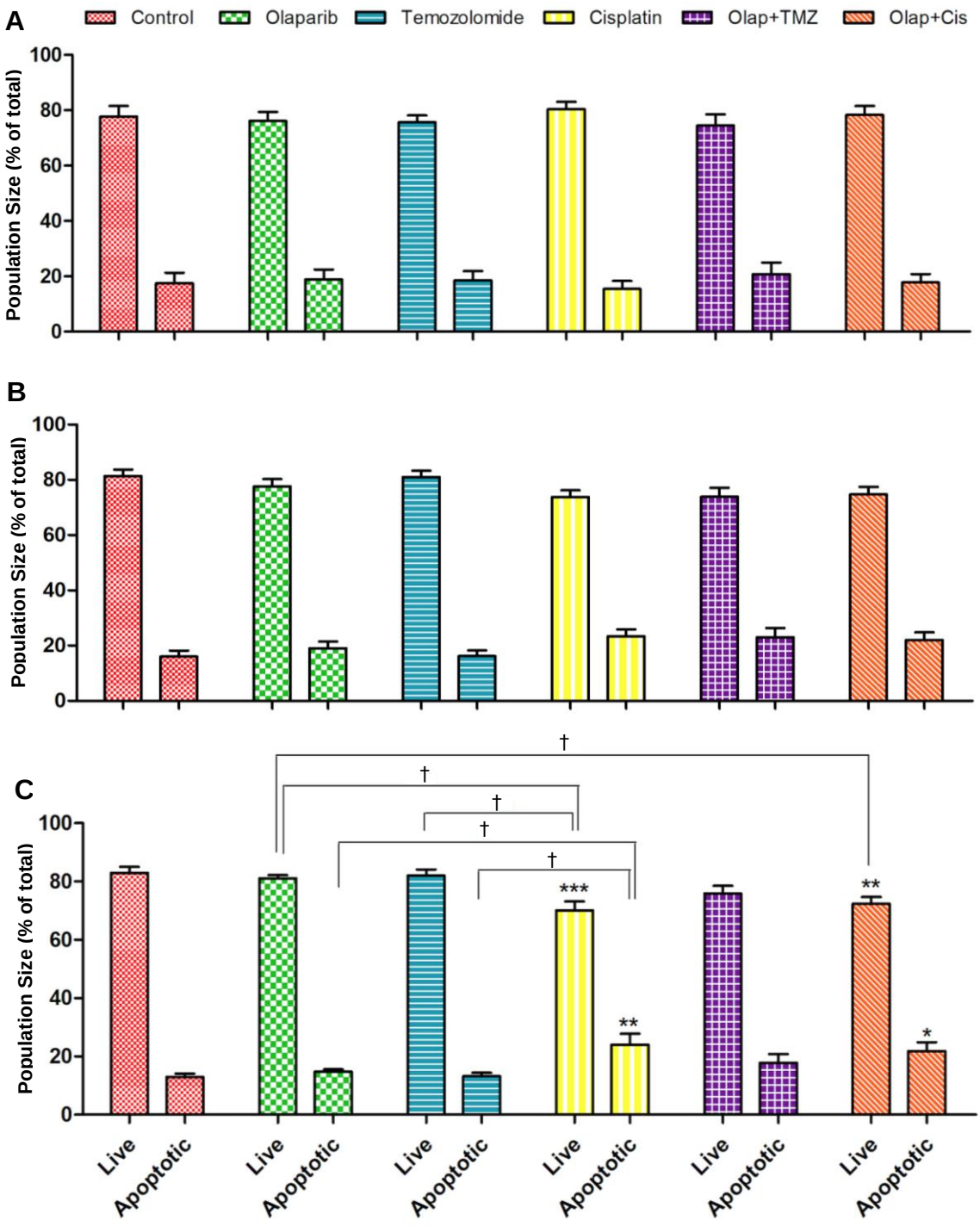

Figure 3.14: Bar charts showing comparisons of various drug treatments on the effects of apoptosis measured by PI and Annexin V fluorescence under normoxia in U87-MG cells. Apoptotic analysis presented as a percentage of the total following (A) 24-, (B) 48-, and (C) 72-hours after single/combined drug treatment in normoxia (21% O_2). Data represent mean±SEM of five independent repeats with significance determined by ANOVA. Significant differences (p<0.05) shown by the asterisks (*) is in comparison to the respective control, and † denotes significance between drug treatments.

3.5.2 Detection of Apoptosis in Hypoxia

A similar pattern was observed in SVG p12 cells as in normoxia. However, combination treatments had the largest effect and were most consistent, as well as cisplatin. While the other drug treatments had little effect at 24-hours (Fig.3.15A), the combination treatment with olaparib and cisplatin (58±4%) caused a significant increase in the apoptotic population compared to the control (44±5%) (p<0.05). Cisplatin (63±4%) (p<0.05), olaparib and TMZ combined (63±3%) (p<0.05) and olaparib and cisplatin combined (65±3%) (p<0.01) all induced a significantly increased proportion of apoptotic cells at 48-hours, in comparison to the control (52±3%) (Fig.3.15B). Interestingly, all drug treatments were effective at 72-hours compared to the non-treated control, though not all were significant (Fig.3.15C). The population of apoptotic cells following treatment with cisplatin (62±4%) (p<0.05), olaparib and TMZ combined (66±3%) (p<0.01) and olaparib and cisplatin combined (64±2%) (p<0.05) caused a significant increase, compared to the control (49±8%). The combination treatment of olaparib and TMZ also caused a significant increase in the proportion of apoptotic cells at 72-hours when compared to olaparib (54±3%) (p<0.05).

In the U87-MG cells, again no change was observed at 24-hours following drug treatment. Only cisplatin and olaparib and cisplatin combined induced any effect at 48- and 72-hours, although, no significant differences were present between them (p>0.05).

When comparing the cell lines, the same results that were obtained in normoxia were observed in hypoxia; with similar patterns for all drug treatments and the proportion of apoptotic cells observed for the non-treated control was higher in SVG p12 cells.

3.5.3 Comparisons of Apoptosis in Normoxia and Hypoxia

Cisplatin was observed to be the most consistent monotherapy with similar efficacy in both conditions, although not significant in U87-MG cells in hypoxia at 72-hours. The combination treatments were the most effective, though again without significance in the U87-MG cells under hypoxia.

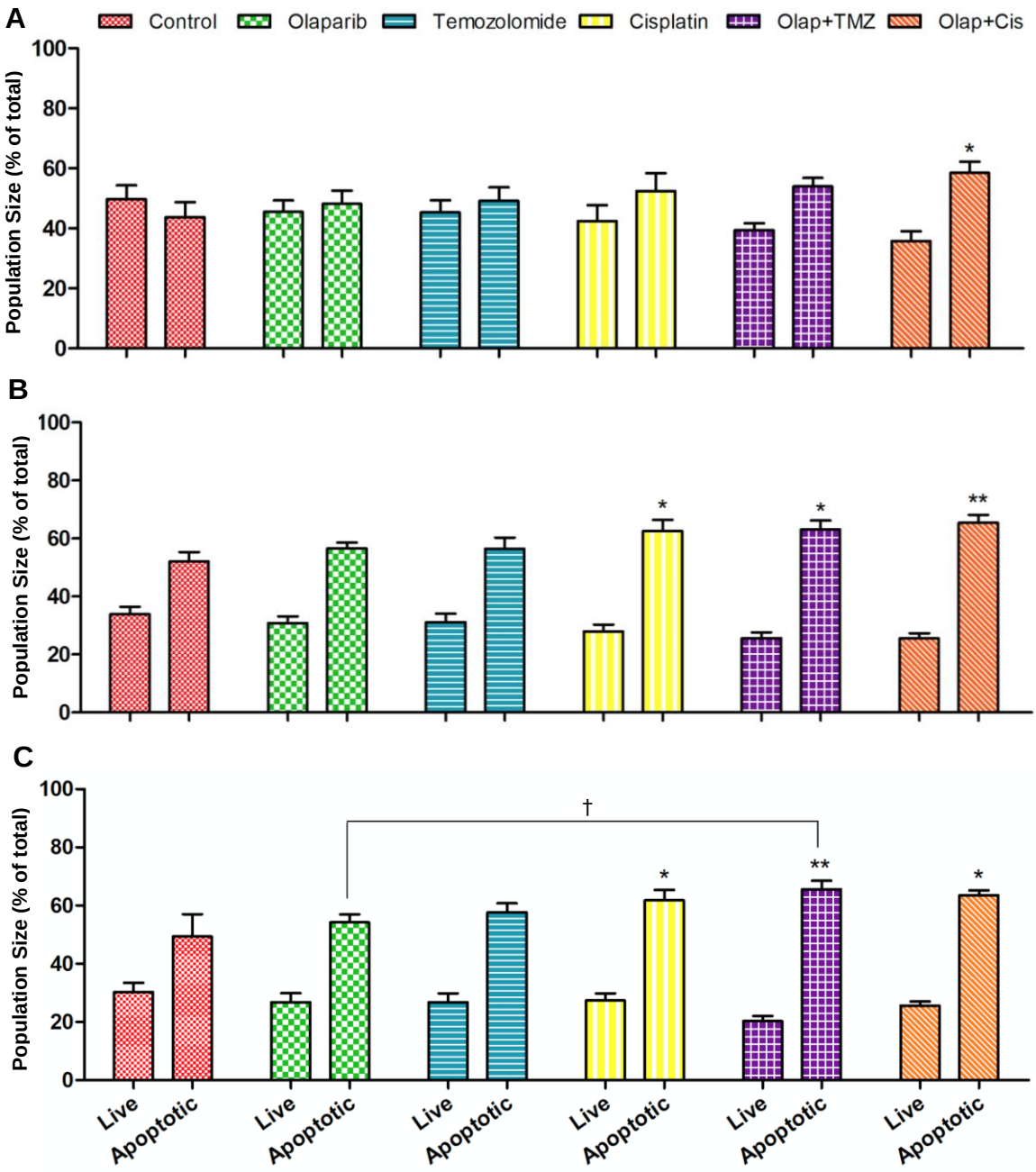

Figure 3.15: Bar charts showing comparisons of various drug treatments on the effects of apoptosis measured by PI and Annexin V fluorescence under hypoxia in SVG p12 cells. Apoptotic analysis presented as a percentage of the total following (A) 24-, (B) 48- and (C) 72-hours after single/combined drug treatment in hypoxia (1% O_2). Data represent mean±SEM of five independent repeats with significance determined by ANOVA. Significant differences (p<0.05) shown by the asterisks (*) is in comparison to the respective control, and † denotes significance between drug treatments.

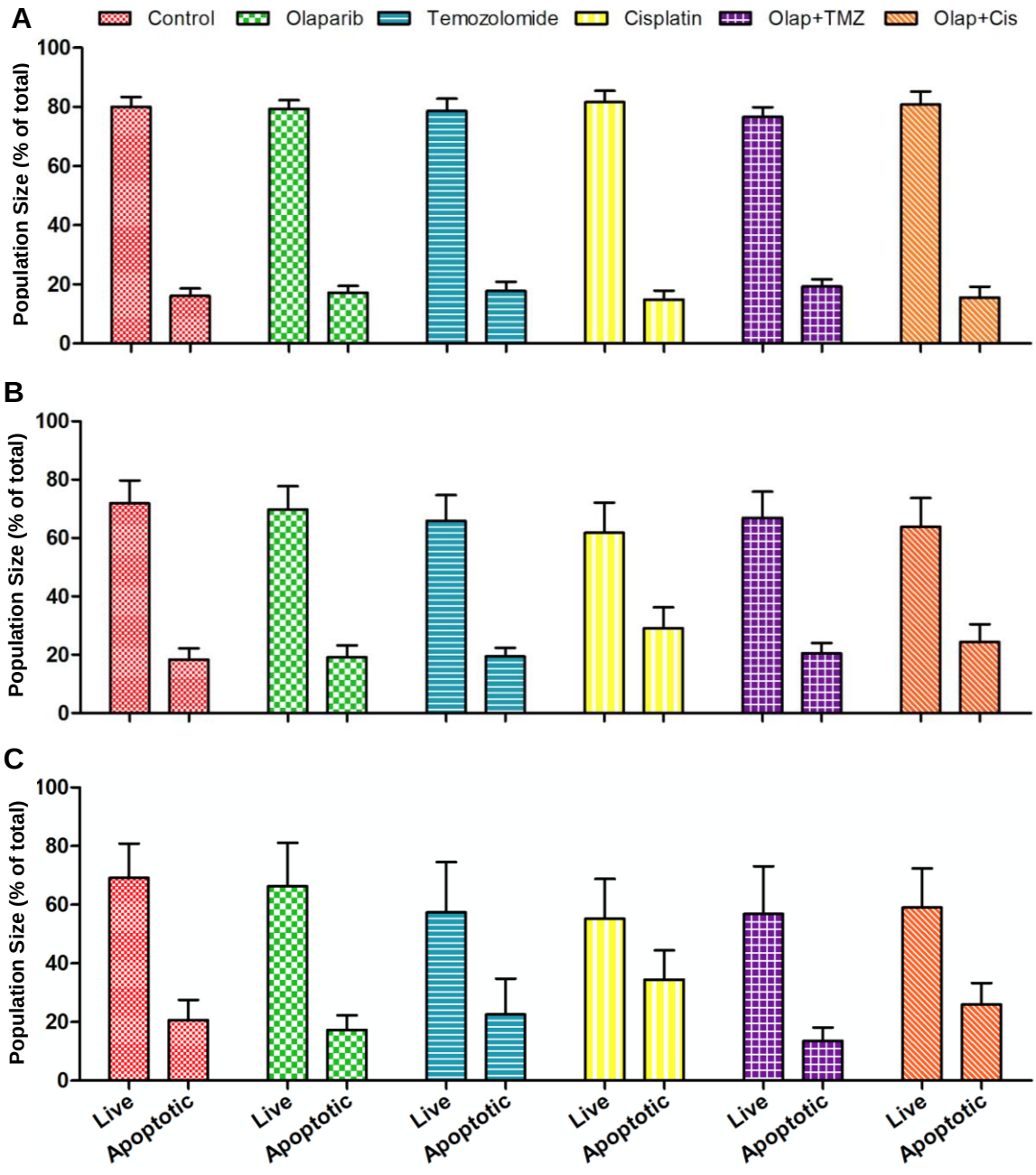

Figure 3.16: Bar charts showing comparisons of various drug treatments on the effects of apoptosis measured by PI and Annexin V fluorescence under hypoxia in U87-MG cells. Apoptotic analysis presented as a percentage of the total following (A) 24-, (B) 48- and (C) 72-hours after single/combined drug treatment in hypoxia (1% O_2). Data represent mean±SEM of five independent repeats with significance determined by ANOVA. Note no significant differences were observed (p>0.05).

3.6 *Autophagy Assay*

Based on the IC_{50} values obtained from the cell viability assay, the effects on the induction of autophagy following drug treatment were investigated under normoxic and hypoxic conditions *in vitro*. A combination treatment of rapamycin and chloroquine was used as a positive control. Figure 3.17 illustrates representative graphs for autophagic fluorescence following 24-hours of drug treatment.

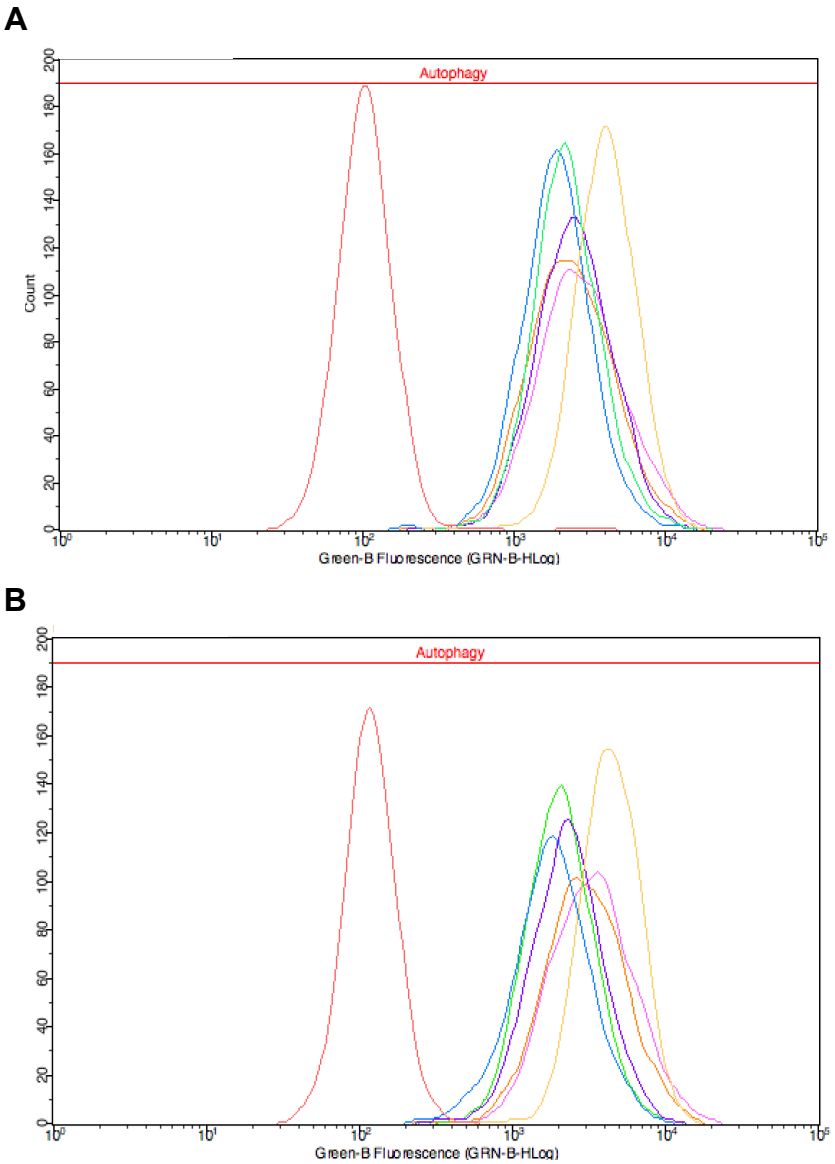

Figure 3.17: Original representative graphs for autophagy following treatment with non-treated control (red), olaparib (green), temozolomide (blue), cisplatin (purple), olaparib and temozolomide (pink), olaparib and cisplatin (orange) and the positive control (yellow) in U87-MG cells measured by CYTO-ID green staining and analysed by flow cytometry. (A) normoxia (21% O_2), (B) hypoxia (1% O_2). Graphs are typical of 5 such different experiments.

3.6.1 Effects on Autophagy in Normoxia

In SVG p12 cells, it was clearly visible that the positive control treatment of rapamycin and chloroquine worked effectively, when compared to the control with a percentage increase of 95±21% (p<0.001) (Fig.3.18A). Overall, a similar pattern to the apoptosis assay was observed, in which cisplatin (113±5%) and the combination treatments of olaparib and TMZ (130±15%) and olaparib and cisplatin (122±5%) appear to have increased autophagy, with maybe a small effect of olaparib (107±6%), when compared to the non-treated control (100±0%). Interestingly, a significant increase was observed in autophagy induction by olaparib and TMZ combination treatment (130±15%) in comparison to TMZ alone (91±5%) (p<0.05).

In U87-MG cells, the positive control treatment also induced a significant increase in autophagy, when compared to the non-treated control as there was a percentage increase of 123±27% (p<0.001) (Fig.3.18B). The greatest effects on autophagy were observed following treatment with olaparib (114±5%), olaparib and TMZ combined (136±9%) and olaparib and cisplatin combined (120±10%), when compared to the control (100±0%), although these differences were not significant.

Comparisons between SVG p12 and U87-MG cells showed a similar pattern of results, although cisplatin monotherapy induced no autophagy in U87-MG cells. The combination treatments were observed to induce the greatest effects on autophagy.

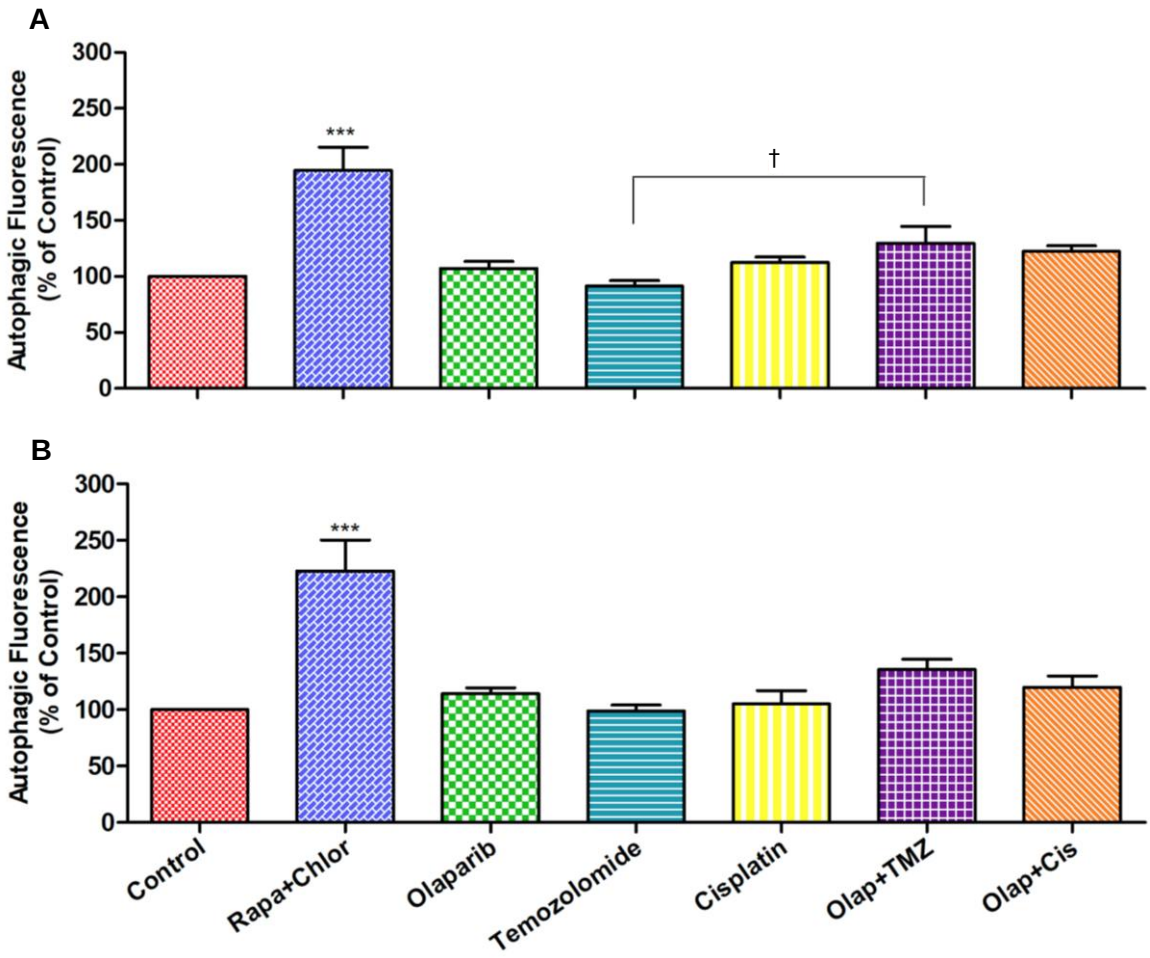

Figure 3.18: Bar charts showing comparisons of various drug treatments on autophagy induction as measured by CYTO-ID green stain fluorescence under normoxia. Autophagic fluorescence presented as a percentage of the respective control following 24-hours after single/combined drug treatment in normoxia (21% O_2). (A) SVG p12, (B) U87-MG. Data represent mean±SEM of five independent repeats with significance determined by ANOVA. Significant differences (p<0.05) shown by the asterisks (*) is in comparison to the respective control, and † denotes significance between drug treatments.

3.6.2 Effects on Autophagy in Hypoxia

In SVG p12 cells, the rapamycin and chloroquine treatment caused an increase of 71±20% in comparison to the control (100±0%) (p<0.001), indicating the positive control has worked (Fig.3.19A). While an increase in autophagy was observed following treatment with the combination of olaparib and cisplatin (137±10%) compared to the non-treated control, the most significant effect was with the combination of olaparib and TMZ, where autophagy was significantly increased (157±9%) (p<0.01). An increase in autophagy was also observed with olaparib (101±5%) and cisplatin (103±10%) in comparison to the control, although not significant. In contrast, TMZ (88±4%) caused a decrease in autophagy when compared to the control. A significant increase was induced by the combination treatments of olaparib and TMZ (157±9%) (p<0.01) and olaparib and cisplatin (137±10%) (p<0.05), compared to olaparib monotherapy (101±5%).

In U87-MG cells, the positive control treatment induced an increase of 150±24% compared to the control (100±0%) (p<0.001) (Fig.3.19B). The combination treatments of olaparib and TMZ (157±11%) (p<0.001) and olaparib and cisplatin (154±11%) (p<0.01) caused a significant increase in autophagy, in comparison to the control. Olaparib (112±7%), TMZ (102±4%) and cisplatin (115±4%) also caused an increase in autophagy, although they were not significant (p>0.05). Olaparib in the combination treatments was significantly better than olaparib on its own. A significant increase was induced by olaparib and TMZ (157±11%) (p<0.01) and olaparib and cisplatin (154±11%) (p<0.05), in comparison to olaparib monotherapy (112±7%).

Comparisons between SVG p12 and U87-MG cells showed a similar pattern of results, although this time, cisplatin monotherapy may have induced an effect in U87-MG cells (115±4%), when compared to SVG p12 cells (103±10%). The combination treatments had the greatest effects in both cell lines.

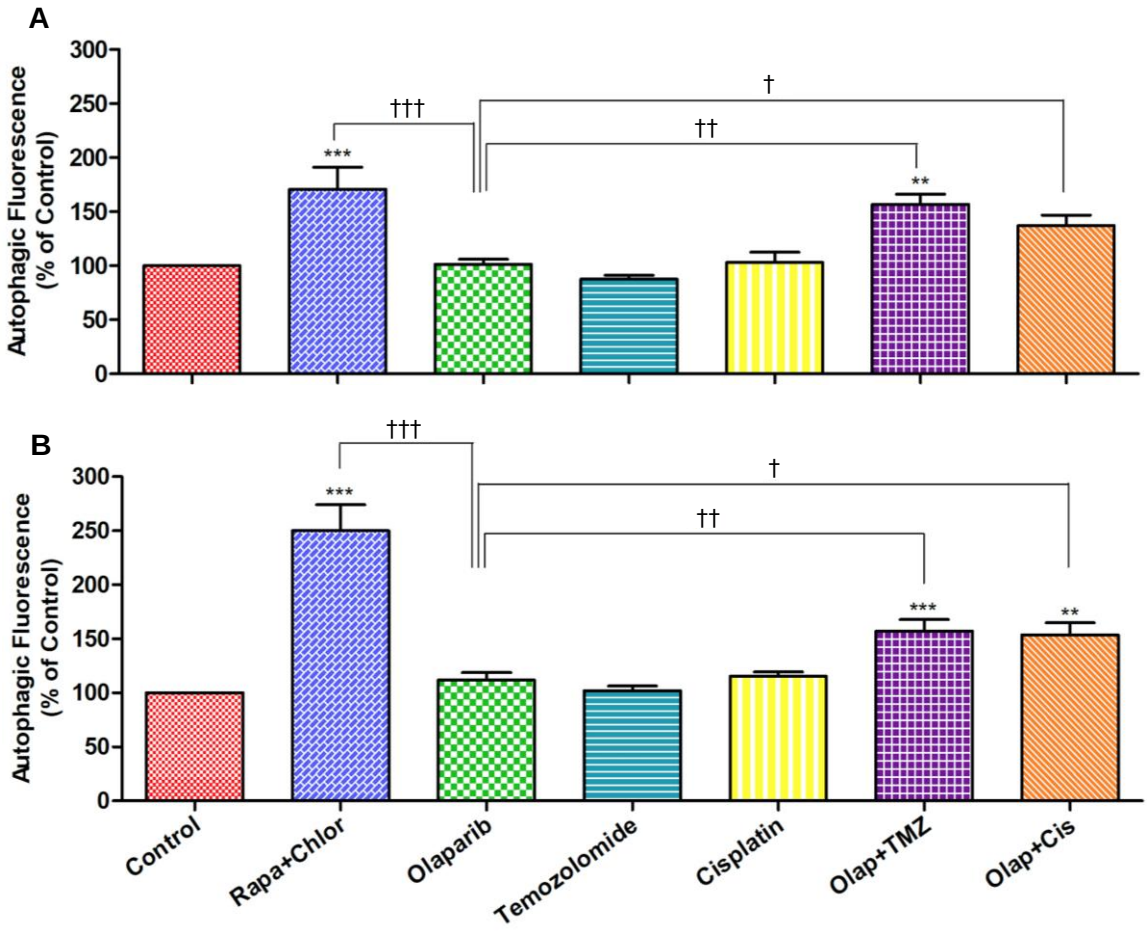

Figure 3.19: Bar charts showing comparisons of various drug treatments on the induction of autophagy as measured by CYTO-ID green stain fluorescence under hypoxia. Autophagic fluorescence presented as a percentage of the respective control following 24-hours after single/combined drug treatment in hypoxia (1% O_2). (A) SVG p12, (B) U87-MG. Data represent mean±SEM of five independent repeats with significance determined by ANOVA. Significant differences (p<0.05) shown by the asterisks (*) is in comparison to the respective control, and † denotes significance of olaparib compared to the other drug treatments.

3.6.3 Comparisons of the Effects of Autophagy in Normoxia and Hypoxia

When SVG p12 cells, in the two conditions, were compared, less autophagy was observed under hypoxia, apart from the combination treatments which caused an increase in autophagy under hypoxia (Fig.3.20A). Olaparib and TMZ combined and olaparib and cisplatin combined induced an increase in autophagy under hypoxia (145±19% and 131±21%, respectively) compared to normoxia (130±15% and 122±5%, respectively). Overall, all drug treatments had a similar efficacy.

In the U87-MG cells, similar levels of autophagy were observed in both conditions. The monotherapies all had a similar efficacy, whereas the combination treatments may be more effective under hypoxia. While olaparib and TMZ combined increased autophagy in hypoxia (158±24%) compared to normoxia (136±9%), the greatest effect was observed with the combination of olaparib and cisplatin with a significant increase in autophagy under hypoxia (155±23%) in comparison to normoxia (120±10%) (p<0.05).

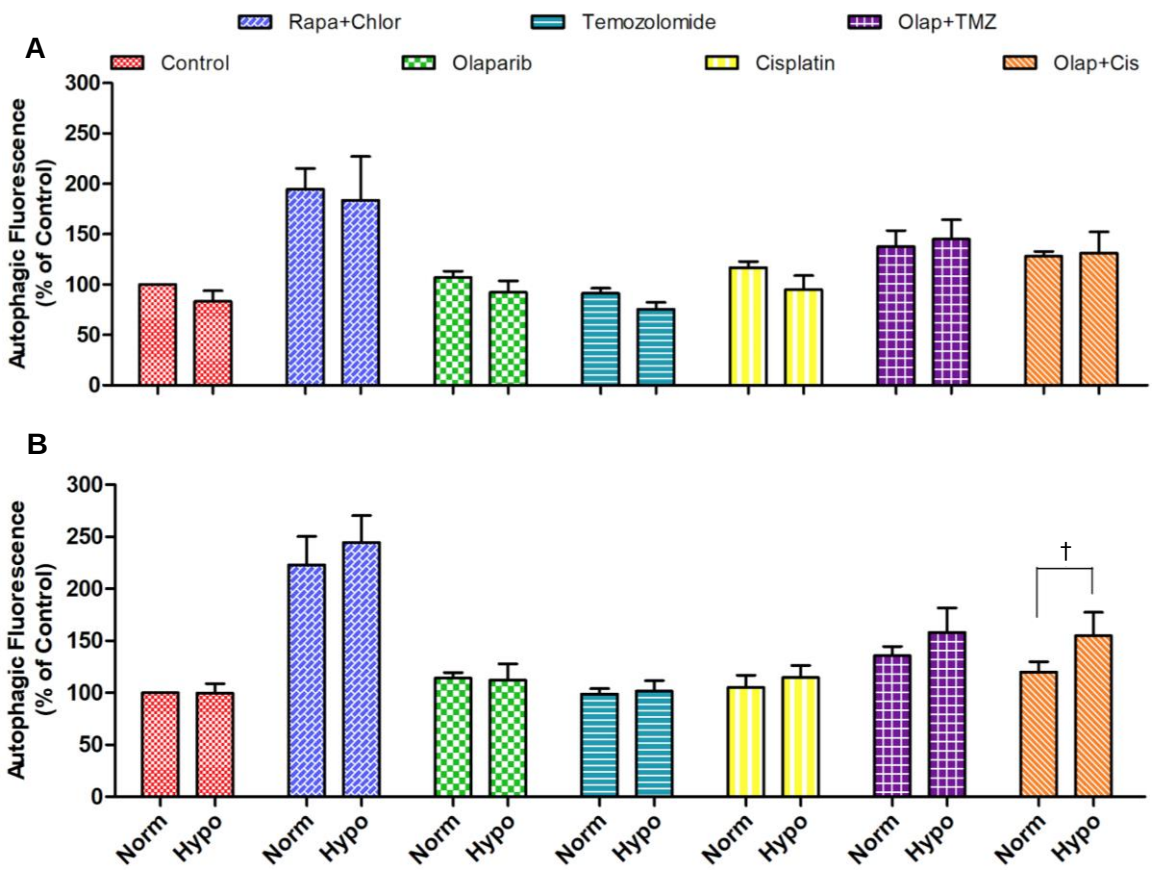

Figure 3.20: Bar charts showing comparisons of the drug treatments on the induction of autophagy as measured by CYTO-ID green stain fluorescence under normoxia and hypoxia. Effects on autophagy showing the comparisons following 24-hours after single/combined drug treatment in normoxia (21% O_2) and hypoxia (1% O_2). (A) SVG p12, (B) U87-MG. Data represent mean±SEM of five independent repeats with significance determined by ANOVA. Significant difference (p<0.05) shown by † denotes significance within the combination drug treatment.

3.7 Comet Assay

Based on the IC_{50} values, the proportion of DNA damage caused following drug treatment was investigated *in vitro*. Figure 3.21 illustrates representative images that were observed after electrophoresis. Two sets of analysis were performed: total intensity/area and the average intensity/unit distance.

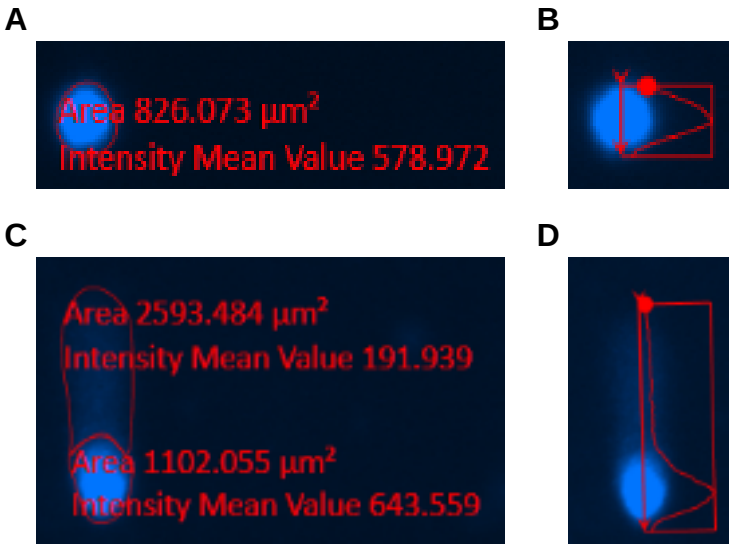

Figure 3.21: Original representative images that were observed following treatment with non-treated control (A, B) and olaparib (C, D) in U87-MG cells, measured by electrophoresis. The two methods of analysis used are shown: total intensity/area (μm^2) (A, C) and average intensity/unit distance (μm) (B, D). Images are typical of 3 such different experiments.

3.7.1 Analysis of the Total Intensity/Area

When the control treatment was compared to the drug treatments in the SVG p12 cells, a range of differences were observed (Fig.3.22A). The positive control of H_2O_2 (83±2) caused a significant increase in the total intensity/area of the tail, compared to the negative control (38±7) (p<0.001), and also a significant decrease in the head (23±2 vs. 78±6) (p<0.001). Similar significance was also observed with TMZ (tail: 74±8) (head: 31±5) (p<0.001). Olaparib caused a decrease in intensity for both the tail (35±6) and head (71±4), when compared to the control, although this was not significant. Cisplatin produced an increase in the total intensity/area in the tail (48±5), but a decrease in the comet head (73±2), in comparison to the control.

Olaparib (35±6) caused a significant decrease in the intensity/area of the tail, when compared to H_2O_2 (83±2) (p<0.001). Whereas, a significant increase occurred in the comet head (71±4 vs. 23±2) (p<0.001). A similar result was present when olaparib was compared to TMZ where significant differences were observed in both the tail (35±6 vs. 74±8), and the comet head (71±4 vs. 31±5) (p<0.001). A significantly lower intensity/area was produced by olaparib in the comet tail, when compared to cisplatin (48±5) (p<0.05). H_2O_2 and TMZ also caused great significant differences when compared to cisplatin. Similarly, a significant decrease in intensity/area was produced in the tail following cisplatin treatment (p<0.001), and a significantly greater intensity/area was seen in the head (p<0.001).

In U87-MG cells, when the control treatment was compared to H_2O_2, a significant decrease in the total intensity/area in the tail (44±4 vs. 86±3) (p<0.001), and a significant increase in the head (79±4 vs. 21±1) (p<0.001) was observed (Fig.3.22B). Similar results were observed when the control treatment was compared to TMZ (tail: 72±6) (head: 31±4) (p<0.001). A significantly lower intensity/area was produced with cisplatin treatment in the comet tail, in comparison to the control (0±0) (p<0.001). Whereas, a significantly greater effect was seen in the comet head (100±0) (p<0.01). Olaparib caused an insignificant decrease in both the comet tail (37±2) and head (71±2), compared to the control.

A significantly lower value for the total intensity/area was produced by olaparib in the tail, when compared to H_2O_2 (37±2 vs. 86±3) (p<0.001). However, a significant increase was present in the head (71±2 vs. 21±1) (p<0.001). Major significant differences were also observed when olaparib was compared to TMZ and cisplatin treatment. A significant decrease in the intensity/area of the tail in olaparib, compared to TMZ (72±6), and a significant increase in the head (31±4) (p<0.001). Whereas, olaparib compared to cisplatin caused a significantly greater intensity/area in the tail (0±0), and a significant decrease in the head (100±0) (p<0.001). H_2O_2 also produced significant differences when compared to TMZ and cisplatin. TMZ caused a minor, but significant decrease in the intensity/area in the comet tail, in comparison to H_2O_2 (p<0.05). Cisplatin produced a significant decrease in the tail, and a significant increase in the head (p<0.001). Significant differences were also present when TMZ was compared with cisplatin; a significant increase in the tail, and a significant decrease in the comet head (p<0.001).

Olaparib treatment in either the U87-MG cells (tail: 37±2, head: 71±2) or the SVG p12 cells (tail: 35±6, head: 71±3) did not produce a significant difference in either the comet tail or head fluorescence intensity. Minor differences were also observed with TMZ in both of the cell lines; with a decrease in intensity/area in the tail, but an increase in the head of U87-MG cells, in comparison to SVG p12 cells. Cisplatin, however, caused a significant decrease in the comet tail, and a significant increase in the comet head of U87-MG cells compared to SVG p12 (p<0.001).

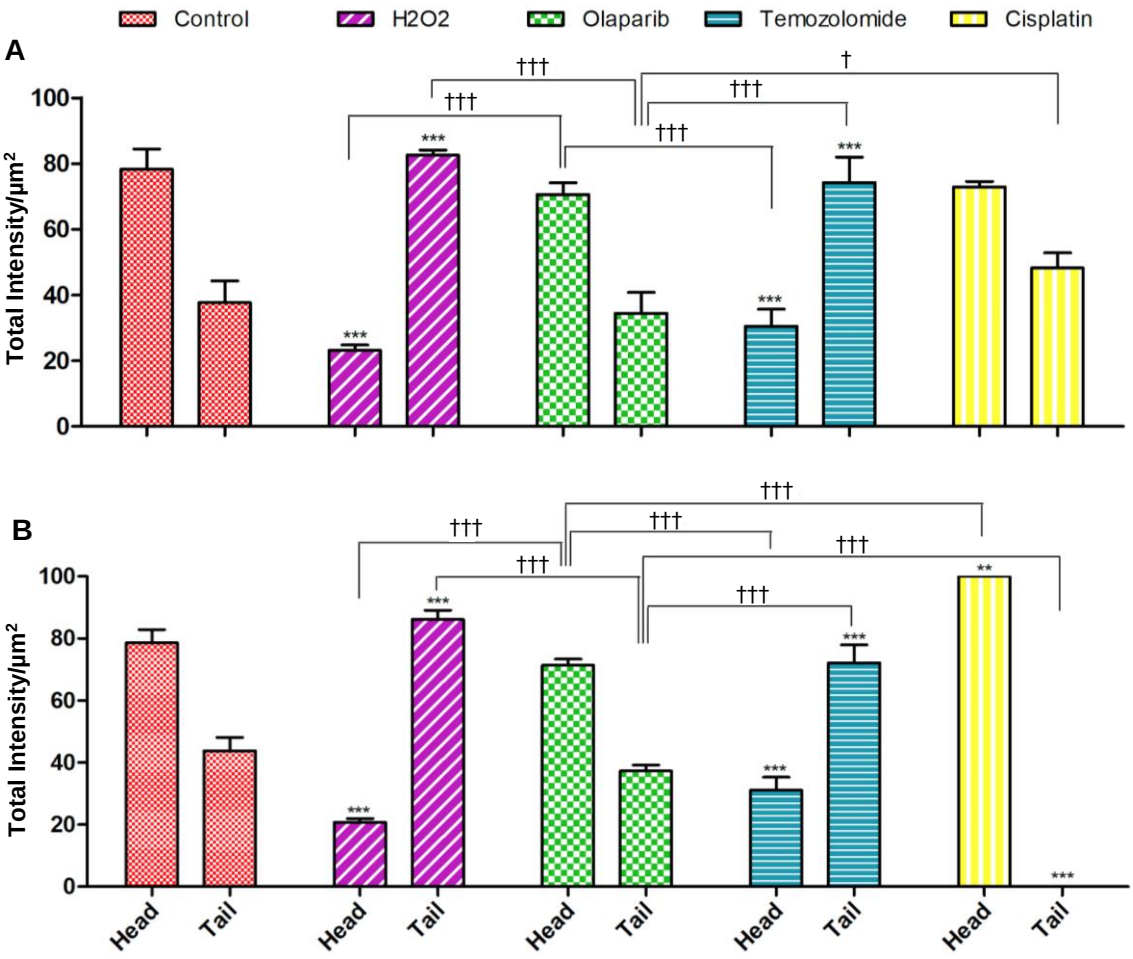

Figure 3.22: Bar charts showing comparisons of the proportion of DNA damage caused following drug treatment measured by electrophoresis. Effects of drug treatment presented by the total intensity/area (µm^2). (A) SVG p12, (B) U87-MG. Data represent mean±SEM of three consecutive independent repeats with significance determined by ANOVA. Significant differences (p<0.05) shown by the asterisks (*) is in comparison to the respective control, and † denotes significance of olaparib only compared to the other drug treatments.

3.7.2 Analysis of the Average Intensity/Unit Distance

In SVG p12 cells, when the control treatment was compared to the other drug treatments various differences were observed (Fig.3.23A). The control, compared to the positive control of H_2O_2, showed a significant increase in the average intensity/unit distance in the comet head (32±3 vs. 20±6) (p<0.01). A greater significant increase was also caused by the control in the comet head, when compared to TMZ (17±2) (p<0.001). A decrease in average intensity/distance was produced by olaparib in the comet head (26±6), in comparison to the control, though not significant.

H_2O_2 caused a significant decrease in the average intensity/distance in the comet head, when compared to cisplatin (20±8 vs. 31±6) (p<0.01). While no significance was present when H_2O_2 and cisplatin was compared to olaparib (p>0.05), a significantly greater average intensity/distance was observed with olaparib in the comet head, when compared to TMZ (26±6 vs. 17±2) (p<0.05). TMZ produced a significantly lower average intensity/distance in the comet head, than cisplatin (31±6) (p<0.001).

Several variations were also present in the U87-MG cells following 24-hours of drug treatment (Fig.3.23B). When the control treatment was compared to the positive control, olaparib and TMZ, no significant differences in average intensity/unit distance were observed (p>0.05). However, when compared to cisplatin, a significant increase in the comet head was present (28±5 vs. 56±7) (p<0.001).

Olaparib caused no difference in the average intensity/distance in the comet tail but did cause a small but non-significant decrease in the comet head, when compared to TMZ (tail: 5±1 vs. 5±1) (head: 21±3 vs. 23±1), though these differences were not significant. Cisplatin produced significantly greater results in the comet head, when compared to all drug treatments (56±7 vs H_2O_2 24±7; olaparib 21±3; TMZ 23±1) (p<0.001).

The average intensity/unit distance of the comet tail and head produced by olaparib in U87-MG cells was lower than in SVG p12 cells (tail: 6±1 vs. 5±1) (head: 21±3 vs. 26±6). TMZ treatment in U87-MG cells caused an increase in the comet head compared to SVG p12 cells (23±1 vs. 17±2). Cisplatin produced a significant decrease in the average intensity/distance of the tail in U87-MG cells, compared to SVG p12 cells (0±0 vs. 9±2) (p<0.05). Whereas, a significant increase of the head was produced in U87-MG cells (56±7 vs. 31±6) (p<0.001).

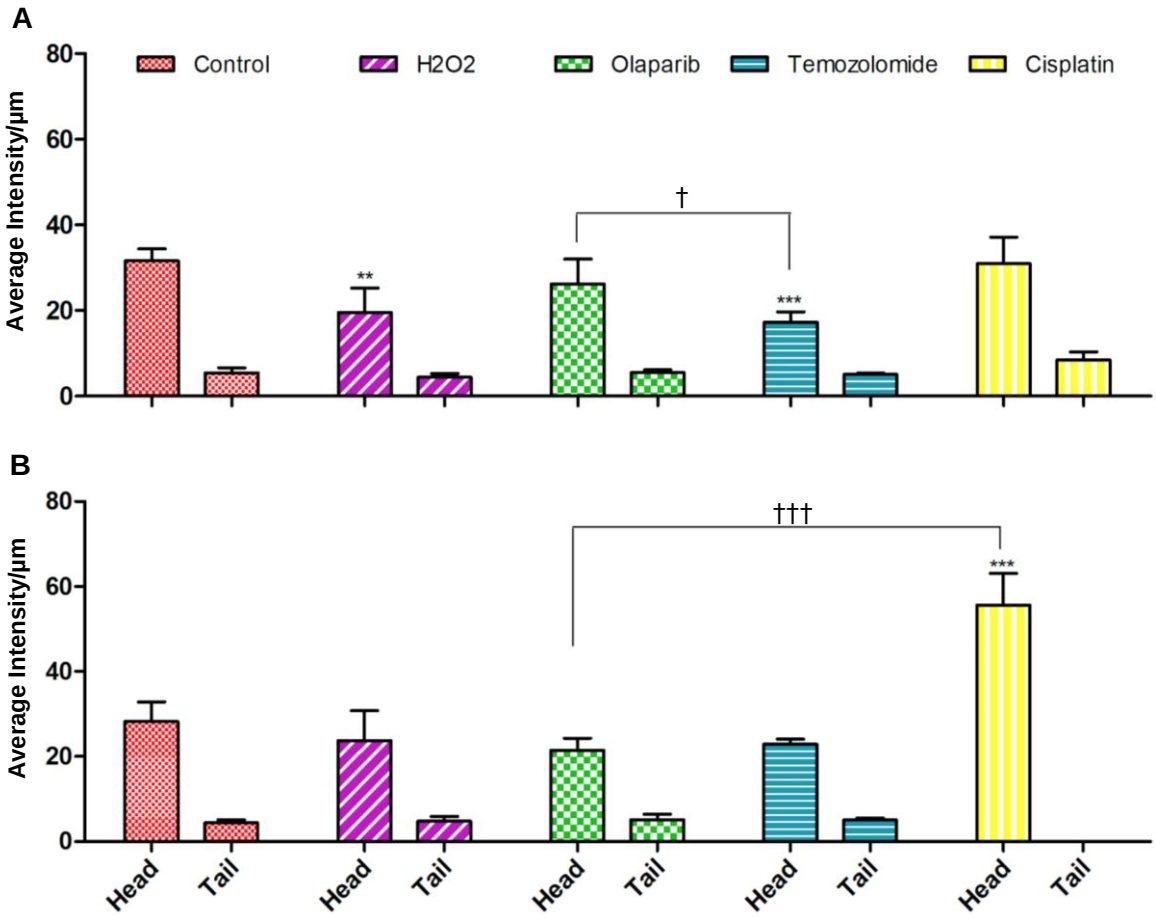

Figure 3.23: Bar charts showing comparisons of the proportion of DNA damage caused following drug treatment measured by electrophoresis. Effects of drug treatment presented by the average intensity/unit distance (µm). (A) SVG p12, (B) U87-MG. Data represent mean±SEM of three consecutive independent repeats with significance determined by ANOVA. Significant difference (p<0.05) shown by the asterisk (*) is in comparison to the respective control, and † denotes significance of olaparib compared to the other drug treatments.

3.8 Clonogenic Assay

Following 10-days of drug treatment in both normoxic and hypoxic conditions, colonies for each treatment in SVG p12 and U87-MG cells were visually counted and recorded.

3.8.1 Clonogenic Analysis in Normoxia

No significant differences (p>0.05) were observed in either of the cell lines in normoxia, though many variations were observed. In SVG p12 cells (Fig.3.24A), olaparib (83±6%) had the greatest effect by producing a lower number of colonies, when compared to the control (100±0%). Whereas, the results for TMZ and cisplatin were similar to the control.

However, in U87-MG cells (Fig.3.24B), when compared to the control all drug treatments caused a decrease in the number of colonies (100±0% vs. olaparib 76±15%; TMZ 60±13%; cisplatin 50±13%).

When the two cell lines were compared, olaparib induced a consistent decrease in colonies, but cisplatin induced the greatest effect in U87-MG (50±13%) compared to SVG p12 cells (100±25%).

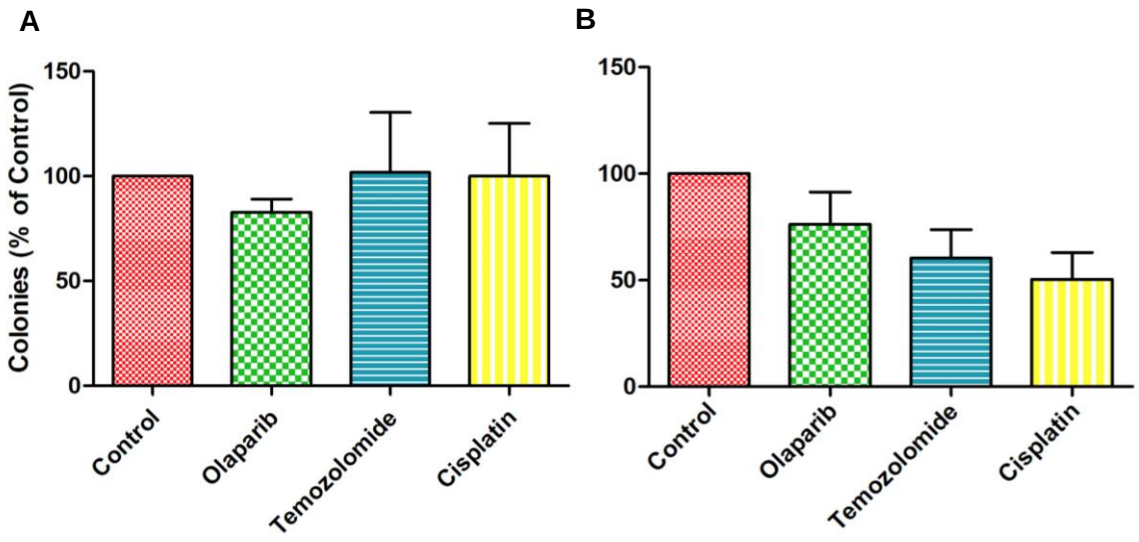

Figure 3.24: Bar charts showing comparisons of the quantity of colonies visualised following drug treatment under normoxia. The quantity of colonies observed presented as a percentage of the respective control following 10-days after drug treatment in normoxia (21% O_2). (A) SVG p12, (B) U87-MG. Data represent mean±SEM of five consecutive independent repeats. Note no significant differences were observed (p>0.05).

3.8.2 Clonogenic Analysis in Hypoxia

In SVG p12 cells (Fig.3.25A), following drug treatment with olaparib (90±6%), TMZ (88±8%) and cisplatin (79±6%), all treatments produced small decreases in colony number, compared to the control (100±0%). Whereas, in U87-MG cells (Fig.3.25B), interestingly olaparib (103±6%) had no effect on colony number in comparison to the control (100±0%). When comparing the cell types, a similar pattern to normoxia was observed, with the exception of olaparib. However, cisplatin induced consistently the largest effect.

3.8.3 Comparisons of Clonogenic Analysis in Normoxia and Hypoxia

Though all comparisons between the two conditions of each drug treatment in each cell line were insignificant ($p>0.05$), various differences were observed. Olaparib treatment produced a higher percentage of colonies in the SVG p12 cells under hypoxia, than in normoxia (90%±6% vs. 83%±6%). A similar comparison was also seen with the U87-MG cells (103%±6% vs. 76%±15%). The TMZ treated SVG p12 cells had a lower percentage of colonies in hypoxia, compared to normoxia (88%±8% vs. 102%±29%). Whereas, in the U87-MG cells, a higher percentage was observed in hypoxia (73%±5% vs. 60%±13%). Cisplatin produced a much lower percentage of colonies in SVG p12 cells in hypoxia, compared to normoxia (79%±6% vs. 100%±25%), but a higher percentage in U87-MG cells in hypoxia, than in normoxia (55%±8% vs. 50%±13%).

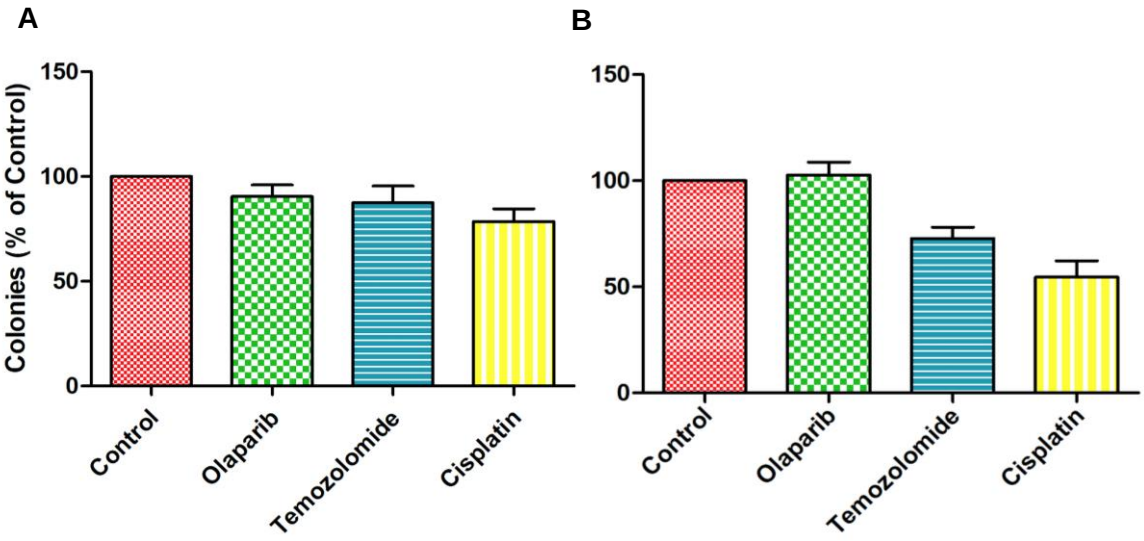

Figure 3.25: Bar charts showing comparisons of the quantity of colonies visualised following drug treatment under hypoxia. The quantity of colonies observed presented as a percentage of the respective control following 10-days after drug treatment in hypoxia (1% O_2). (A) SVG p12, (B) U87-MG. Data represent mean±SEM of five consecutive independent repeats. Note no significant differences were observed (p>0.05).

Chapter 4:

Discussion

Currently, there are only limited therapeutic options available for GBM and other high-grade gliomas due to several reasons, including the presence of the BBB, the heterogeneity of the tumours, and their ability to become resistant to drug treatments (Karpel-Massler, *et al*., 2014). Also due to the median overall survival (<15 months) of GBM patients, the requirement to develop new treatment strategies has increased (Karpel-Massler, *et al*., 2014). In previous work, evidence has established that PARP1 is widely expressed in GBM, and that interfering with PARP1 function may be a beneficial strategy to overcome drug resistance and also enhance cytotoxicity of existing therapies (Karpel-Massler, *et al*., 2014).

The main aim of this study was to investigate the effect of olaparib, alone and in combination with other chemotherapeutics, on a GBM cell line *in vitro*. While variation was observed between assays, evidence has been obtained in this project of the effects of olaparib in U87-MG GBM cells, resulting in decreases in cell proliferation, accompanied by impairment of cell cycle progression and an increase in apoptosis and DNA damage.

4.1 Drug Effects on Cell Viability

Initially, this study was designed to examine the effect of olaparib on cell viability in SVG p12 and U87-MG cells. As the oxygen levels in the intra-tumoural environment can affect the efficacy of drug treatments, the assays were performed under both normoxia (21% O_2) and hypoxia (1% O_2), with the exception of the comet assay.

Olaparib produced decreases in both SVG p12 cell and U87-MG cell viability, although its effects were clearly not as potent and rapid as TMZ and cisplatin. With an increase in concentration and over a 72-hour time period, olaparib was observed to cause a reduction in cell viability at the highest concentration of 0.3 mM in both cell lines and in both conditions. This result agrees with findings from a study by Karpel-Massler, *et al*., (2014), who concluded that olaparib alone elicited mild to moderate effects on U87-MG cell viability, though only a 10 µM concentration of olaparib for 48-hours was used. Rasmussen, *et al*., (2016) found PARP inhibition by olaparib to be efficient in causing cytotoxicity in GBM cells *in vitro* and *in vivo*, even when administered alone. They used three xenografted GBM cell lines, and a concentration of olaparib based on the IC_{50} values for each cell line (9.0 µM, 11.7 µM, 724.9 nM), and cell viability was measured over 7-days (Rasmussen, *et al*., 2016). Many mechanisms can explain olaparib's cytotoxicity due to PARP1 having a functional role in transcriptional regulation,

cell death as well as in DNA repair. Therefore, interfering with PARP1 can lead to synthetic lethality in all of these pathways, even when extensive DNA damage is not present (Ko & Ren, 2012). A potent effect of olaparib was not observed in this project, this may be due to the different cell lines used and that cell viability was only measured over 3-days and not longer.

Temozolomide and cisplatin demonstrated their cytotoxic effects by causing a decrease in cell viability of both cell lines in a concentration- and time-dependent manner, under both normoxia and hypoxia. This result was expected due to these drugs being potent chemotherapeutic agents. Castro, *et al*., (2015) found that TMZ-treated U87-MG cells, at a concentration of 25 µM, after 24-hours of treatment showed 80% viability. This study measured cell viability over 3-days, and at 72-hours was when the largest decrease was observed. Kumar-Thakor, *et al*., (2017) also found cisplatin (10^{-7}-10^{-4}M) to induce a concentration- and time-dependent decrease in U87-MG cells' viability under normoxia, over 3-days. These results from previous studies agree with the results gained from the current study.

In this project, olaparib had similar efficacy on cell viability in both cell lines under both conditions. When compared to TMZ and cisplatin treatment, olaparib had less of an effect in both cell lines under both normoxia and hypoxia. TMZ and cisplatin, in this study, were observed to induce greater reductions in cell viability 48-hours after treatment. They are extremely effective cancer treatments (Lee, 2016; Rocha, *et al*., 2014), and due to the mechanism of action of cisplatin which exerts cytotoxicity by producing DNA lesions, and TMZ being an alkylating agent (Fig. 4.1), may be the reason why rapid reductions in cell viability were observed 48-hours after drug treatment. This statement agrees with findings by Kumar-Thakor, *et al*., (2017) who concluded that cisplatin might have a delayed effect until after 48-hours of treatment. Similarly, Rasmussen, *et al*., (2016) found olaparib can decrease cell viability over 7-days. Therefore, it would be expected for TMZ and cisplatin to induce their effects quicker than olaparib, which suggests even though olaparib may be a better alternative for normal cells due to the delayed cytotoxicity, is not as effective as the current therapies on reducing GBM cell viability.

Based on the results obtained in this project for this assay, scope for future work may include the use of different cell lines, such as the xenografted GBM cell lines used in the 2016 study by Rasmussen *et al*. and also to measure cell viability over a longer period of time, such as 7-days, instead of only 3-days.

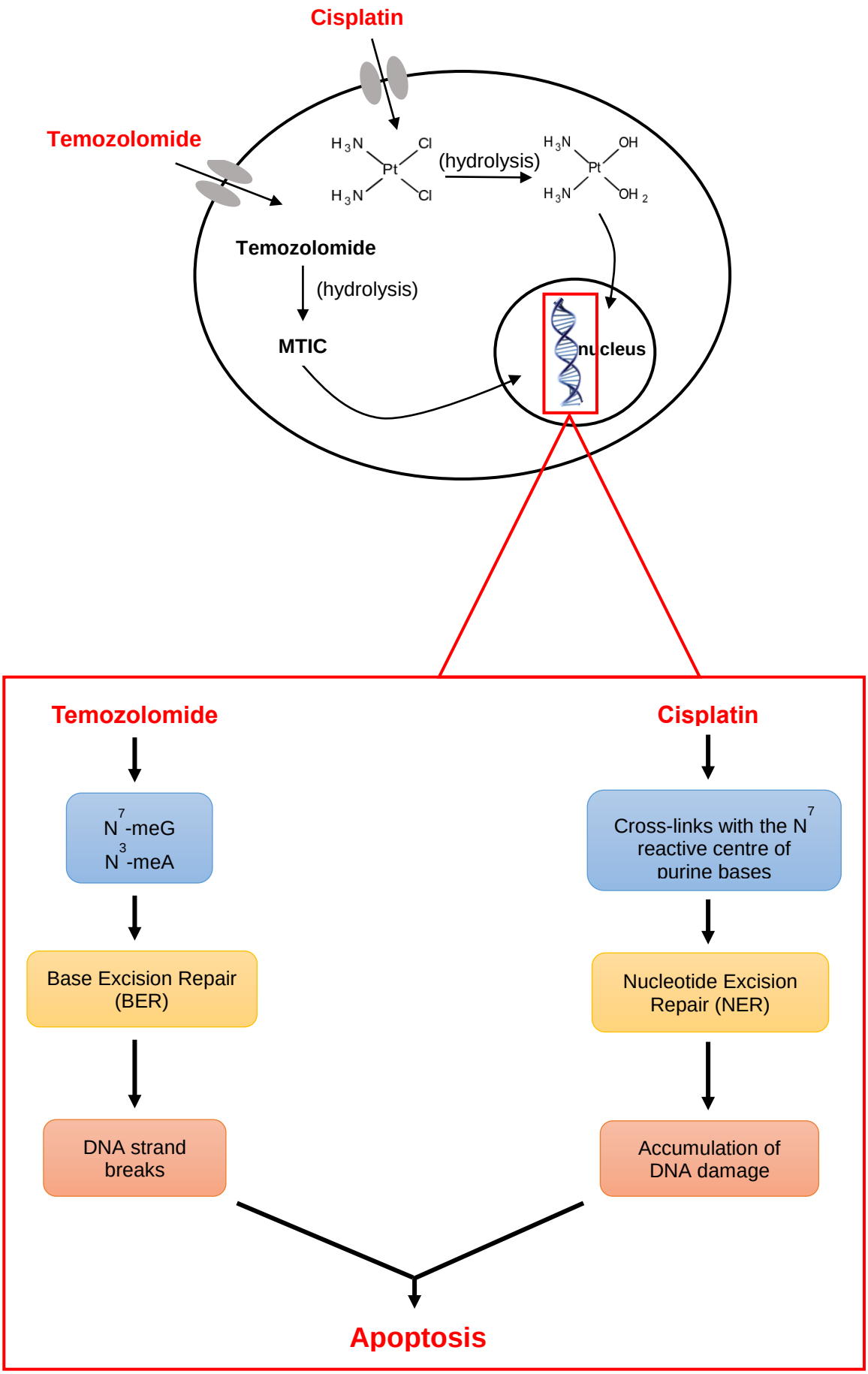

Figure 4.1: Diagram showing the mechanisms of action of temozolomide and cisplatin in cells, and how they ultimately induce apoptosis of the cells.

4.2 Olaparib Decreased Cell Proliferation Over 7 days

As cell viability is determined by many factors or mechanisms, this study subsequently decided to examine the effects of olaparib on cell proliferation. Findings from this assay indicate a decline over 7-days in CFDA-SE fluorescence in the GBM and SVG p12 cell lines under normoxia and hypoxia conditions. A decrease in fluorescence corresponds to proliferation of cells over the time period, though variation between the cell lines and treatments were present. Olaparib caused a decrease in proliferation over the 7-days, especially in the U87-MG cells under normoxia. These results correlate with the study by Karpel-Massler, *et al*., (2014), who obtained findings that olaparib caused inhibition of proliferation in U87-MG cells, although this was concentration-dependent.

The results for TMZ and cisplatin do not coincide with what would be presumed to be seen. This would be a halt in proliferation in both cell lines. Yu, *et al*., (2016) determined TMZ to have concentration-dependent inhibitory effects on proliferation in U87 cells, at a concentration range of 0-3.2 mM for 72-hours. Similarly, Kutwin, *et al*., (2017) found cisplatin to also decrease proliferation in U87 and U118 GBM cell lines 24-hours after treatment, though at an unknown concentration. In this study, although results were not significant, cisplatin definitely inhibited proliferation in U87-MG cells under normoxia, and SVG p12 and U87-MG cells under hypoxia.

TMZ and cisplatin under normoxia caused more of a time-dependent decrease in CFDA-SE fluorescence in the SVG p12 cells than in the U87-MG cells, implying the SVG p12 cells were proliferating more quickly. In contrast, the opposite effect was observed in hypoxia. A similar efficacy of olaparib on proliferation was observed in SVG p12 cells under both conditions, though a significant effect was seen in the U87-MG cells under hypoxia compared to normoxia. This may be due to the involvement of hypoxia-inducible factors (HIFs) in hypoxic conditions. Previous studies have found that cancer cell proliferation and invasion are linked to HIF expression, and also that they contribute to the hypoxic tumoural microenvironment (Yang, *et al*., 2015). HIF-induced transcription regulates many genes which promote proliferation (Monteiro, *et al*., 2017). Gonzalez-Flores, *et al*., (2014) reported that PARP1 regulates HIF-1 activity, but also that PARP1 interacts with HIF-2α and inhibition of PARP1 affected complex formation and protein stability of HIF-2α. The HIF-α subunits are regulated by oxygen availability and under hypoxic conditions, hydroxylation is inhibited which causes increased HIF-α stability. PARP1 was found to be present at the HIF-2α promoter, therefore PARP1 inhibition considerably decreased HIF-2α mRNA and protein levels, as well as HIF-2-dependent genes' transcription. Thus, Gonzalez-Flores, *et al*., (2014) concluded that inhibition of

PARP1 results in multiple regulatory effects on the HIF-2-mediated hypoxic response at both the transcriptional and post-transcriptional level. While this is known about the crosstalk between HIF and PARP, exactly how this relates to the results from the current study would require further investigation.

Based on the proliferation results obtained in this project, scope for future work may include to measure proliferation of the cell lines following drug treatment in both a time- and concentration-dependent manner. This would allow for proliferation to be measured at a range of different concentrations of the drugs, as well as over a period of 7-days.

4.3 Olaparib Caused Cell Cycle Arrest

As olaparib was found to inhibit cell proliferation, this study next examined cell cycle distribution using propidium iodide staining and flow cytometry. In normoxic conditions, olaparib induced the greatest population of GBM and SVG p12 cells to arrest in the G2/M phase. This was also the same for the SVG p12 cells in hypoxic conditions. Although the greatest population of GBM cells were not present in G2/M in hypoxia, there was a definite increase when compared to the control. Studies examining olaparib's effects on cell cycle arrest in either cell line were not found, however another study by Rasmussen, *et al*., (2016) investigated olaparib in three other GBM cell lines under normoxia. They found olaparib to induce cell cycle arrest during the G2/M phase in all three of these cell lines. Even though they used different GBM cells, this result coincides with the findings gained from this project.

Under normoxia, TMZ caused a decrease in the percentage of the population of GBM cells in the G0/G1 phase, the percentage of apoptotic cells increased, G2/M increased, but S phase was unchanged, when compared to the non-treated control. These results partly correlate with a study by Carmo, *et al*., (2011). Although they used the U-118 glioma cell line, they did find similar results with TMZ (Carmo, *et al*., 2011). Other studies have also found TMZ to induce cell cycle arrest during the G2/M phase (Filippi-Chiela, *et al*., 2013; Tiek, *et al*., 2018). Wang, *et al*., (2017) found that the proportion of GBM cells in the G2/M phase increased in a concentration- and time-dependent manner following TMZ treatment. They stated that the G2/M arrest by TMZ was induced by DNA damage. The use of alkylating agents during chemotherapy enhances genotoxic-stress induced DNA damage, and the most vital biological response to this is cell death. Activation of cellular mechanisms, including DNA repair and cell cycle arrest regulate this biological response immediately following DNA damage.

GADD45A, a downstream gene of the tumour-suppressor TP53, has been found to be immediately induced by DNA damage by genotoxic drugs, such as TMZ and cisplatin. GADD45A is a stress-induced protein that interacts with other cellular molecules involved in maintaining genomic stability, regulation of the cell cycle at the G2/M checkpoint, apoptosis and DNA repair (Wang, *et al*., 2017). Thus, it is tempting to suggest that *GADD45A* may be involved in causing the TMZ-treated GBM cells to arrest the cell cycle during the G2/M phase.

Cisplatin also caused an increase in the population of U87-MG cells in the apoptotic and G2/M phase, and a decrease in the G0/G1 phase under normoxia, though these results were not significant when compared to the non-treated control. A 2015 study by Jia, *et al*., observed cisplatin to significantly induce cell cycle arrest during the apoptotic phase in U87-MG cells. Kumar-Thakor, *et al*., (2017) also found cisplatin to cause a decrease in the proportion of U87-MG cells in the G0/G1 phase and an increase in the G2/M phase, following 48-hours of treatment. Findings from both of these previous studies correlate with the results from this current study. Cisplatin induces cytotoxicity *via* DNA intercalation which can cause apoptosis and alterations in the cell cycle (Kumar-Thakor, *et al*., 2017). Interestingly, an effect that was replicated in this study where cell cycle arrest was observed during the G2/M phase under normoxia.

Under hypoxic conditions, the cell cycle for TMZ-treated cells was G0/G1 dominant, and cisplatin was G2/M dominant. Findings from the study by Kumar-Thakor, *et al*., (2017) do not correlate with the results from the present study as they found cisplatin treatment to cause a lower proportion of cells to arrest in the G2/M phase under hypoxia compared to normoxia. They reported that hypoxic conditions slow the progression of the cell cycle, whereas oxygen levels at 1%, also known as moderate hypoxia, induces pre-S-phase arrest in cells and cells in other cell cycle phases progress to late G1 phase before they arrest. It has been suggested that this transient arrest in the G1 phase is a mechanism to protect cells from proceeding into the S phase, where they are more susceptible to hypoxia-related DNA damage (Kumar-Thakor, *et al*., 2017). The G1 phase cell cycle checkpoints are activated in response to stress, such as hypoxia, and also when the tumour suppressor gene p53 accumulates in response to DNA damage (Graeber, *et al*., 1994). Thus, indicating that under hypoxia the treatments would be expected to arrest the cell cycle during the G0/G1 phase, this correlates with current findings in this study for TMZ, but not for cisplatin. The present results do indicate though that TMZ and cisplatin can inhibit proliferation in the U87-MG cell line.

In the SVG p12 cells, TMZ induced a G2/M arrest and this correlates with the results for U87-MG cells where a similar increase in the proportion of cells were seen, when compared to the control under normoxia. Whereas, cisplatin caused an increase in the apoptotic population and potentially a decrease in the G2/M phase, though this does not correlate with the U87-MG cells result where a G2/M arrest was observed. Under hypoxia, TMZ caused an increase in the proportion of cells in the S phase and cisplatin induced the greatest percentage of arrest during the G2/M, similar to the U87-MG cells.

Scope for future work based on these results may be to measure cell cycle arrest using different GBM cell lines, such as the U-118 cell line. Previous studies obtained results that correlated with the findings from this project, though they examined the effects of olaparib and TMZ in other GBM cell lines. Also, the effects of the drug treatments on cell cycle arrest could be measured in a concentration-dependent manner.

4.4 *Olaparib Monotherapy Did Not Induce Apoptosis*

Another factor-determining change in cell viability is cell death, in particular apoptosis. Using PI and Annexin V staining this study examined any effects of olaparib. In U87-MG GBM cells, olaparib did not induce apoptosis in a time-dependent manner under either normoxia or hypoxia. Karpel-Massler, *et al*., (2014) investigated the effects of olaparib on apoptosis in the U251 GBM cell line and they found olaparib to induce apoptosis after 24-hours of treatment, a finding which coincides with previous results from this study where olaparib was observed to have minor cytotoxic effects on the U87-MG cells.

Under normoxia, TMZ caused an increase in the proportion of live GBM cells over the 3-day period, but no change in apoptotic cells. Previous studies have found correlating results regarding TMZ-induced apoptosis in U87-MG cells. Knizhnik, *et al*., (2013) concluded that TMZ in U87-MG cells induces apoptosis 120-hours and onwards following treatment at a concentration of 35 mM. Wang, *et al*., (2017) also found the effects of TMZ (25 µg/ml) in U87 and U373 cells on apoptosis to be more prominent 4-days after treatment. Findings have been established that numerous genes involved in genome stability, cell survival and DNA repair are up-regulated in response to the cytotoxic effects that occur after TMZ treatment. Certain genes, such as GADD45A, have been suggested to have anti-apoptotic and protective roles in GBM. Thus, possibly suggesting why TMZ treatment takes longer to induce its apoptotic effects, however this is yet to be established (Wang, *et al*., 2017). In hypoxia, TMZ induced a decrease in the

percentage of live GBM cells. This suggests the cytotoxic effects of TMZ may be enhanced in low oxygen conditions, which would be beneficial due to the intra-tumoural environment of GBM being hypoxic (Jawhari, *et al*., 2016). However, no change was observed in the apoptotic population. Resistance to chemotherapy and radiation is generally associated with hypoxia, and findings from a 2012 study by Sun, *et al*., concluded that hypoxic tumours have survival benefits, hence indicating TMZ to not significantly induce apoptosis in hypoxic conditions. Ahmed, *et al*., (2018) reported the downregulation of HIF-1α increased sensitivity of U87 GBM cells to TMZ.

In this study, the results show that cisplatin caused a significant increase in the population of apoptotic U87-MG cells under normoxia; a result that correlates with a previous study conducted which investigated cisplatin, at a concentration of 10 µM, over 72-hours on U87-MG and SVG p12 cell lines (Kumar-Thakor, *et al*., 2017). Cytotoxic effects of cisplatin can cause variations in the DNA structure which interfere with DNA replication. Cisplatin uses passive diffusion to enter cells and induces cytotoxicity by DNA intercalation, hence initiating apoptosis (Kumar-Thakor, *et al*., 2017). In this project, cisplatin induced significantly greater apoptotic effects in hypoxia on GBM cells; though not a result which corresponds to a study by Kumar-Thakor, *et al*., (2017), whom established the efficacy of cisplatin to be reduced in hypoxia. HIFs are known to be the primary mediators of hypoxic responses. The HIF factor, HIF-1α has been found to stimulate glioma cancer stem cells survival under hypoxic conditions, and HIF-2α is believed to be associated to the GBM stem cell phenotype within the hypoxic niche (Ahmed, *et al*., 2018). A decrease in oxygen levels activates transcription of HIF, which results in changes in cellular metabolism, and this is caused by transcription of various genes including *EGFR* (epidermal growth factor receptor), *VEGFR* (vascular endothelial growth factor receptor) and *GLUT-1* (glucose transporter-1). Hypoxia promotes the malignant phenotype of cancerous cells, and an enhanced resistance to chemotherapy and radiation is often exhibited (Kumar-Thakor, *et al*., 2017). In another study, Ahmed, *et al*., (2018) determined that the downregulation of HIF-2α increased sensitivity of U87 cells to cisplatin, thus, suggesting why previous studies did not observe an increase in apoptosis under hypoxia.

The combination treatment of olaparib and TMZ under normoxia produced only a slightly higher percentage of apoptotic GBM cells over the 3-days. This may have been expected due to the lack of an effect from TMZ alone. The combination of PARPi and TMZ has been suggested to enhance the apoptotic rate of a cell population (Dréan, *et al*., 2016). A study by Engert, *et al*., (2015) observed an increase in apoptosis following 48-hours of treatment with the combination of olaparib (0.3 µM/L) and TMZ (50 µM/L)

using Ewing sarcoma cell lines. A similar decrease in the proportion of live and apoptotic cells over the 72-hour time-period was observed under hypoxia for this combination treatment. Previous studies have not yet established an explanation for this, as it is still an area for research. However, from previous findings in this project, olaparib and TMZ alone were observed to have enhanced effects in hypoxic conditions.

Olaparib combined with cisplatin induced significant increases in apoptosis in both normoxia and hypoxia. Cisplatin's mechanism of action is largely based on DNA damage and the production of DNA adducts. Previous studies discovered that PARPi did not change the quantity of DNA adducts formed by cisplatin, but rather delayed the repair of them (Dréan, *et al*., 2016; Miknyoczki, *et al*., 2003); agreeing with the suggestion that PARPi do not potentiate chemo-resistance, but that the effects observed of combination treatment are additional (Dréan, *et al*., 2016; Murai, *et al*., 2014). Previous research regarding olaparib and cisplatin combined in hypoxia was not found, but from the results of this study, this combination treatment induced a greater percentage of apoptosis, also implying from what we know of that enhanced cytotoxicity is caused in low oxygen conditions.

Some of the results obtained for the SVG p12 cell line were not anticipated. This may be due to several reasons, but one study has established a possible cause. Henriksen, *et al*., (2014) determined that SVG p12 cells specifically obtained from the American Type Culture Collection contain the infectious BK polyomavirus (BKPyV) of strain UT and various defective mutants. Strain UT had been discovered in urine and in tumours of different patients beforehand but is also commonly used in research. Therefore, it is not clear whether BKPyV was present in the brain tissue which was used to produce the cell line or whether it is contamination (Henriksen, *et al*., 2014). Thus, this cell line is not 100% representative of normal glial cells and this may have also affected the results for the SVG p12 cells in this study.

Based on the results obtained in this project, future work may include examining the effects of apoptosis following drug treatment over a range of time periods rather than just 3-days. Different GBM cell lines could also be used, as some previous studies have. Western blotting could be conducted to identify the different proteins involved in the signalling pathways. Previous studies who investigated the effects of apoptosis following the combination treatments under hypoxic conditions were not found, therefore this would also be scope for future work.

4.5 Olaparib, Alone and in Combination, Induced Autophagy

Autophagy is a survival mechanism for cells that precedes apoptosis. Using CYTO-ID staining solution and flow cytometric analysis, the effects of olaparib were investigated. Olaparib produced similar effects on autophagic fluorescence in both normoxic and hypoxic conditions. Very limited research investigating olaparib on autophagy in U87-MG cells was found in the literature to support these results, suggesting this area of research requires attention. However, previous studies investigating olaparib in ovarian cancer cells determined that olaparib did induce autophagic effects (Sui, *et al*., 2015), which partly coincides with our findings. However, the method used by Sui, *et al*., (2015) was to inject the cell lines into mice and treated them once daily at a dose of 30 mg/kg for 3-weeks, so any disparity may be as a result of this. From the other autophagy results, it may also be expected that olaparib would induce greater autophagy in hypoxia, though this was not observed.

TMZ treatment in GBM cells caused little change in autophagic fluorescence compared to the non-treated control. Previous studies have reported TMZ treatment to induce autophagy in GBM cells. Knizhnik, *et al*., (2013) found that glioma cells underwent autophagy in a specific time-dependent manner following 24-144-hours after TMZ (100 µM) treatment in U87-MG and LN-229 cell lines. However, even though TMZ induces autophagy, it provides GBM cells with resistance to the treatment (Jawhari, *et al*., 2016). In the current study, under hypoxia, TMZ caused no change in autophagic fluorescence when compared to normoxia. Autophagy is a highly regulated mechanism that can be activated in response to certain stimuli, such as conditions of starvation including hypoxia (Knizhnik, *et al*., 2013). Therefore, as hypoxia has been found to induce autophagy (Jawhari, *et al*., 2016) the effects of hypoxia and TMZ treatment combined should have caused a greater percentage of fluorescence, than in normoxia, though this was not observed in current results. However, this study only tested autophagy induction following 24-hours of drug treatment, so this may have been too early to observe any effects.

Similar findings were observed for cisplatin where an increase in autophagic fluorescence was induced in hypoxic conditions, when compared to the non-treated control and also compared to under normoxia. A study by Zhang, *et al*., (2015) reported cisplatin (10 µg/ml) can induce autophagy, and their findings supported the results of the present study; though they treated U251 GBM cells for 6, 12, and 24-hours. As a cytotoxic agent, cisplatin is hypothesised to cause cell death by DNA damage and inhibition of DNA synthesis, however it has been established that cisplatin can also

induce cell death through endoplasmic reticulum (ER) stress *in vitro* and *in vivo* (Zhang, *et al*., 2015). The ER is the location of regulating protein synthesis, protein folding following synthesis and accumulation, stress reaction, and regulating calcium ion levels. Changes in the microenvironment of tumour cells, such as hypoxia, or anti-tumour drugs, can cause ER stress, including accumulation of unfolded and misfolded proteins in the ER and an abnormality in the intracellular calcium ion balance. Eventually, proteins that fail to be folded correctly are degraded by the proteasomal and autophagy pathways (Zhang, *et al*., 2015). Hence concluding ER stress, caused by cisplatin, hypoxia or a combination of both can induce autophagy. This observation suggests the reason why an increased effect was observed in the results of the present study in low oxygen conditions, compared to normoxic conditions.

Both of the combination treatments with olaparib produced increases in autophagic fluorescence under both normoxia and hypoxia, with significant increases under hypoxia. These results correlate closely with those obtained in this study following TMZ and cisplatin treatment alone, as they also induced a higher percentage of fluorescence in hypoxic conditions. Therefore, these findings suggest when TMZ and cisplatin are combined with olaparib, greater effects are exerted on the GBM cells. Previous studies have not established results for these combination treatments on autophagy in U87-MG cells, however various studies have determined how combined treatments with a PARPi enhances cytotoxicity in GBM (Dréan, *et al*., 2016). Therefore, based on the MOA of TMZ and cisplatin, it is logical for olaparib to increase autophagy.

Some of the results for autophagy can be associated with those of the apoptosis assay. Previous studies (Knizhnik, *et al*., 2013) that have investigated TMZ, after comparing the time course of apoptosis and autophagy after TMZ treatment, established that autophagy precedes apoptosis. These studies demonstrated how a single-type of DNA lesion induced by TMZ, O^6-methylguanine (O^6MeG), produces three different end-points in glioma cells: autophagy, senescence and apoptosis. The authors found that 72-hours after treatment autophagy was significantly induced, which reaches a maximum at 96-hours and then decreases thereafter; cellular senescence was induced 72-hours following treatment which steadily increases with time; while apoptosis is the last response that becomes significant 120-hours after treatment; this was investigated in LN-229 GBM cells (Knizhnik, *et al*., 2013). Therefore, this may explain why in the current results, TMZ alone and in combination with olaparib only induced apoptosis slightly. This may also be a reason for olaparib treatment due to its MOA, though this is not fully known.

Very limited research is present in the literature that investigates olaparib and the combination of olaparib with TMZ or cisplatin in GBM cells on autophagy in both normoxic and hypoxic conditions, therefore this is scope for future work. In this project, autophagy was measured 24-hours after drug treatment, however previous studies that examined TMZ found that glioma cells underwent autophagy in a specific time-dependent manner. Therefore, autophagy could be measured following 24-144-hours after drug treatment. Other studies also used different GBM cell lines to measure the effects of drug treatments on autophagy. Therefore, these are possibilities for future work.

4.6 Olaparib Induced DNA Damage in U87-MG GBM Cells

The comet assay detects the amount of DNA damage a drug treatment can induce following treatment. These results can confirm the data of previous assays including the apoptosis assay as the proportion of DNA damage caused can be observed clearly. Olaparib was observed to induce DNA damage in the U87-MG GBM cells, which even though this does not correlate with the apoptosis results, these findings do confirm olaparib alone does cause DNA damage. Previous studies have not investigated the effects of olaparib treatment alone on DNA damage in U87-MG cells. However, other research was found in the literature to support the effects of olaparib in other cancers. Wang, *et al*., (2016) performed the comet assay and found that olaparib can induce minor DNA damage in ovarian cancer cells; though it was 48-hours after drug treatment. Kwon, *et al*., (2016) observed a moderately high level of DNA damage in cisplatin-resistant head and neck cancer cells. This was determined 72-hours after olaparib treatment. Thus, the time-point used in the current study may have been too early to effectively assess the effect of olaparib on DNA damage.

TMZ treatment, when compared to the non-treated control, induced the greatest amount of DNA damage in the U87-MG cells. This was expected for TMZ as it is a potent chemotherapeutic agent. Castro, *et al*., (2015) found results that partly correlate with the present findings regarding TMZ (25 µM) and that they observed DNA damage in U87 cells, though only at an intermediate level.

Cisplatin was predicted to induce DNA damage similar to TMZ, as cisplatin is also a potent chemotherapeutic drug that induces DNA damage by crosslinking to the purine bases on DNA (Dasari & Tchounwou, 2014), however, this was not observed in the present study. This finding does not coincide with a study by Kutwin, *et al*., (2017), who determined cisplatin to induce lethal DNA damage in U87 GBM cells. The comet assay

is considered sensitive in detecting both SSB and DSBs (Braafladt, *et al*., 2016). However, this assay is commonly used for detecting SSBs as the initial damage produced by a treatment (Kawaguchi, *et al*., 2010). An explanation for cisplatin's results could not be discovered, suggesting that this is an area for further research. However, previous findings from this study have shown cisplatin to induce apoptosis and a decrease in cell viability, at an identical concentration of 300µM and also after 24-hours of treatment.

The DNA damage caused in the SVG p12 cells, when compared to the U87-MG cells, was fairly similar. Olaparib, however, induced a higher level of DNA damage in the GBM cells than in the SVG p12 cells. Previous studies were not found that have investigated DNA damage by olaparib on normal glial cell lines, however Fulton, *et al*., (2018) reported that even though PARP1 is regularly over-expressed in GBM, it is barely detectable in normal brain. Thus, this observation suggests olaparib may induce fewer adverse effects on normal cells than the current treatments.

Two different analysis methods were used in this study to interpret the results of the comet assay. The first method obtained the total intensity of both the head and the tail individually by drawing around each segment point-by-point. Whereas, the second method only provides an average of the intensity of the entire comet, and this was gained by starting at the top of the comet tail and drawing a straight line to the bottom. Also, the results from both methods for the H_2O_2 and TMZ treatments do not correlate. H_2O_2 was used as a positive control so the results obtained from the first method were expected. This finding suggests the second method of analysis is less effective at detecting DNA damage in the comet assay. Gyori, *et al*., (2014) performed the comet assay on rat muscle cell lines, and conducted analysis using the intensity profile method. This correlates closely with the first method employed in the current study. No previous studies were found that used the second method of image analysis. This indicates that it has not yet been fully established by previous studies which analysis method is more effective, therefore further research is required.

Based on the findings obtained in this project for the comet assay, scope for future work may include further investigation of the effects of olaparib on DNA damage in GBM cells, and also over a longer period of time, as this project only measured DNA damage following 24-hours of drug treatment. Further research is also required to examine different analysis methods to interpret results to establish which method is more effective in detecting DNA damage.

4.7 Drug Effects on Colony Formation

The clonogenic assay is based on the ability of a single cell to grow into a colony, and it was performed to further investigate the drug treatments on the survival and proliferation of the cells under normoxia and hypoxia. Olaparib induced an expected minor reduction in colony-formation in the U87-MG cells under normoxia. This finding coincides with a study by Irwin, *et al*., (2014) who also reported that olaparib did induce a reduction in the number of surviving colonies in U87 GBM cells. A similar result was not obtained under hypoxia, instead no change was observed. This result was not what would be expected due to PARP1's involvement with the HIF factors, and inhibition of PARP1 led to multiple regulatory effects on the HIF-2-mediated hypoxic response at both the transcriptional and post-transcriptional level (Gonzalez-Flores, *et al*., 2014). Previous studies relating to this finding were not found though; therefore, further research would be required.

In normoxia, TMZ and cisplatin induced clear decreases in the number of colonies observed in the U87-MG cells, which was expected from these positive control treatments. Pasi, *et al*., (2014) reported TMZ to induce a reduction in clonogenicity, when compared to the control, in T98G and U251-MG cells; though in a different GBM cell line, these findings correlate with the results of the present study. Cisplatin in U87 cells was investigated by Combs, *et al*., (2012), and they found it to reduce clonogenic survival with increasing concentrations. Similar findings for TMZ and cisplatin were also obtained in hypoxic conditions. Though previous studies who examined TMZ or cisplatin in GBM cell lines were not found, another study by Abyaneh, *et al*., (2017) investigated cisplatin (33.2µM) under hypoxia in MDA-MB-231, a triple negative breast cancer cell line. After 24-hours of treatment, they found that cells cultured under hypoxia had a significantly higher number of colonies than under normoxia. Therefore, even though a decrease in colony formation under hypoxia was seen in my results, other studies do not correlate with this. All drug treatments were observed to be less effective under hypoxia compared to normoxia, which suggests the cells could have been treated for longer prior to counting the colonies.

The findings obtained for the SVG p12 cells under normoxia, especially, were not what would be expected for TMZ and cisplatin treatments, but instead a decrease should have been observed, similar to what was seen with the U87-MG cells. The variation of these results was wider than the others, however, the results under hypoxia were not as varied. The reasoning behind the unusual SVG p12 results may be due to the high temperature in the laboratory when this assay was conducted. A study by Bergs, *et al*.,

(2016) investigated the effects of hyperthermia on a human squamous lung carcinoma cell line. Hyperthermia is known to be a very potent chemo- and radiosensitiser, that can be effective even at mild temperatures. It was determined that temperatures of 42-48ºC for 30-120 minutes can induce genotoxic effects (Bergs, *et al*., 2016). Therefore, if temperatures in the laboratory were extremely higher than normal, the effects of the drug treatments should have increased. A decrease in colony formation should have also been observed for the non-treated control, however this was not seen, especially as for this assay the colonies were not counted until 10-days later.

Scope for future work based on the results of this assay include further research on the effects of olaparib, TMZ and cisplatin on colony-formation in GBM cells under hypoxia. In this project, the colonies were counted after 10-days, however by doing this only a single result was obtained. Therefore, the assay could be stopped at different timepoints to count the colonies formed, in order to generate a range of results and ensure the drug treatments are effective.

4.8 Conclusion

Figure 4.2 summarises the main findings of this study. The results from this study have demonstrated that olaparib does induce cytotoxic effects on U87-MG GBM cells *in vitro*, and fewer effects were induced on the SVG p12 cells, compared to TMZ and cisplatin. Stronger cytotoxicity in the GBM cells was observed when administered in combination with other drug treatments, compared to when olaparib was given alone. Therefore, combination treatments with olaparib may be a better treatment option for GBM. As the dual effects of PARP inhibition by olaparib and the DNA damage by either TMZ or cisplatin would be expected to induce enhanced cytotoxicity in GBM tumours *in vivo* to potentially provide an improved prognosis and increase long-term survival of patients.

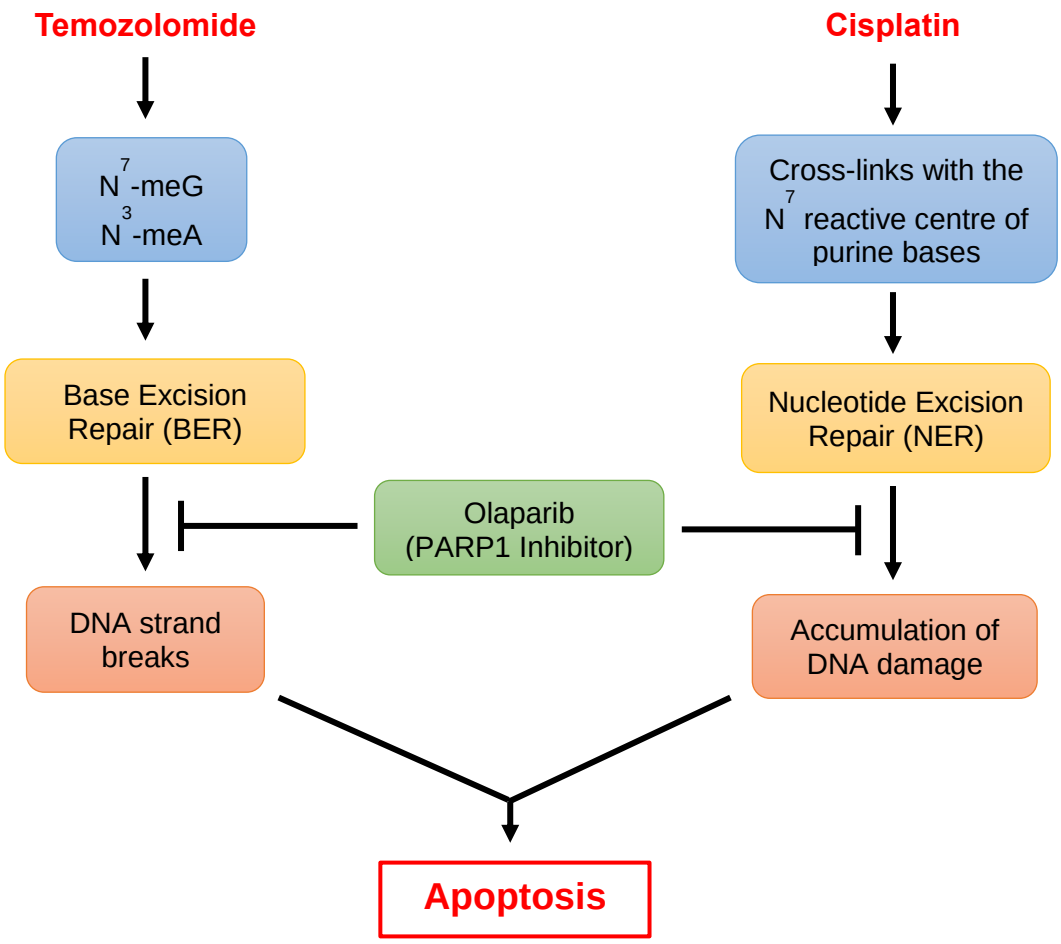

Figure 4.2: Diagram showing the mechanism of action of temozolomide and cisplatin, and how with the inhibition of PARP1 by olaparib, apoptosis of the cells is ultimately induced.

4.9 Future Work

In this project, while significant work has been completed, due to the variability in the results, certain assays, such as the apoptosis and clonogenic assays, may need repeating to verify the results. As Knizhnik, *et al*., (2013) stated apoptosis is not observed until 120-hours and onwards after drug treatment. Therefore, it would be beneficial to perform this assay over a longer period of time to ensure the effects of drug treatment on apoptosis is observed. For the clonogenic assay, because the results obtained in this study were not as expected, it would be required to repeat this assay in order to verify the results.

The comet assay could also be performed under hypoxic conditions to determine the proportion of DNA damage induced in hypoxia, when compared to normoxia. All other

assays in this project were conducted under both conditions for comparisons to be made. Also, as the microenvironment of a GBM tumour is extremely hypoxic (Jawhari, *et al*., 2016), it would be beneficial to establish the effects of drug treatments under hypoxic conditions, as well as normoxic conditions.

The effects of olaparib in the SVG p12 cell line were unexpected at times during the study, which may be because the cells are not 100% representative of normal glial cells due to the BKPyV infection. Therefore, this would require further research in order to clearly establish to what extent normal cells would be affected. Using primary cells or short-term cultures may be beneficial, as a better understanding of how the drug treatments induce effects could be established.

Administration of combination drug treatments requires additional investigation to determine the effects of olaparib and TMZ or cisplatin in all assays. This would provide a wider understanding on whether combination treatments enhance the therapeutic effects for GBM.

Triplet combination therapies of PARP inhibition, radiotherapy and TMZ have been observed to induce extra synergistic lethality, compared to doublet therapy (Lim & Tan, 2017), so this is another field for further research.

Further study on the mechanism(s) of action of olaparib as a PARP1 inhibitor is required. Studies have stated that olaparib is an inhibitor for both PARP1 and PARP2 (Rasmussen, *et al*., 2016), therefore future studies could determine how olaparib exerts its effects on GBM cells. An siRNA approach could be used to do this; knocking down the expression of PARP1 could establish whether olaparib is inducing its effects through that particular enzyme or others. This would be useful as an siRNA is a very selective knockdown approach, and no previous studies have conducted this before.

Olaparib has been observed to induce cytotoxicity in *BRCA*-mutated cancers, including ovarian and breast tumours. When either *BRCA1* or *BRCA2* is defective, HR, which is essential for DSBs repair, becomes dysfunctional. If HR cannot repair the damage, alternative repair mechanisms are activated. Therefore, if a patient is deficient in *BRCA* and olaparib inhibits PARP, the unrepaired DNA SSBs and DSBs will ultimately result in cell death (Lorusso, *et al*., 2018). Currently, an association between *BRCA* germline mutation and GBM malignancy has not been established. However, Boukerroucha, *et al*., (2015) investigated two patients with a *BRCA1* germline mutation treated for breast cancer, who developed GBM a few years later. They concluded that

the loss of heterozygosity did not occur as the tumour-suppressor protein expression is maintained in GBM at the protein and mRNA levels, implying that a *BRCA* mutation is not associated with GBM development. Another study by Elmariah, *et al*., (2006) reported a *BRCA1*-mutated patient who developed GBM, though they did not investigate this further. Studies on the risk of brain tumour development in *BRCA* carriers were conducted in 1994 and 2002 (Boukerroucha, *et al*., 2015); since then techniques have immensely evolved. Therefore, whether there may be a hidden link between *BRCA* mutation and GBM development is an extensive area for further research and whether olaparib treatment could potentially be more beneficial in these patients, as well as in GBM overall.

5 References

Abyaneh, H.S., Gupta, N., Radziwon-Balicka, A., Jurasz, P., Seubert, J., Lai, R. and Lavasanifar, A. (2017). STAT3 but Not HIF-1α Is Important in Mediating Hypoxia-Induced Chemoresistance in MDA-MB-231, a Triple Negative Breast Cancer Cell Line. *Cancers,* 9(10): 137-153.

Ahmed, E.M., Bandopadhyay, G., Coyle, B. and Grabowska, A. (2018). A HIF-independent, CD133-mediated mechanism of cisplatin resistance in glioblastoma cells. *Cellular Oncology (Dordrecht),* 41(3): 319-328.

Allen, M., Bjerke, M., Edlund, H., Nelander, S. and Westermark, B. (2016). Origin of the U87MG glioma cell line: Good news and bad news. *Science Translational Medicine*, 8(354): 1-4.

Annovazzi, L., Mellai, M. and Schiffer, D. (2017). Chemotherapeutic Drugs: DNA Damage and Repair in Glioblastoma. *Cancers,* 9(6): 57-73.

AstraZeneca. (2018). *Lynparza tablets receive EU approval for the treatment of platinum-sensitive relapsed ovarian cancer.* [Online] Available at: https://www.astrazeneca.com/media-centre/press-releases/2018/lynparza-tablets-receive-eu-approval-for-the-treatment-of-platinum-sensitive-relapsed-ovarian-cancer08052018.html [Accessed 10 July 2018].

Ben-Hur, E., Chen, C.C. and Elkind, M.M. (1985). Inhibitors of Poly(adenosine Diphosphoribose) Synthetase, Examination of Metabolic Perturbations, and Enhancement of Radiation Response in Chinese Hamster Cells. *American Association for Cancer Research,* 45(5): 2123-2127.

Bergs, J.W., Oei, A.L., Ten-Cate, R., Rodermond, H.M., Stalpers, L.J., Barendsen, G.W. and Franken, N.A. (2016). Dynamics of chromosomal aberrations, induction of apoptosis, BRCA2 degradation and sensitization to radiation by hyperthermia. *International Journal of Molecular Medicine,* 38(1): 243-250.

Boukerroucha, M., Josse, C., Segers, K., El-Guendi, S., Frères, P., Jerusalem, G. and Bours, V. (2015). BRCA1 germline mutation and glioblastoma development: report of cases. *BMC Cancer,* 15(1): 181-187.

Braafladt, S., Reipa, V. and Atha, D.H. (2016). The Comet Assay: Automated Imaging Methods for Improved Analysis and Reproducibility. *Scientific Reports,* 6(1): 32162-32171.

Bray, F., Ferlay, J., Soerjomataram, I., Siegel, R.L., Torre, L.A. and Jemal, A. (2018). Global cancer statistics 2018: GLOBOCAN estimates of incidence and mortality worldwide for 36 cancers in 185 countries. *CA: A Cancer Journal for Clinicians*, 68(6): 394-424.

Brown, G.L., Eckley, M. and Wargo, K.A. (2010). A Review of Glioblastoma Multiforme. *Pharmacist,* 35(5): 3-10.

Brown, J.S., Kaye, S.B. and Yap, T.A. (2016). PARP inhibitors: the race is on. *British Journal of Cancer,* 114(7): 713-715.

Cancer Research UK. (2018). *Cancer Statistics for the UK.* [Online] Available at: https://www.cancerresearchuk.org/health-professional/cancer-statistics-for-the-uk#heading-Three [Accessed 9 December 2018].

Carmo, A., Carvalheiro, H., Crespo, I., Nunes, I. and Lopes, M.C. (2011). Effect of temozolomide on the U-118 glioma cell line. *Oncology Letters,* 2(6): 1165-1170.

Castro, G.N., Cayado-Gutiérrez, N., Zoppino, F.C.M., Fanelli, M.A., Cuello-Carrión, F.D., Sottile, M., Nadin, S.B. and Ciocca, D.R. (2015). Effects of temozolomide (TMZ) on the expression and interaction of heat shock proteins (HSPs) and DNA repair proteins in human malignant glioma cells. *Cell Stress & Chaperones,* 20(2): 253–265.

Chalmers, A. (2017). *A trial looking at olaparib with temozolomide for glioblastoma that has come back (OPARATIC).* [Online] Available at: http://www.cancerresearchuk.org/about-cancer/find-a-clinical-trial/a-trial-looking-at-olaparib-with-temozolomide-glioblastoma-has-come-back#undefined [Accessed 20 September 2017].

Chalmers, A., Jackson, A., Swaisland, H., Watts, C., Halford, S., Hargrave, D. and McCormick, A. (2016). DDIS-19. Olaparib Penetrates Tumour Margins As Well As Contrast Enhancing Regions Of Glioblastoma At Therapeutic Levels: Interim Results Of The Oparatic Trial NCT01390571. *Neuro-Oncology,* 18(6): (an abstract).

Chen, A. (2011). PARP inhibitors: its role in treatment of cancer. *Chinese Journal of Cancer,* 30(7): 463-471.

Cohen, A., Holmen, S. and Colman, H. (2013). IDH1 and IDH2 Mutations in Gliomas. *Current Neurology and Neuroscience Reports,* 13(5): 345-351.

Coluccia, D., Figueiredo, C.A., Wu, M.Y., Riemenschneider, A.N., Diaz, R., Luck, A., Smith, C., Das, S., Ackerley, C., O'Reilly, M., Hynynen, K. and Rutka, J.T. (2018). Enhancing glioblastoma treatment using cisplatin-gold-nanoparticle conjugates and targeted delivery with magnetic resonance-guided focused ultrasound. *Nanomedicine: Nanotechnology, Biology and Medicine,* 14(4): 1137-1148.

Combs, S.E., Zipp, L., Rieken, S., Habermehl, D., Brons, S., Winter, M., Haberer, T., Debus, J. and Weber, K.J. (2012). In vitro evaluation of photon and carbon ion radiotherapy in combination with chemotherapy in glioblastoma cells. *Radiation Oncology,* 7(1): 9-14.

Dasari, S. and Tchounwou, P.B. (2014). Cisplatin in cancer therapy: molecular mechanisms of action. *European Journal of Pharmacology,* 740(1): 364-378.

Davis, M.E. (2016). Glioblastoma: Overview of Disease and Treatment. *Clinical Journal of Oncology Nursing,* 20(5): 2-8.

Dréan, A., Lord, C.J. and Ashworth, A. (2016). PARP inhibitor combination therapy. *Critical Reviews in Oncology/Hematology,* 108: 73-85.

Dziadkowiec, K.N., Gąsiorowska, E., Nowak-Markwitz, E. and Jankowska, A. (2016). PARP inhibitors: review of mechanisms of action and BRCA1/2 mutation targeting. *Menopause Review,* 15(4): 215-219.

Elmariah, S.B., Huse, J., Mason, B., LeRoux, P. and Lustig, R.A. (2006). Multicentric glioblastoma multiforme in a patient with BRCA-1 invasive breast cancer. *The Breast Journal,* 12(5): 470-474.

FDA. (2018). *FDA approves olaparib for germline BRCA-mutated metastatic breast cancer.* [Online] Available at: https://www.fda.gov/drugs/informationondrugs/approveddrugs/ucm592357.htm [Accessed 4 September 2018].

Filippi-Chiela, E.C., Thomé, M.P., Bueno-e-Silva, M.M., Pelegrini, A.L., Ledur, P.F., Garicochea, B., Zamin, L.L. and Lenz, G. (2013). Resveratrol abrogates the Temozolomide-induced G2 arrest leading to mitotic catastrophe and reinforces the Temozolomide-induced senescence in glioma cells. *BMC Cancer,* 13(1): 147-160.

Fulton, B., Short, S.C., James, A., Nowicki, S., McBain, C., Jefferies, S., Kelly, C., Stobo, J., Morris, A., Williamson, A. and Chalmers, A.J. (2018). PARADIGM-2: Two parallel phase I studies of olaparib and radiotherapy or olaparib and radiotherapy plus temozolomide in patients with newly diagnosed glioblastoma, with treatment stratified by MGMT status. *Clinical and Translational Radiation Oncology,* 8: 12-16.

Gonzalez-Flores, A., Aguilar-Quesada, R., Siles, E., Pozo, S., Rodríguez-Lara, M.I., López-Jiménez, L., López-Rodríguez, M., Peralta-Leal, A., Villar, D., Martín-Oliva, D., del Peso, L., Berra, E. and Oliver, F.J. (2014). Interaction between PARP-1 and HIF-2α in the hypoxic response. *Oncogene,* 33(7): 891-898.

Goodenberger, M. and Jenkins, R. (2012). Genetics of adult glioma. *Cancer Genetics,* 205(12): 613-621.

Graeber, T.G., Peterson, J.F., Tsai, M., Monica, K., Fornace, A.J. Jr. and Giaccia, A.J. (1994). Hypoxia induces accumulation of p53 protein, but activation of a G1-phase checkpoint by low-oxygen conditions is independent of p53 status. *Molecular and Cellular Biology,* 14(9): 6264-6277.

Gyori, B.M., Venkatachalam, G., Thiagarajan, P.S., Hsu, D. and Clement, M.V. (2014). OpenComet: An automated tool for comet assay image analysis. *Redox Biology,* 2: 457-465.

Haar, C.P., Hebbar, P., Wallace, G.C., Das, A., Vandergrift, W.A., Smith, J.A., Giglio, P., Patel, S.J., Ray, S.K. and Banik, N.L. (2012). Drug Resistance in Glioblastoma: A Mini Review. *Neurochemical Research,* 37(6): 1192-1200.

Henriksen, S., Tylden, G.D., Dumoulin, A., Sharma, B.N., Hirsch, H.H. and Hanssen-Rinaldo, C. (2014). The Human Fetal Glial Cell Line SVG p12 Contains Infectious BK Polyomavirus. *Journal of Virology,* 88(13): 7556–7568.

Holohan, C., Van Schaeybroeck, S., Longley, D.B. and Johnston, P.G. (2013). Cancer drug resistance: an evolving paradigm. *Nature Reviews Cancer,* 13(10): 714-726.

Irwin, C.P., Portorreal, Y., Brand, C., Zhang, Y., Desai, P., Salinas, B., Weber, W.A. and Reiner, T. (2014). PARPi-FL - a Fluorescent PARP1 Inhibitor for Glioblastoma Imaging. *Neoplasia,* 16(5): 432-440.

Jawhari, S., Ratinaud, M.H. and Verdier, M. (2016). Glioblastoma, hypoxia and autophagy: a survival-prone ‘ménage-à-trois'. *Cell Death & Disease,* 7(10): 1-10.

Jenkins, R. (2017). *PARP-inhibitor olaparib shows promise for glioblastoma.* [Online] Available at: https://www.oncology-central.com/2017/11/08/parp-inhibitor-olaparib-shows-promise-glioblastoma/ [Accessed 10 June 2018].

Jia, W.Z., Zhao, J.C., Sun, X.L., Yao, Z.G., Wu, H.L. and Xi, Z.Q. (2015). Additive anticancer effects of chrysin and low dose cisplatin in human malignant glioma cell (U87) proliferation and evaluation of the mechanistic pathway. *Journal of Balkan Union of Oncology,* 20(5): 1327-1336.

Karpel-Massler, G., Pareja, F., Aimé, P., Shu, C., Chau, L., Westhoff, M.A., Halatsch, M.E., Crary, J.F., Canoll, P. and Siegelin, M.D. (2014). PARP Inhibition Restores Extrinsic Apoptotic Sensitivity in Glioblastoma. *PLoS One,* 9(12): 1-24.

Kawaguchi, S., Nakamura, T., Yamamoto, A., Honda, G. and Sasaki, Y.F. (2010). Is the Comet Assay a Sensitive Procedure for Detecting Genotoxicity?. *Journal of Nucleic Acids,* 2010(1): 541050.

Knizhnik, A.V., Roos, W.P., Nikolova, T., Quiros, S., Tomaszowski, K.H., Christmann, M. and Kaina, B. (2013). Survival and Death Strategies in Glioma Cells: Autophagy, Senescence and Apoptosis Triggered by a Single Type of Temozolomide-Induced DNA Damage. *PLoS One,* 8(1): 1-12.

Ko, H.L. and Ren, E.C. (2012). Functional Aspects of PARP1 in DNA Repair and Transcription. *Biomolecules,* 2(4): 524-548.

Kuhnt, D., Becker, A., Ganslandt, O., Bauer, M., Buchfelder, M. and Nimsky, C. (2011). Correlation of the extent of tumor volume resection and patient survival in surgery of glioblastoma multiforme with high-field intraoperative MRI guidance. *Neuro-Oncology,* 13(12): 1339-1348.

Kumar-Thakor, F., Wan, K.W., Welsby, P.J. and Welsby, G. (2017). Pharmacological effects of asiatic acid in glioblastoma cells under hypoxia. *Molecular and Cellular Biochemistry,* 430(1): 179-190.

Kutwin, M., Sawosz, E., Jaworski, S., Wierzbicki, M., Strojny, B., Grodzik, M. and Chwalibog, A. (2017). Assessment of the proliferation status of glioblastoma cell and tumour tissue after nanoplatinum treatment. *PLoS One,* 12(5): 1-14.

Kwon, M., Jang, H., Kim, E.H. and Roh, J.L. (2016). Efficacy of poly (ADP-ribose) polymerase inhibitor olaparib against head and neck cancer cells: Predictions of drug sensitivity based on PAR–p53–NF-κB interactions. *Cell Cycle,* 15(22): 3105-3114.

Lacroix, M., Abi-Said, D., Fourney, D.R., Gokaslan, Z.L., Shi, W., De Monte, F., Lang, F.F., McCutcheon, I.E., Hassenbusch, S.J., Holland, E., Hess, K., Michael, C., Miller, D. and Sawaya, R. (2001). A multivariate analysis of 416 patients with glioblastoma multiforme: prognosis, extent of resection, and survival. *Journal of Neurosurgery,* 95(2): 190-198.

Lee, S.Y. (2016). Temozolomide resistance in glioblastoma multiforme. *Genes & Diseases,* 3(3): 198-210.

Lim, J.S. and Tan, D.S. (2017). Understanding Resistance Mechanisms and Expanding the Therapeutic Utility of PARP Inhibitors. *Cancers,* 9(8): 109-122.

Longworth, L. (2005). *Carmustine implants and temozolomide for the treatment of newly diagnosed high-grade glioma.* [Online] Available at: https://www.nice.org.uk/guidance/ta121/documents/glioma-overview2 [Accessed 10 June 2018].

Lorusso, D., Tripodi, E., Maltese, G., Lepori, S., Sabatucci, I., Bogani, G. and Raspagliesi, F. (2018). Spotlight on olaparib in the treatment of BRCA-mutated ovarian cancer: design, development and place in therapy. *Drug Design, Development and Therapy,* 12(1): 1501-1509.

Louis, D.N., Perry, A., Reifenberger, G., von Deimling, A., Figarella-Branger, D., Cavenee, W.K., Ohgaki, H., Wiestler, O.D., Kleihues, P. and Ellison, D.W. (2016). The 2016 World Health Organization Classification of Tumors of the Central Nervous System: a summary. *Acta Neuropathologica,* 131(6): 803-820.

Louis, D.N., Schiff, D. and Batchelor, T. (2018). *Classification and pathologic diagnosis of gliomas.* [Online] Available at: https://www.uptodate.com/contents/classification-and-pathologic-diagnosis-of-gliomas [Accessed 23 August 2018].

Major, E.O., Miller, A.E., Mourrain, P., Traub, R.G., de Widt, E. and Sever, J. (1985). Establishment of a line of human fetal glial cells that supports JC virus multiplication. *Proceedings of the National Academy of Sciences of the United States of America,* 82(4): 1257-1261.

Malyuchenko, N.V., Kotova, E.Y., Kulaeva, O.I., Kirpichnikov, M.P. and Studitskiy, V.M. (2015). PARP1 Inhibitors: antitumor drug design. *ActaNaturae,* 7(3): 27-37.

Mann, J., Ramakrishna, R., Magge, R. and Wernicke, A.G. (2017). Advances in Radiotherapy for Glioblastoma. *Frontiers in Neurology,* 8(1): 748-759.

Miknyoczki, S.J., Jones-Bolin, S., Pritchard, S., Hunter, K., Zhao, H., Wan, W., Ator, M., Bihovsky, R., Hudkins, R., Chatterjee, S., Klein-Szanto, A., Dionne, C. and Ruggeri, B. (2003). Chemopotentiation of temozolomide, irinotecan, and cisplatin activity by CEP-6800, a poly(ADP-ribose) polymerase inhibitor. *Molecular Cancer Therapeutics,* 2(4): 371-382.

Monteiro, A.R., Hill, R., Pilkington, G.J. and Madureira, P.A. (2017). The Role of Hypoxia in Glioblastoma Invasion. *Cells,* 6(4): 45-69.

Moody, C.L. and Wheelhouse, R.T. (2014). The Medicinal Chemistry of Imidazotetrazine Prodrugs. *Pharmaceuticals,* 7(7): 797-838.

Murai, J., Zhang, Y., Morris, J., Ji, J., Takeda, S., Doroshow, J.H. and Pommier, Y. (2014). Rationale for poly(ADP-ribose) polymerase (PARP) inhibitors in combination therapy with camptothecins or temozolomide based on PARP trapping versus catalytic

inhibition. *The Journal of Pharmacology and Experimental Therapeutics,* 349(3): 408-416.

Murnyák, B., Kouhsari, M.C., Hershkovitch, R., Kálmán, B., Marko-Varga, G., Klekner, Á. and Hortobáhvi, T. (2017). PARP1 expression and its correlation with survival is tumour molecular subtype dependent in glioblastoma. *Oncotarget,* 8(28): 46348–46362.

NHS. (2016). *Overview: Cancer.* [Online] Available at: https://www.nhs.uk/conditions/cancer/ [Accessed 9 December 2018].

Ohgaki, H. and Kleihues, P. (2013). The Definition of Primary and Secondary Glioblastoma. *Clinical Cancer Research,* 19(4): 764-772.

Ostrom, Q.T., Bauchet, L., Davis, F.G., Deltour, I., Fisher, J.L., Eastman Langer, C., Pekmezci, M., Schwartzbaum, J.A., Turner, M.C., Walsh, K.M., Wrensch, M.R. and Barnholtz-Sloan, J.S. (2014). The epidemiology of glioma in adults: a “state of the science” review. *Neuro-Oncology,* 16(7): 896-913.

Ozdemir-Kaynak, E., Qutub, A.A. and Yesil-Celiktas, O. (2018). Advances in Glioblastoma Multiforme Treatment: New Models for Nanoparticle Therapy. *Frontiers in Physiology,* 9(1): 170-184.

Pasi, F., Paolini, A., Nano, R., Di Liberto, R. and Capelli, E. (2014). Effects of Single or Combined Treatments with Radiation and Chemotherapy on Survival and Danger Signals Expression in Glioblastoma Cell Lines. *BioMed Research International,* 2014: 1-9.

Pontén, J. and Macintyre, E.H. (1968). Long term culture of normal and neoplastic human glia. *Acta Pathologica et Microbiologica Scandinavica,* 74(4): 465-486.

Powell, M.A. (2014). *Perspectives on PARP Inhibitors in Ovarian Cancer: Has the Time Come for Individualized Care?.* [Online] Available at: https://www.medscape.org/viewarticle/830282_2 [Accessed 7 September 2018].

Purdy, M.C. (2014). *The Source.* [Online] Available at: https://source.wustl.edu/2014/08/study-reveals-one-reason-brain-tumors-are-more-common-in-men/ [Accessed 7 December 2018].

Ramakrishna, R. (2017). *Glioblastoma Multiforme (GBM).* [Online] Available at: http://weillcornellbrainandspine.org/condition/glioblastoma-multiforme-gbm/diagnosing-and-treating-glioblastoma-multiforme [Accessed 20 August 2018].

Rasmussen, R.D., Gajjar, M.K., Jensen, K.E. and Hamerlik, P. (2016). Enhanced efficacy of combined HDAC and PARP targeting in glioblastoma. *Molecular Oncology,* 10(5): 751-763.

Rocha, C.R.R., Garcia, C.C.M., Vieira, D.B., Quinet, A., de Andrade-Lima, L.C., Munford, V., Belizário, J.E. and Menck, C.F.M. (2014). Glutathione depletion sensitizes cisplatin- and temozolomide-resistant glioma cells in vitro and in vivo. *Cell Death & Disease,* 5(10): 1-10.

Sharples, N. (2017). *FDA Approves Olaparib as Maintenance Therapy for Recurrent Ovarian Cancer.* [Online] Available at: https://www.cancer.gov/news-events/cancer-currents-blog/2017/fda-olaparib-ovarian-cancer-maintenance [Accessed 4 September 2018].

Stupp, R., Hegi, M.E., Mason, W.P., van den Bent, M.J., Taphoorn, M.J., Janzer, R.C., Ludwin, S.K., Allgeier, A., Fisher, B., Belanger, K., Hau, P., Brandes, A.A., Gijtenbeek, J., Marosi, C., Vecht, C.J., Mokhtari, K., Wesseling, P., Villa, S., Eisenhauer, E., Gorlia, T., Weller, M., Lacombe, D., Caimcross, J.G. and Mirimanoff, R.O. (2009). Effects of radiotherapy with concomitant and adjuvant temozolomide versus radiotherapy alone on survival in glioblastoma in a randomised phase III study: 5-year analysis of the EORTC-NCIC trial. *The Lancet: Oncology,* 10(5): 459-466.

Stupp, R., Mason, W.P., van den Bent, M.J., Weller, M., Fisher, B., Taphoorn, M.J., Belanger, K., Brandes, A.A., Marosi, C., Bogdahn, U., Curschmann, J., Janzer, R.C., Ludwin, S.K., Gorlia, T., Allgeier, A., Lacombe, D., Caimcross, J.G., Eisenhauer, E. and Mirimanoff, R.O. (2005). Radiotherapy plus Concomitant and Adjuvant Temozolomide for Glioblastoma. *The New England Journal of Medicine,* 352(10): 987-996.

Sui, H., Shi, C., Yan, Z. and Li, H. (2015). Combination of erlotinib and a PARP inhibitor inhibits growth of A2780 tumor xenografts due to increased autophagy. *Drug Design, Development and Therapy,* 9(1): 3183-3190.

Sun, S., Lee, D., Lee, N.P., Pu, J.K., Wong, S.T., Lui, W.M., Fung, C.F. and Leung, G.K. (2012). Hyperoxia resensitizes chemoresistant human glioblastoma cells to temozolomide. *Journal of Neuro-Oncology,* 109(3): 467-475.

Sun, T., Warrington, N.M., Luo, J., Brooks, M.D., Dahiya, S., Snyder, S.C., Sengupta, R. and Rubin, J.B. (2014). Sexually dimorphic RB inactivation underlies mesenchymal glioblastoma prevalence in males. *The Journal of Clinical Investigation,* 124(9): 4123-4133.

Thakkar, J.P., Dolecek, T.A., Horbinski, C., Ostrom, Q.T., Lightner, D.D., Barnholtz-Sloan, J.S. and Villano, J.L. (2014). Epidemiologic and Molecular Prognostic Review of Glioblastoma. *Cancer Epidemiology, Biomarkers & Prevention,* 23(10): 1985-1996.

Tiek, D.M., Rone, J.D., Graham, G.T., Pannkuk, E.L., Haddad, B.R. and Riggins, R.B. (2018). Alterations in Cell Motility, Proliferation, and Metabolism in Novel Models of Acquired Temozolomide Resistant Glioblastoma. *Scientific Reports,* 8(1): 7222-7232.

Wang, D., Li, C., Zhang, Y., Wang, M., Jiang, N., Xiang, L., Li, T., Roberts, T.M., Zhao, J.J., Cheng, H. and Liu, P. (2016). Combined inhibition of PI3K and PARP is effective in the treatment of ovarian cancer cells with wild-type PIK3CA genes. *Gynecologic Oncology,* 142(3): 548-556.

Wang, H.H., Chang, T.Y., Lin, W.C., Wei, K.C. and Shin, J.W. (2017). GADD45A plays a protective role against temozolomide treatment in glioblastoma cells. *Scientific Reports,* 7(1): 8814-8828.

Yang, C., Hong, C.S. and Zhuang, Z. (2015). Hypoxia and glioblastoma therapy. *Aging,* 7(8): 523-524.

Young, R.M., Jamshidi, A., Davis, G. and Sherman, J.H. (2015). Current trends in the surgical management and treatment of adult glioblastoma. *Annals of Translational Medicine,* 3(9): 121-135.

Yu, Z., Zhao, G., Li, P., Li, Y., Zhou, G., Chen, Y. and Xie, G. (2016). Temozolomide in combination with metformin act synergistically to inhibit proliferation and expansion of glioma stem-like cells. *Oncology Letters,* 11(4): 2792–2800.

Zhang, R., Wang, R., Chen, Q. & Chang, H. (2015). Inhibition of autophagy using 3-methyladenine increases cisplatin-induced apoptosis by increasing endoplasmic reticulum stress in U251 human glioma cells. *Molecular Medicine Reports,* 12(2): 1727-1732.

Zhao, S., Wu, J., Wang, C., Liu, H., Dong, X., Shi, C., Shi, C., Liu, Y., Teng, L., Han, D., Chen, X., Yang, G., Wang, L., Shen, C. and Li, H. (2013). Intraoperative Fluorescence-Guided Resection of High-Grade Malignant Gliomas Using 5-Aminolevulinic Acid–Induced Porphyrins: A Systematic Review and Meta-Analysis of Prospective Studies. *PLoS One*, 8(5): 1-10.